Studies on Slow Electrons in Gases

by

Isobel C. Walker (née Bain)

Thesis presented for the Degree of Doctor of Philosophy.

University of Edinburgh May 1965.

To my Parents

and

Jamieson

INDEX.

I. INTRODUCTION.

INTRODUCTION.

1.1. The interaction that takes place when a free electron and a gas molecule collide depends on the energy of the electron and the nature of the molecule. Perhaps the best known such interaction is that of ionisation.

$$e + M \rightarrow M^{+} + 2e$$

This is the reaction occurring in the ion source of a mass spectrometer. To effect ionisation, the colliding electron must have a kinetic energy that at least equals the ionisation potential of the molecule. Less energetic electrons might cause electronic transitions within the molecule.

$$e + M \rightarrow M^{*} + e$$

Reactions of this kind are being studied at the present time in electron-impact spectroscopy. This can be compared with optical spectroscopy, the incident photons being replaced by electrons. Electron-impact spectroscopy is of particular interest because the electronic transitions are not limited by the optical selection rules, and "forbidden" transitions have been observed in some spectra.(7). The "slow electrons" with which this thesis deals are still less energetic and may be conveniently defined as electrons which are not sufficiently energetic to excite electronic transitions within the molecules with which they collide. They are, therefore, electrons of up to about 1 eV energy. An electron of energy 1 eV is moving with a velocity of 5.9×10^{7} cm s^{-1} and has an associated wave length of 12 A^{o}.

In general, slow electron/molecule collisions may be classified into three types according to the nature of the resulting interaction.

(a) Elastic Collisions. These are impacts in which only kinetic energy is exchanged between electron and molecule. If momentum and kinetic energy are to be conserved in an elastic impact between a body of mass m and another of mass M, simple physics shows that the lighter body loses a fraction of its kinetic energy λ to the heavier, λ being given by:-

$$\lambda = \frac{2m(1 - \cos\Theta)}{M}$$

θ is the angle through which m is scattered. If scattering is isotropic (all θ are equally probable) then $\overline{1 - \cos\theta} = 1$, and $\lambda = 2m/M$. For an elastic impact between an electron and a molecule $m/M \doteqdot 10^{-4}$. So, if the electron is a slow one, the kinetic energy transferred to the molecule is very small and indeed will be scarcely noticed by the molecule.

(b) Inelastic Collisions. These are impacts in which the molecule gains internal energy from the electron. For slow electrons, the only inelastic processes energetically possible are rotational or vibrational excitation of the molecules.

(c) Superelastic Collisions. These are impacts in which internal energy from the molecule is handed on to the electron. The molecule must, therefore, be initially in an excited state.

Since early this century, evidence of inelastic impacts between slow electrons and molecules has been accumulating.[1,3,4] It indicates that, in some cases, rotational or vibrational excitation may be very efficient. Some of the processes involved - especially in rotational excitation are well understood; others less well so. In particular, large energy losses appear to take place when electrons of energy in the region of one vibrational quantum collide with some molecules.[1.] In order to excite a vibration "directly" an electron must hand over one quantum of kinetic energy to vibrational kinetic energy of the molecule. However, we have pointed out that the Principles of Conservation of Energy and Momentum limit the exchangeable kinetic energy to a very small fraction of the incident energy - too small to cause vibrational excitation. In view of this apparently anomolous excitation, and of the importance to chemists of energy transfer, this present study was undertaken in an attempt to elucidate further the nature of inelastic interactions between slow electrons and molecules.

1.2. Methods of Study.

Two experimental methods are available for the study of slow electron/molecule interactions - namely electron beam and electron swarm techniques. In the former, a beam of electrons as nearly monoenergetic as possible, is passed into a chamber containing gas at a very low pressure. Experimental conditions are chosen so that an electron makes no more than one collision with a gas molecule. Then, usually by looking at the scattered electrons, one gets information on single impact phenomena.

Electron beam experiments involve great practical difficulties. Swarm experiments, on the other hand, are relatively simple to carry out, but their results are difficult to interpret. They involve pushing an electron swarm through a gas by means of a d.c. electric field. The average energy of the electron swarm can, to a certain extent, be controlled. The gas pressure is such that each electron makes many collisions with gas molecules. By looking at the speed with which the electrons move through the gas and the extent to which they diffuse sideways, information on the nature of the electron/molecule collisions may be obtained.

1.3. Definitions:- Collision and Collision Cross-Section.

Collisions are usually described in terms of collision cross-section, and so it is important that the two terms - collision and collision cross-section - be rigidly defined.

Classically, a collision may be simply defined in terms of position and velocity of the colliding particles. This is not possible when dealing with electron/molecule impacts. The electron/molecule interaction may be a very long-range one, making it difficult to say when a collision has taken place. In addition, the wave nature of the electron cannot be neglected. This means that the collision cross-section is a property, not of the scattering molecule alone, but of the whole system - electron plus molecule. It is, therefore, a function of the incident electron energy.

The following is one of a number of possible definitions for the term "collision" when applied to electron/molecule impacts. An electron/molecule impact is said to have occurred, if any physical change can be

detected after the distance between electron and molecule has been first decreased, and then increased. This physical change may be simple deflection, kinetic energy change, etc. etc..

Collision Cross-Section is defined as the probability that an electron makes a collision in going 1 cm distance through the gas at unit density. Therefore, in travelling distance dx through a gas of density N molecules/cm^3, the probability that an electron collides is

$$P = Q.N.dx$$

and Q

$$Q = P/N.dx.$$

Q is the collision cross section and may be seen to have the dimensions of area. Classically, because of the long range electron/molecule interaction, there is always a finite probability that the electron is deflected, and, therefore, according to the present definition, the cross-sections will be always infinite. Quantum mechanically, on the other hand, one can say that scattering has occurred only if the deviation of the electron is large compared with the indeterminancy in the direction of motion of the electron. This is given by Heisenberg's Uncertainty Principle. It can be shown that if the scattering field U(r) decreases more rapidly than $1/r^n$ where $n \geqslant 3$ the cross-section is finite.[8] The electron mean free path is given by l:-

$$l = I/NQ$$

where N is the gas density in molecules cm^{-3}.

Total collision cross-sections can be subdivided into elastic and inelastic cross-sections which combine additively

$$Q = Q \text{ elastic} + Q \text{ inelastic.}$$

These cross-sections are usually expressed in units of πa_o^2 where a_o is the radius of the first Bohr orbit of the hydrogen atom.

$$a_o = 0.5292 \times 10^{-8} \text{cm}$$
$$\pi a_o^2 = 8.806\ 10^{-17} \text{cm}^2$$

The differential cross-section makes allowance for scattering of the electrons through different angles. The differential cross-section for a given element of solid angle $d\Omega$ is related to the probability that an electron be scattered elastically or inelastically into that solid angle. If θ is the scattering angle and ϕ the azimuth scattering angle, $d\Omega = \sin\theta\, d\theta\, d\phi$. The probability that the electron be scattered into $d\Omega$ is $P(\theta) \sin\theta\, d\theta\, d\phi$. The differential cross-section for scattering into $d\Omega$ is defined as $Q\, P(\theta) \sin\theta\, d\theta\, d\phi$.

$$Q\, P(\theta) \sin\theta\, d\theta\, d\phi = I(\theta) \sin\theta\, d\theta\, d\phi$$

The total cross-section is the differential cross-section integrated over the entire range of angular scattering.

$$Q = \int_0^{\pi} \int_0^{2\pi} I(\theta) \sin\theta\, d\theta\, d\phi.$$

The momentum transfer cross-section is also defined to allow for angular scattering. An electron scattered elastically through an angle θ loses a fraction of its energy given by $2(1-\cos\theta)m/M$. The mean fractional loss per collision is

$$\frac{2m}{M} \int_0^{\pi} \int_0^{2\pi} (1-\cos\theta) \sin\theta\, P(\theta)\, d\theta\, d\phi = \frac{2m\, Q_D}{M\, Q}$$

where $$Q_D = \int_0^{\pi} \int_0^{2\pi} Q\, P(\theta)\, (1-\cos\theta) \sin\theta\, d\theta\, d\phi$$

and is known as the momentum transfer, or diffusion cross-section. In travelling a distance x in a gas of density N atoms cm^{-3}, an electron makes $N\, Q\, x$ collisions. So, the fractional energy loss by an electron in travelling a distance x is

$$\frac{2m}{M} \frac{Q_D}{Q} N\, Q\, x = \frac{2m}{M} Q_D\, N\, x$$

just as if λ were taken as $2m/M$ and Q replaced by Q_D. Q_D will be the same as Q if scattering is isotropic. If there is a concentration of forward scattering $Q_D < Q$, and if there is preferential backward scattering $Q_D > Q$

These various cross-sections describe completely any impact. We shall now describe how they may be measured experimentally.

Fig.1.4.1.

Ramsauer Apparatus

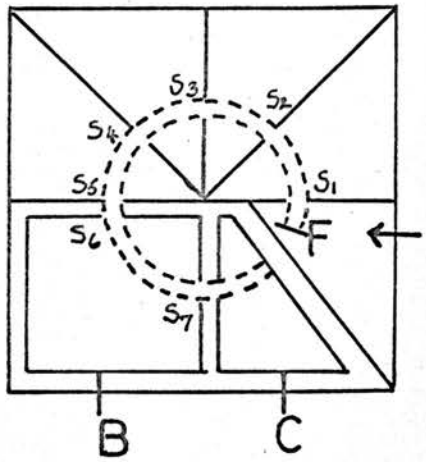

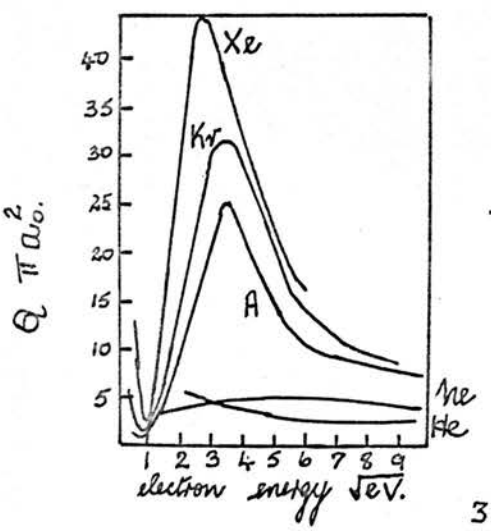

Fig 1.4.2.

Total Collision Cross-Sections

Fig.1.4.3.

Cross-Sections

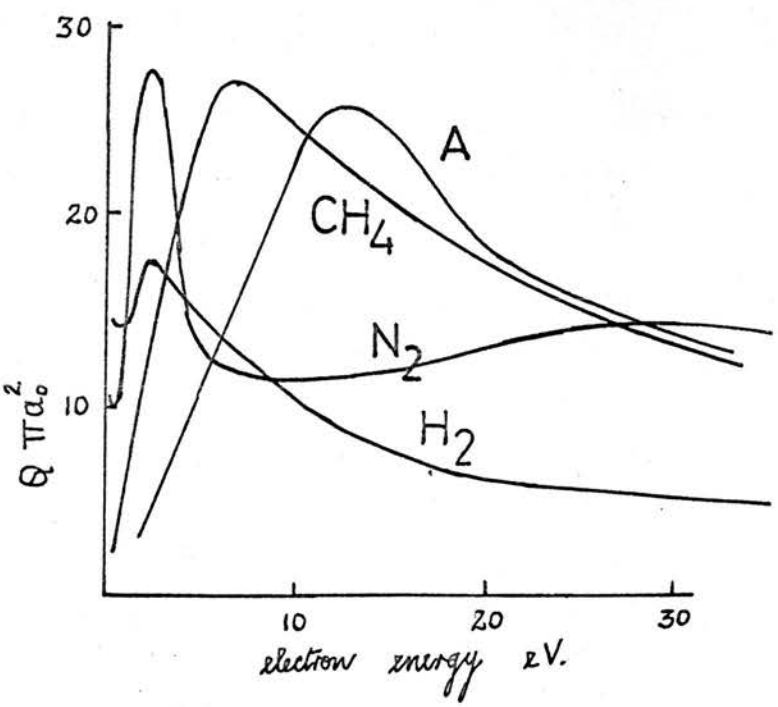

1.4. Measurement of Total Collision Cross-sections.

Quantitative measurements on total collision cross-sections date from about 1920, when Ramsauer described quite a simple method for measuring them[9]. The Ramsauer apparatus is illustrated in fig. 1.4.1. Electrons ejected from a zinc plate F by a u.v. beam are accelerated to the desired velocity before passing through slit S_1. A magnetic field perpendicular to the plane of the paper causes the electrons to describe a circular path through slits S_1 to S_7 to collector C. All scattered electrons fail to get through the slits. If at any point, the electron beam current is given by I_o, in travelling a distance dx this is diminished by dI.

$$dI = N Q \, dx$$

$$I = I_o \exp(-N Q x)$$

$$= I_o \exp(-\alpha x)$$

I is the current after distance x. α is known as the absorption coefficient. This expression is used to evaluate Q as follows: With a gas pressure P_1 Torr in the apparatus, the currents i_1 to C alone and j_1 to B and C together are measured. If x is the path length between S_6 and S_7

$$i_1 = j_1 \exp(- P_1 \alpha x)$$

where α is the absorption coefficient at a pressure of one Torr.
If i_2 and j_2 are similar currents at P_2 Torr

$$i_2 = j_2 \exp(-\alpha P_2 x)$$

So

$$(P - P_2) x = \log \frac{j \, i_2}{j_2 i}$$

From this α and hence Q is found.

Total collision cross-sections for the following species have been measured by Ramsauer and others. (9 - 13)
Helium, neon, krypton, xenon, zinc, cadmium, mercury, sodium, tellurium, hydrogen, oxygen, nitrogen, carbon monoxide, hydrogen chloride,

nitric oxide, carbon dioxide, water, nitrous oxide, methane, ethane, propane, butane, ethylene, acetylene, methyl chloride, dichloromethane, trichloromethane, carbon tetrachloride, fluoromethane, methanol, methylamine, trimethylamine, isobutane, dimethylether and ethanol.

1.4(a) Ramsauer-Townsend Effect. Total collision cross-sections for the rare gases are shown in fig. 1.4.2. Ar, Kr, and Xe display striking variations in cross-section over the low energy region. The minimum in Q occurring in Ar at 1 eV was seen independently by Townsend in a swarm experiment[14] and it is therefore known as the Ramsauer-Townsend Effect. This effect must be an elastic one.

Consider the elastic scattering of an electron from an atom. It may be treated qualitatively as follows.[1] The scattering centre may for simplicity, be represented by a potential well of depth D. i.e. $V(r) = -D$ for $r < a$ and $V(r) = 0$ for $r > a$. Consider a head-on collision. The incident electron constitutes a wave-train, the wave length of which is h/mu for $r > a$ and $\frac{h}{(m^2u^2+2Dm)^{1/2}}$ for $r < a$. The two wave-trains must join smoothly at $r = a$. To do this, and keep the amplitude of the wave finite at the centre, a phase change must be introduced into the train for $r > a$, relative to that which would exist if the potential barrier were not there. An observer at infinity detects the scattering through this phase shift, and if it is 2π or $2n\pi$ he will not notice it. Then the collision cross-section is effectively zero. This simple picture shows that Q is a function of the phase shift produced in the incident electron by the potential field of the scattering atom. An electron which has an angular momentum about the atom may also experience a phase shift provided it is not too far distant from the atom. Angular momentum is quantised.

$$J = \left[l(l+1)\right]^{\frac{1}{2}}h$$

η_l is the phase shift of the electron of quantum number l
Scattering theory shows that [15]

$$Q = \frac{4\pi}{k^2}\ (2l+1)\ \sin^2\eta_l$$

The summation is over all l and $k = \frac{2\pi}{\text{wave length}}$ To produce a noticeable phase shift in an electron train of impact parameter p

$$V(p) > \tfrac{1}{2} m u^2$$

But for a slow electron to have even unit angular momentum it must have a high impact parameter

$$p = 2h / mu$$

So for slow electrons only $l = 0$ is significant and

$$Q = \frac{4\pi}{k^2} \sin^2 \eta_0$$

The minima observed in the cross-sections of atoms occur where the potential of the atom is sufficiently strong to introduce a phase shift of $n\pi$ at a particular electron energy. So, the similar behaviour in Ar, Kr, and Xe is due to the fact that in going from Ar to Kr the atomic field becomes just strong enough to introduce an additional half wave length within the incident wave train. Similarly for Xe. The fields of He and Ne are too weak to do this.

Some molecular cross-sections measured by the Ramsauer method, are illustrated in fig. 1.4.3. The behaviour of methane is very like that of Ar.

The extension of collision theory to molecules is complex because spherical symmetry is no longer preserved and stronger electron/molecule interactions are possible. Particularly in polar molecules higher order phase shifts must be considered in the expression for Q (elastic). In addition there may be inelastic contributions to the cross-section at low energies.

The total angular momentum of an electron about the scattering molecule is no longer a constant of motion. Instead, the component of angular momentum about the internuclear axis is quantised, the allowed values being mh, for m = 0,1,2,....

The incident wave may be resolved into partial waves, for which $m = 0,1,2,\ldots$ For each such partial wave, a phase shift $\eta_{\ell m}$ is introduced by the scattering field, and the total cross-section becomes

$$Q = \sum_{\ell m} q(\ell m)$$

where

$$q = \frac{2\pi}{k^2} \sin^2 \eta_{\ell m} \qquad m=0$$

$$= \frac{4\pi}{k^2} \sin^2 \eta_{\ell m} \qquad m \neq 0$$

As the electron energy tends to zero, all the partial cross-sections except q_{oo} tend to zero.

Fisk (16) did extensive calculations on the phase shifts in electron scattering from molecules and was able to reproduce the cross-section peak in N_2 at 2.3 eV. However, recent work in N_2 shows that it has a high inelastic cross-section at 2.3 eV, and it may mean that the maximum in the Ramsauer cross-section is due to this inelastic process. When applied to chlorine, Fisk's theory gave cross-sections much smaller than those observed experimentally.

The similarity between the cross-sections of methane and argon has also been explained in terms of elastic processes. CH_4 has a high degree of symmetry. Buckingham, Massey and Tibbs[17] calculated a spherically symmetrical field for the methane molecule and then found the phases for scattering of electrons by this field. According to their calculations, the Ramsauer-Townsend effect in CH_4 arises because the molecular field is just strong enough to introduce exactly two extra half-waves into the low energy partial waves with zero angular momentum, while the Ar field produces three, Kr four and Xe five.

1.5. Measurement of Inelastic Cross-sections

The cross-sections obtained from Ramsauer-type experiments are total, elastic plus inelastic. Recently, Schulz and others at the Westinghouse laboratories have perfected beam techniques whereby inelastic cross-sections may be measured. Two experimental methods have

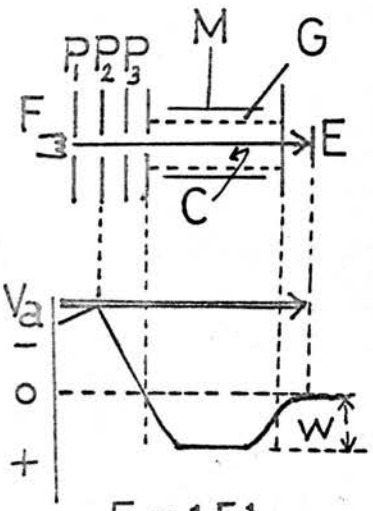

Fig 1.5.1.
Electron Trap

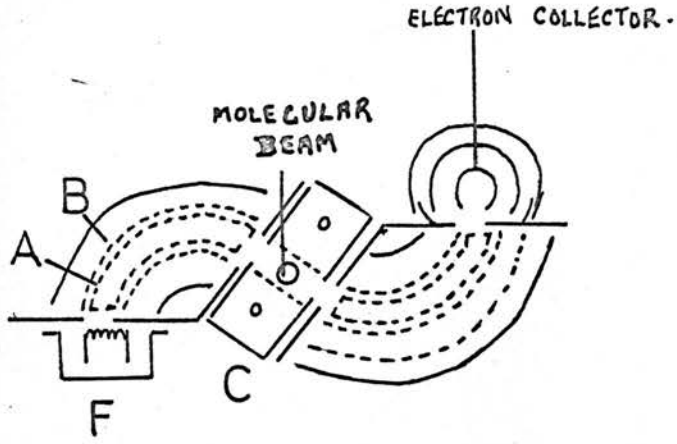

Fig.1.5.2.
Electrostatic Analyzer

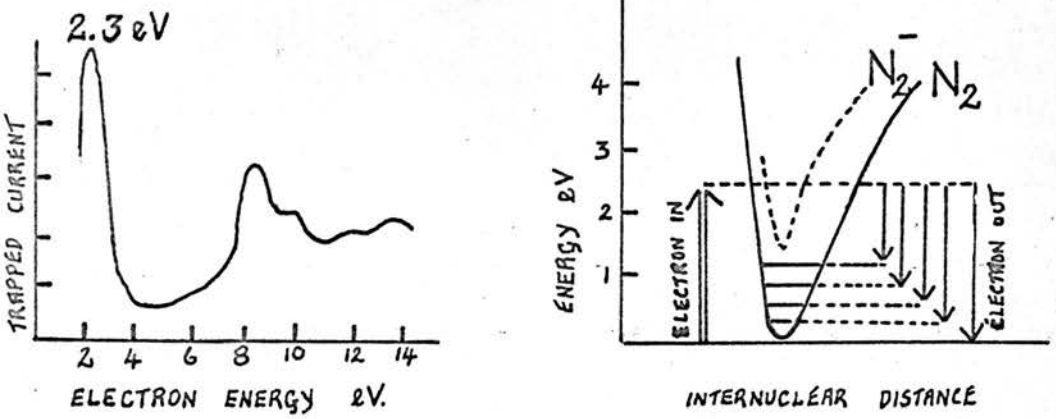

Fig 1.5.3.
Inelastic Scattering from N_2

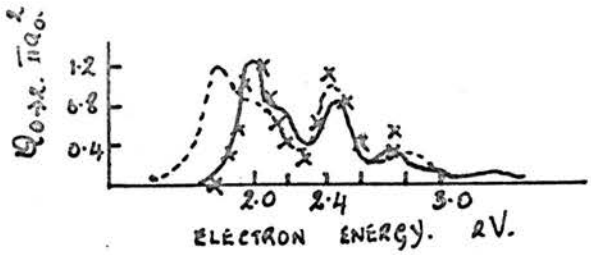

Fig 1.5.4.
Vibrational X-Section
$Q_{0\to 2}$ N_2.

—— CHEN

---- HERZENBERG + MANDL

× × SCHULZ.

been used, the so-called "electron trap" and the double electrostatic analyser.[18-24].

(a) Electron Trap A typical electron trap is shown in fig.1.5.1. It consists of an electron gun, a collision chamber C and an electron collector E. The electron source is the filament F. Electron energy is controlled by the retarding potential difference method as follows. Electrode P_3 is positive with respect to F and draws electrons from it. P_2 is maintained at a potential V_A which is slightly negative with respect to F. P_2 thus provides a potential barrier which is surmountable only by the higher energy electrons. P_1 and P_3 are equipotential and the collision chamber is at potential V_A with respect to P_2. Electrons getting over V_A are aligned by a magnetic field and pass into C which contains a gas at a low pressure (10^{-4} Torr). If V_A is increased slightly to $V_A + dV_A$, the distribution of electrons getting into the collision chamber is cut off sharply at a slightly different energy. Thus by the method of differences one can measure the events in the collision chamber caused by electrons in the energy band dV_A. The collision chamber consists of the grid G and entrance and exit plates all at the same potential. M is an electron collector which is well insulated from G. A potential, positive with respect to G can be applied to M. A small part of this potential penetrates to the collison chamber, so that the situation is as illustrated in fig. 1.5.1. An electron in C has energy $V_A + w$ where w is the depth of the potential well created by the potential on M. If this electron collides inelastically losing energy between V_A and $V_A + w$ it finds itself with insufficient energy to get out of the potential well and eventually arrives at M. By measuring this trapped electron current for different V_A and w one can estimate the probabilities of inelastic processes occurring, as a function of electron energy.

(b) Double Electrostatic Analyser The apparatus is illustrated in fig. 1.5.2. The collision chamber C is situated between two identical electrostatic analysers. In the first one, cylindrical grids A and B deflect the electrons emitted from filament F and focus them on the exit slit. The essentially monoenergetic beam which emerges passes

into the collision chamber where it is crossed by a molecular beam. Those electrons scattered in the forward direction (or any other chosen direction) pass into the second analyser where they are energy analysed and collected on a highly shielded electron collector. This method enables one to obtain directly the energy lost by the scattered electrons. It is, however, less sensitive than the electron trap, so, if an inelastic cross-section is low, the double electrostatic analyser cannot be used.

Schultz has examined inelastic processes in nitrogen,[19,20,24] oxygen,[23] carbon monoxide,[19,24] nitrous oxide,[22] water[21] and hydrogen.[24]

Fig. 1,5.3(a) shows the results obtained for N_2 in the electron trap.[19] Trapped electron current is given as a function of electron energy. This current shows a well defined maximum at 2.3 eV indicating an inelastic process at that energy. The lowest electronic state in N_2 has an excitation threshold of 6 eV. Haas[25], in a swarm-type experiment had previously demonstrated that 2.3 eV electrons collide inelastically with N_2 and he suggested vibrational excitation by an indirect mechanism, involving the formation of an intermediate negative ion which undergoes decay to the vibrationally excited parent molecule.

$$N_2 + e \rightarrow (N_2)^- \rightarrow N^*_2 + e$$

Schulz interpreted his results similarly. A hypothetical potential energy diagram, the energies in which are chosen to conform with experimental figures is given in fig. 1.5.3 (b). This illustrates how an electron of 2.3 eV energy may excite several vibrational levels in N_2. This kind of impact may be compared with the classical "soft" impact, i.e. one where the coefficient of restitution is less than unity. Schulz also looked at N_2 in the electrostatic analyser[20] and was able to separate out the scattered electrons according to the energy they had lost. He thus obtained relative cross-sections for excitation of vibrational levels from $\nu = 1$ to $\nu = 8$. All the cross-sections showed sharp thresholds at energies greater than 1.7 eV. except that for the $0 \rightarrow 1$ excitation which had a long low energy tail. This

could only be interpreted as "direct" excitation of the first vibrational level, but no mechanism was suggested.

The problem of resonance scattering of electrons (i.e. via a negative intermediate) has been studied theoretically by several groups of workers. Herzenberg and Mandl[26] compared the negatively charged intermediate to the resonance states encountered in nuclear physics and assumed that the inelastic peaks are due to resonances of the incident electron in the well represented by the molecule. Using the quantal theory of Kapur and Pieirls, they derived equations for the scattering amplitudes to different vibrational states of the target molecule. The equations were applied to N_2 and solved numerically. The general features of inelastic scattering by N_2 were reproduced fairly well. In this treatment, they discussed the lifetime of the intermediate resonant state, comparing it with the duration of a vibration. Two situations were considered:

(1) Lifetime long compared with the vibration time.

(2) Lifetime short compared with the vibration time.

Schulz had found that the cross-sections for excitation to different levels had maxima at slightly different energies. This is to be expected if (2) holds.

More recently Chen[27] made a similar calculation based on a treatment advanced by Fesbach. He obtained absolute cross-section for excitation of N_2 to the various vibrational levels. The partial cross-sections for excitation of the second level as calculated by Chen and Herzenberg and Mandl and as measured by Schulz are shown in fig. 1.5.4. Those of Schulz and Herzenberg and Mandl have been normalised to Chen's calculated values. Haas estimated the inelastic cross-section at 2.3 eV to be $3 \times 10^{-16} cm.^2$ Chen's value is 4×10^{-16} cm^2. It is interesting that the inelastic cross-section and total cross-section have a maximum at 2.3 eV. It may be, that the latter is also due to the formation of a negative species and not - as was supposed by Fisk - to an elastic phenomenon.

CO which is isoelectronic with N_2 appears to interact similarly with slow electrons[19,24]. The inelastic cross-section shows a maximum at 1.7 eV, presumably due to excitation via $[CO^-]$ "Direct" excitation of the first level also shows up. On the other hand

excitation of H_2[24] has a threshold energy of 1 eV (not 0.53 eV corresponding to a "direct" $0 \rightarrow 1$ excitation) and a maximum at 2 eV. Absolute cross-sections for excitation of O_2[23] were obtained in the electron trap, but in this case it was not possible to distinguish whether the excitation is direct or indirect. In N_2O,[22] the trapped current was found to consist of some negative ions as well as electrons. By reducing the potential of M to almost zero, only the ions could be collected. Subtracting this from the total trapped current gave the electron current. The negative ion was identified as O^- from its mass spectrum. This and the trapped current values suggests the following mechanism for 2.2 eV electrons and N_2O.

$$N_2O + e \rightarrow N_2O^- \begin{cases} \nearrow N_2 + O^- \\ \searrow N_2O + e \end{cases}$$

A negative ion is formed and two processes compete for its decay.

1.6. Electron Swarms

Low energy electron beam techniques have been developed only in recent years. The practical difficulties involved have already been pointed out, and it is doubtful whether they can be used at very low energies, say < 0.5 eV. Swarm experiments are relatively easy to carry out and they provide the only means whereby interactions between very slow electrons and molecules may be studied.

Swarm theory and experimentation were developed by J.S. Townsend.[28] He started work at the end of the last century on the motion of negative ions in gases. When it was noticed that, in some gases, free electrons as well as negative ions carried current,[29] future effort was concentrated on the study of the drift and diffusion of free electrons in gases. Much work on this subject was done by the Townsend school during the nineteen twenties and thirties and recently interest in the subject has

been reawakened.

Consider a swarm of electrons in a gas. The electrons have mass m and average random velocity $\bar{u}$. The molecules have mass M and average random velocity $\bar{V}$. If T is the ambient temperature

$$\tfrac{1}{2} m u^2 = \tfrac{1}{2} M V^2 = \frac{3}{2} \frac{R}{No} T$$

R is the gas constant and N_o is Avogadro's number.
A d.c. electric field of strength E is applied to the system. The neutral gas molecules do not interact with the field. But the field does work on the electrons - work which causes an increase in electron energy. Because of their very small mass, the electrons, when they collide with gas molecules do not lose all the energy gained from the field, but continue to move in all directions with an increased thermal velocity. After several collisions a state of motion is obtained in which the electron energy remains constant. Then the energy gained from the field between collisions equals that lost to the molecules during collisions. In addition there is an overall drift of electrons in the direction of the applied field. The velocity of drift, W, is less than the random velocity u of the electrons. u and W are both functions of E/P, where P is the gas pressure. Both are increased by the field doing work on the electrons - work which is opposed by the gas molecules. However, at any given E/P, there is an inverse relation between u and W. This means that, if, at any E/P, u were suddenly to decrease, this would be reflected in an increase in W. The reason for this apparent anomoly is as follows. W is a measure of the rate at which electrons gain energy from the field. If the energy of a group of electrons suddenly falls, the rate at which this group regains energy from the field must rise in order to restore the agitational energy to its original value. u falls when inelastic impacts set in. So, by looking at u and W as functions of E/P, one can get an indication of the kind of electron/molecule collisions that are occurring. If u and W are known for corresponding E/P values, average total collision cross-sections may be calculated. An additional quantity is also calculable,

namely the fraction of its energy lost by an electron in a collision. This gives inelastic contributions to the cross-section.

Electron Swarm Theory The electrons in a swarm have an ill-defined distribution of velocities, and each electron makes several collisions with gas molecules. Thus, in swarm experiments, one observes some mean properties of the electron swarm and must relate them to individual collision phenomena. The theory involved in the interpretation of experimental data is complex, and involves many approximations and simplifying assumptions. The following approach is taken from Huxley.[31,30]

Consider a group of electrons in a gas travelling radially from a common origin $x = 0$. Let there be n_o electrons at the origin and let n_1 be the number that reach the point x without colliding. All electrons have the same speed u. If the number of electrons that collide between x and $(x + dx)$ is dn_1 the differential equation for n_1 is

$$dn_1 = -N\,Q(u)\,n_1\,dx \qquad \text{1.6.1.}$$

where N is the number of gas molecules present. An electric field is applied to the system. This causes the electron speed to increase along its trajectory so that at distance x it is $u + \Delta u(x)$. Then at distance x the cross-section is $Q(u) + (dQ/du)\,\Delta u(x)$, neglecting terms in higher powers of x. The proportion of the group of electrons that collides at distance greater than x is

$$n_1/n_o = \exp -\left[N\,Q\,x + N \int (dQ/du)\,u(x)\,dx\right] \qquad \text{1.6.2.}$$

The proportion that collides between x and $x + dx$ is

$$dn_1/n_o = \left[NQ + N\left(\frac{dQ}{du}\right)\Delta u(x)\right] dx \exp\left[-NQx - N\int \frac{dQ}{du}\Delta u(x)\,dx\right] \qquad \text{1.6.3.}$$

When $u(x)/u$ is small, this expression is approximately the same as

$$\begin{aligned} dn_1/n_o &= \left[NQ + N\left(\frac{dQ}{du}\right)\Delta u(x)\right]\left[1 - N\int\left(\frac{dQ}{du}\right)\Delta u(x)\,dx\right] dx \exp(-NQx) \\ &= \left[NQ - N\left(\frac{dQ}{du}\right)\left\{NQ\int \Delta u(x)\,dx - \Delta u(x)\right\}\right] dx \exp(-NQx) \end{aligned} \qquad \text{1.6.4.}$$

In terms of mean free path l, this becomes

$$dn/n_o = \left[\frac{1}{l} + \frac{1}{l^2}\frac{dl}{du}\left\{\int \Delta u(x)\,\frac{dx}{l} - \Delta u(x)\right\}\right] dx \exp\left(\frac{-x}{l}\right) \qquad \text{1.6.5.}$$

Now consider a group of electrons moving in a steady state of motion in a gas, and let the number whose agitational speed lies between u and (u + du) be

$$dn_u = n\, f(u)\, du \qquad \text{1.6.5.}$$

In time dt the average number of free paths traversed by each member of the group is udt/l. W will be given by the product of u dt/l and the mean displacement in the direction of E along these free paths. To evaluate this mean displacement, assume isotropic scattering. Consider electrons colliding at O. In the absence of E these electrons make their next collision at P. Application of E deflects the electrons to Q In travelling the distance x, electrons are subject to a force $\frac{Ee}{m}\sin\theta$ at right angles to OP. The time of transit is x/u. s. So, the displacement of the electrons is $\frac{1}{2}\frac{Ee}{m}\sin\theta\left(\frac{x}{u}\right)^2$ at right angles to OP. And the displacement in the field direction is $\frac{1}{2}\frac{Ee}{m}\left(\frac{x}{u}\right)^2\sin^2\theta$. In addition to this they travel a distance $x\cos\theta$ in the direction of E in the course of their free flight.

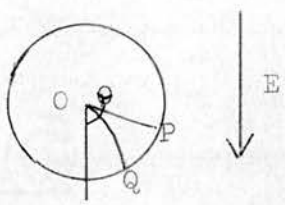

The increment in speed $\Delta u(x)$ along the path x is given by (acceleration) (time) = $\frac{Ee}{m}\cos\theta\left(\frac{x}{u}\right)$. The proportion of those setting out in the direction θ that collide between x and x + dx is given by substituting this in equation 1.6.5. It then follows that the mean displacement of a particle of the group dn taken over all θ and all free paths is

$$\frac{1}{2}\int_0^{\pi}\int_0^{\infty}\left(\frac{Ee}{2m}\left(\frac{x}{u}\right)^2\sin^2\theta + x\cos\theta\right)\left(\exp\frac{-x}{l}\right)\left[\frac{I}{l} + \frac{I}{l^2}\frac{dl}{du}\left(\frac{x}{2l} - I\right)x\cos\theta\,\frac{Ee}{mu}\right]\sin\theta\, d\theta\, dx.$$

$$= \frac{2}{3}\frac{Ee}{m}\left(\frac{l}{u}\right)^2 + \frac{1}{3}\frac{Ee}{m}\left(\frac{l}{u}\right)\frac{dl}{du}$$

$$= \frac{I}{3}\frac{Ee}{m}\frac{1}{u}\cdot\frac{I}{u^2}\frac{d(lu^2)}{du} \qquad \text{1.6.6.}$$

The number of collisions made by the group dn_u in time dt is $\frac{u}{l}$ dt dn_u. So the sum of the displacements in the direction of E experienced by the group in time dt is obtained by multiplying

equ. 1.6.6. by $\frac{u}{l}$ dt dn_u giving

$$S\,dt = \frac{I}{3}\frac{Ee}{m}\frac{I}{u^2}\frac{d}{du}(lu^2)\,dt\,dn_u. \qquad \text{——————} \quad 1.6.7.$$

The displacement of the centroid of the whole group is

$$dt\left[\int\frac{S\ dn}{n}\right] = dt\int S\ f(u)\ du \quad \text{—} \quad 1.6.8.$$

Drift velocity W is displacement divided by time

$$W = \int S\ f(u)\ du = \frac{Ee}{3m}\left[\overline{u^{-2}\frac{d}{du}lu^2}\right] \qquad \text{——} \quad 1.6.9.$$

$$l = I/N\,Q$$

where N is the gas density.

$$\therefore \quad W = \frac{E\,e}{3\,m\,N}\left[\overline{u^{-2}\frac{d}{du}\frac{u^2}{Q}}\right] \quad \text{——} \quad 1.6.10.$$

This expression was derived on the assumption that scattering is isotropic. If this is not so, the expression is modified simply by substituting $1/(I - \cos\theta)$ for l, or replacing Q by Q_D the momentum transfer cross-section.

$$W = \frac{E\,e}{3\,m\,N}\left[\overline{u^{-2}\frac{d}{du}\frac{u^2}{Q_D}}\right] \qquad 1.6.11.$$

The bracketed portion may be evaluated only if the electron velocity distribution f(u) and the form of the energy dependence of Q_D are known.

Coefficienty of Diffusion The electrons in a swarm tend to diffuse outwards to create a uniform electron distribution within the collision chamber. The diffusion coefficient D describes this tendency.

If, at any point the electron density is n cm^{-3} and the local velocity of electron flow in the x direction is v then

$$n\,v = -D \text{ grad } n \qquad \text{1.6.12}$$

i.e. the rate of flow of electrons in any direction is proportional to the concentration gradient in that direction. D depends on the electron energy and the electron mean free path. It can be shown to be given by [32]

$$D = \frac{1}{3}\overline{l\,u} \qquad \text{1.6.13}$$

In a chamber containing a swarm of electrons diffusing and drifting, the spacial distribution of the electrons depends on the ratio W/D. Combining equations 1.6.10 and 1.6.13

$$W/D = \frac{E\,e}{m}\left[\overline{u^{-2}\frac{d}{du}\frac{u^2}{Q_D}}\right] \Big/ \left(\frac{\overline{u}}{Q}\right)_D \qquad \text{1.6.14}$$

The electron energy in a swarm is usually expressed in terms of Townsend's coefficient k, the ratio of electron energy to the energy of the gas molecules.

$$k = \frac{\overline{mu^2}}{3\frac{R}{N_0}T} \qquad \text{1.6.15}$$

N_0 is Avogrado's number; so at T^0 A,

$$\overline{u^2} = 45.5\ 10^{10}\ kT$$

Equation 1.6.14 may be rewritten

$$W/D = \frac{E\,e}{\frac{1}{2}m\,\overline{u^2}}\ F \qquad \text{1.6.16}$$

F is the dimensionless factor $\dfrac{\overline{u^2}\left[\overline{u^{-2}\dfrac{d}{du}\left(\dfrac{u^2}{Q_D}\right)}\right]}{2\left(\dfrac{\bar{u}}{Q_D}\right)}$

In terms of k, W/D becomes

$$W/D = 7.73\,\frac{E\ 10^3}{k\ T}\ F \qquad \text{——————} \qquad 1.6.17.$$

W/D is a measurable quantity. So, if F may be evaluated, k may be obtained as a function of E/P.

Inelastic Energy Losses. Under steady state conditions, the energy gained by the electrons from the field in between collisions is balanced by the energy lost to the molecules during collisions. The collision frequency of electrons of velocity $\bar{u}$ and mean free path $\bar{l}$ is $(\overline{u/l})$ s^{-1}. λ represents the fractional energy lost by an electron in an impact; so, in one second, the energy transferred from an electron to the molecules is given by $(\overline{u/l})\ \lambda\ \frac{1}{2}\ m\overline{u^2}$. The energy gain in this time is E e W.

$$(\overline{u/l})\ \tfrac{1}{2}m\overline{u^2} = E\ e\ W \qquad \text{——————} \qquad 1.6.18$$

From equation 1.6.11:

$$E\ e = \frac{3\ m\ W}{\overline{u^{-2}\dfrac{d}{du}\left(l\ u^2\right)}}$$

$$= \frac{W^2}{u^2}\ K \qquad \text{——————} \qquad 1.6.19$$

K is the dimensionless factor given by

$$\frac{I}{K} = \frac{I}{6}\left[\left(\frac{\bar{u}}{l}\right)\ \overline{u^{-2}\frac{d}{du}\left(l\ u^2\right)}\right]$$

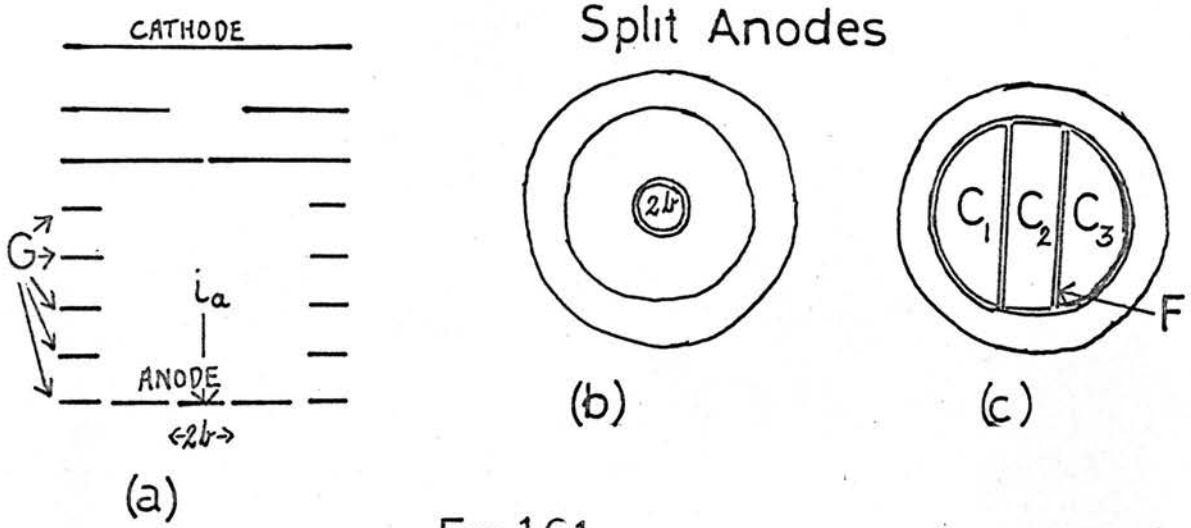

Fig 1.6.1.

Townsend Diffusion Apparatus

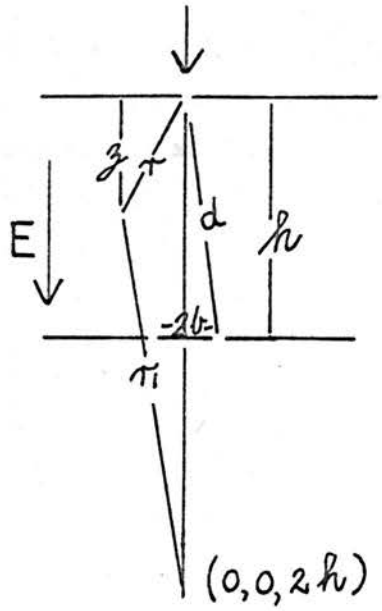

Fig 1.6.2.

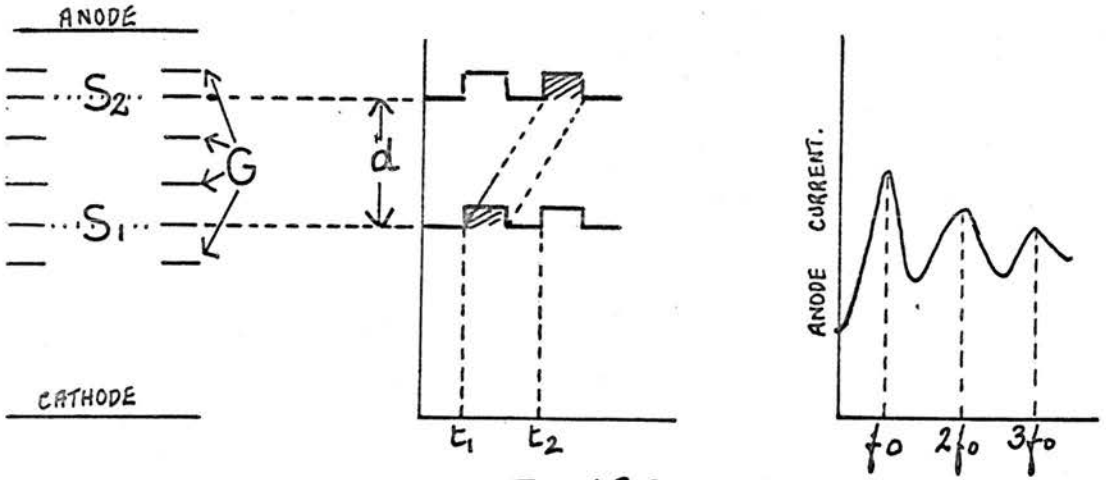

Fig 1.6.3.

Electron Shutter

$$= \frac{1}{6}\left[\overline{(u\,Q_D)}\;\overline{u^{-2}\frac{d\,u^2}{du\,Q_D}}\right]$$

$W = W\,(E/P)$ is measurable. Thus, provided the energy dependent factors K and F (equ. 1.6.16) may be evaluated, $\lambda = \lambda(u)$ can be calculated.

The above theory indicates the difficulties involved in interpreting swarm data. Before discussing this in detail, we shall describe some of the methods available for finding the various measurable quantities.

(a) Measurement of W/D The method most commonly used for measuring W/D was devised by Townsend at the end of the last century.[28,32] He used it originally in the study of the diffusion of ions. The form of the apparatus is shown in fig. 1.6.1. It comprises a diffusion chamber bounded at one end by an electrode in which there is a small orifice and at the other by an anode which is divided into insulated portions as shown. Guard rings G maintain a uniform potential gradient down the chamber. Photoelectrons entering the chamber through the orifice have already steady state drift motion through the gas at pressure P. In the absence of a field, the flow of electrons in the x direction is given by

$$n\,v = -D\,\text{grad}\,n \qquad \text{1.6.12.}$$

When a field E is applied in the x direction, the drift velocity is superposed on this, giving

$$n\,v = -D\,\text{grad}\,n + n\,W \qquad \text{1.6.20}$$

The equation of continuity in this system must be satisfied, i.e.

$$\text{div}\,n\,v = 0$$

$$\text{div}\,(-D\,\text{grad}\,n + n\,W) = 0$$

$$n = W/D\,\text{grad}\,n \qquad \text{1.6.21.}$$

This equation must be solved in accordance with given boundary conditions to give an expression for n at various positions within the chamber.[33]

The boundary conditions are that n = o everywhere at the anode, and n = 0 everywhere at the entrance electrode except at the orifice which is taken as the origin. These conditions can be satisfied if it is supposed that, in addition to the source at the origin, and image source of suitable strength is placed at the point (0,0,2h) to make n = 0 over the anode. Then

$$n = A\, e^{gx} \left[\frac{x}{r} \frac{d}{dr} \frac{(\exp - gr)}{r} + \frac{z - 2h}{r_1} \frac{d}{dr_1} \frac{(\exp - gr_1)}{r_1} \right] \quad \text{1.6.22.}$$

where the distances are as shown in fig 1.6.2.
If i_a is current falling on the central disc of radius b and i_t is the total current arriving at the anode, then
$R = i_a/i_t$ is

$$R = 1 - \left(\frac{h}{d} - \frac{1}{gh} + \frac{h}{d^2 g}\right)\left(\frac{h}{d}\right) \exp -g\,(d-h) \qquad \text{1.6.23}$$

g here is W/2D. (This is more often denoted by λ , but we shall not use this so as to avoid confusion with fractional energy loss of a colliding electron.)
In practice, this solution, which accurately satisfies the prescribed boundary conditions, does not accord with experimental results. Consistent results are obtained from[34]

$$R = 1 - \frac{h}{d} \exp -g(\,d - h\,) \qquad \text{1.6.24}$$

and this empirically correct formula is the one used by most workers. However, experimental conditions can be chosen so that the discrepancy between results obtained from 1.6.23 and 1.6.24 is negligible compared with other experimental errors.[35]

By measuring R at different E and P, one can evaluate g and hence W/D as a function of E/P. This is related to electron energy by equation 1.6.17.

Below is a list of gases in which W/D has been evaluated. Those of the Townsend school date from 1920 - 1930. Others are more recent.

Townsend School Helium,[36] neon,[37] argon,[38] hydrogen,[39] nitrogen,[39] oxygen,[39,40,41] air,[42,43] chlorine,[44] bromine,[45] iodine,[46] carbon monoxide,[47] nitric oxide,[47,48] carbon dioxide,[49,50] nitrous oxide,[47,51] water,[52] ammonia,[52,53,54] pentane,[55] ethylene,[56] hydrogen chloride,[52,53] methane.[57]

Others Helium,[58] argon,[58] hydrogen,[58,59,60,33,65] deuterium,[58,61] nitrogen,[58,59,60,65] air,[62,63] carbon monoxide,[58] carbon dioxide,[58,60] methane,[60] cyclopropane.[60]

(b) Measurement of Drift Velocity Several methods are available for the determination of electron drift velocities.

Magnetic Deflection. This method was devised by Townsend[5]. The cell he used was identical to that employed for measuring W/D except that the anode was split differently. (fig. 1.6.1) In order to determine W the cell was placed between two large vertical coils so that the electrons could move under the combined influence of a vertical electric field and a horizontal magnetic field, the magnetic field being parallel to C (fig. 1.6.1 (c)). When the magnetic field was applied, the electron swarm was deflected. H and E were chosen so that the axis of the deflected beam fell on F as shown by equal currents arriving on C_3 and $C_1 + C_2$. Applying the theory of the Hall effect to this system, Townsend calculated that, if θ is the angle of deflection of the beam

$$W = \frac{E}{H}\tan\theta = \frac{E}{H}\frac{b}{h} \qquad 1.6.25$$

Huxley[64] later discovered this to be in error and gave a corrected formula.

$$W = \frac{E}{H}\frac{b}{h}\frac{4}{3}\frac{(\overline{u^{-1}})^2}{(\overline{u^{-2}})} \qquad 1.6.26$$

Many of the early drift velocity measurements were made in this kind of apparatus. However, the evaluation of W from experimental figures requires a knowledge of the form of the electron velocity distribution curve, so it is inferior to other methods which give an average drift velocity directly. Drift velocities in the gases listed under "Townsend School" in section (a) have been measured by the deflection method.

Electron Shutter An electron shutter apparatus was first used for the measurement of electron drift velocities by Bradbury and Nielson.[65,66] Their drift cell is shown diagramatically in fig. 1.6.3. Electrons travel from a photocathode to an anode under the influence of an electric field. Guard rings G ..... maintain the field uniform. S_1 and S_2 are identical grids constructed of fine wire strung across an insulating frame. Alternate wires of each grid are connected together (fig. II.1.2) so that a potential difference may be applied between adjacent wires. Electrons pass through the grids when the p.d. between the wires is zero or nearly zero. Otherwise, they are swept sideways to the grid wires. An alternating in-phase potential is applied to S_1 and S_2. S_1 acts as a chopper, transmitting a series of electron pulses which travel towards S_2. These pulses reach the anode only if they find S_2 open when they arrive there. Bradbury and Nielson applied sinusoidal waves of variable frequency and amplitude to their grids. However, in fig. 1.6.3 we illustrate the situation for square waves, which give sharper electron pulses. If conditions are such that an electron pulse travels the distance d (the distance between S_I and S_2) in ($t_2 - t_I$) seconds, then a current maximum will show at the anode. Experimentally, the switching frequency is altered until a current maximum registers on the anode. Then that frequency f_o equals $I/(t_2 - t_I)$. Subsidiary maxima are recorded at frequencies $2f_o$, $3f_o$, ... nf_o for then S_2 has opened and shut (n-I) times while a pulse travels from S_I to S_2
W is therefore given by the equation

$$W = \frac{df_o}{n}$$

Other means for measuring the drift times have been developed from this. Phelps and Co.[67] have used an interrupted u.v. source ejecting pulses of electrons from the cathode. A short rectangular pulse applied to S_I makes it transmit a time t after an electron pulse has left the cathode. t is varied until t_o, the time at which the anode current is maximum, is found. Then the electrons have travelled from cathode to S_I in time t_o. This measurement may be checked by pulsing S_2 in a similar way giving the time of drift between cathode and S_2. Phelps and Co.[67] made measurements at very low E/P where the switching potential is liable to distort E in the region of the shutters. To reduce this distortion, they employed a so-called zero-bias method. In this, a pulsed electron source is still used, but the grids are normally open and are closed by the application of sharp rectangular pulses. The anode current is then minimum when $t = t_o$.

The shutter method is regarded as one of the most satisfactory for measuring drift velocities, at moderate to low E/P, and is the method we used to obtain electron drift velocities in a number of gases. Our apparatus is described in detail in section II. A continuous light source was used, together with two shutters operated by square waves.

Some of the errors sources of error in this kind of experiment are obvious. The shutters must switch in phase; the field in which the electrons drift must be uniform; the electron concentrations must be such that anode current may be measured reliably, but low enough to avoid space-charge effects etc. The elimination of these errors lies in the experimental set-up. Other errors are less obvious and less easy to control. They have been studied in detail by the Australian School of Crompton.[69.71] We shall discuss them here with particular reference to our apparatus, i.e. one in which the switching potential is a square wave of variable frequency.

As an electron pulse moves down the drift tube, diffusion of the electrons distort the pulse form. Some electrons diffuse backwards to be absorbed by S_I after it has shut. This causes a displacement of the pulse centre slightly forward, so that the maximum electron current is

recorded on the anode before the centre of the pulse reaches the anode. Lowke[71] has estimated that, in the limiting case when the shutters are open for a very short period of time, the relative error introduced by this back diffusion is $r = \frac{2}{d(W/D)}$

Additional errors due to diffusion other than backward diffusion also arise. The leading edge of a pulse is disturbed by the second shutter which may absorb some of the leading electrons before it opens. Because of diffusion while the leading edge is being collected, the frequency corresponding to maximum electron current is not equal to the frequency corresponding to maximum electron density of the undisturbed pulse at the second shutter. In addition, curves of anode current against frequency are not symmetrical about each maximum, for there is continuous decay of the maximum current density of the pulse while it is passing through the second shutter.

The differential equation describing the electron distribution in the system is

$$\nabla^2 n = \frac{W}{D}\frac{\partial n}{\partial x} + \frac{I}{D}\frac{\partial n}{\partial t}$$

where n is the electron density, x is the distance from the first shutter and t is time. Lowke has solved this equation imposing the necessary boundary conditions and has calculated that, if the relative errors due to these diffusion factors combine additively, then the total relative error is $r = \frac{3}{d(W/D)}$

Experiments suggest that the order of magnitude of this factor is correct.[71] The diffusion coefficient D is a function of P, so diffusion errors are lower at high P, and at long d.

Hornbeck's Method. This method was devised by Herreng[72] and developed by Hornbeck[73] for electron drift velocity measurements. In the drift tube are two large, circular, parallel plates - the anode and cathode. A flash of u.v. light produces, at the cathode, an initial pulse of photo-

electrons which then travels to the anode under the influence of a uniform electric field. The anode current pulse is amplified and viewed oscillographically so that a photograph of the pulse may be obtained. Omitting influences due to diffusion, the current travelling in the gap is given by $i = neW/d$ where d is the cathode/anode distance. Thus, as electrons are produced in the chamber the current rises to a constant level which is maintained while the electrons traverse the gap. Then, as they are absorbed at the anode, the current decreases becoming zero when the pulse is completely absorbed. The transit time of the pulse is taken as $t_2 - t_I$ where t_I and t_2 are the times at which the current is half its maximum value. The position of t_I is determined by the rising characteristics of the current pulse. The procedure in determining t_2 is based on the assumption that, when half the electrons have been absorbed, the centre of the pulse is then at the collecting anode. This is not quite true, as the collecting anode distorts the shape of the pulse, but this may be allowed for.[71]

This method has been widely used for electron drift velocity measurements on the common gases and some hydrocarbons.[74-80]

Time of flight Investigations. Hurst[81] et al have recently reported a new method of evaluating W and W/D based on a solution of the time dependent transport equation in one dimensional space. Under suitable conditions the distribution of the time of arrival of electrons at a point on a plane which is L cm from another plane releasing electrons at a time t = 0, is a function of W and D. The geometrical situation is

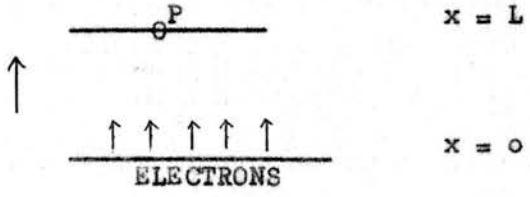

P is an electron detector. Hurst used a Geiger-Mueller tube connected to the collision chamber via a small hole. E(t) is the number of electrons entering the detector in the interval between t and (t+dt).

t_m is the time when an electron is most likely to arrive. Then $W = L/t_m$, and, if t_I is the time at which the function $E(t)$ has the value $e^{-I}E(t_m)$, $\delta t = |t_I - t_m|$, and D is given by the equation

$$D = \frac{L^2 (\delta t)^2}{4t_m^3}$$

The function $E(t)$ is constructed by repeated measurements of the probability that a single electron arrives at P between the time t and $(t + dt)$. Single electrons can be counted on P. Experimentally, a pulsed u.v. lamp generates photo-electrons from x=0 at the time t=0. The time of flight of an individual electron is measured from t=0 to the time when its arrival is recorded at P. The distribution $E(t)$ is stored in an analyser and W and D obtained from it.

Hurst and Co. obtained W and D for electrons in carbon dioxide and ethylene, and the results give reasonable agreement with those obtained by the established methods. The experiment has the disadvantage that P has to be filled with the gas in the collision chamber. This limits the number of gases which may be studied. However, with another method of electron detection it could be extended to give valuable information on electron transport through gases.

Other methods are available for drift velocity measurements at high E/P. This is outwith the region in which we are interested and so they will not be described here. Details of them are given in ref. 3.

1.7 Simplified Analysis of Swarm Data

Early workers made many simplifying assumptions and approximations in analysing swarm data - assumptions which Heylen et al later showed to be justified. Recall the equations:-

$$W = \frac{E\,e}{3mN} \left[\frac{\overline{u^{-2} \frac{d}{du} u^2}}{Q_D} \right] \qquad \text{1.6.11}$$

$$W/D = \frac{E\,e}{m} \left[\frac{\overline{u^{-2}\,\underline{d}\,u^{2}}}{du\,Q_D} \right] \Big/ \left(\overline{u/Q_D} \right) \qquad \text{1.6.14}$$

$$\lambda = \frac{W^2}{u^2} \left[\frac{6}{\overline{uQ_D}\,\overline{u^{-2}\,\underline{d}\,u^{2}}} \right] \qquad \text{1.6.19}$$

Assume that the cross-section does not vary rapidly with electron energy, so that at each E/P (or E/N) Q_D may be replaced by $\overline{Q}_D$, - an average value. Then:-

$$W = \frac{2}{3}\,\frac{E\,e}{m\,N}\,\frac{I}{\overline{Q}_D}\,\overline{u^{-I}} \qquad \text{1.7.1.}$$

$$W/D = \frac{Ee}{m}\,\frac{2}{\bar{u}}\,\overline{u^{-I}} \qquad \text{1.7.2.}$$

$$\lambda = \frac{W^2 10^{-10}}{45.5\,kT}\,\frac{3}{\bar{u}\,\overline{u^{-1}}} \qquad \text{1.7.3.}$$

If the electron velocity distribution is assumed to be Maxwellian, i.e.

$$\frac{dn}{n} = A \exp(-Bu^2)\,u^2 du$$

then the various factors involving the velocity averages may be evaluated from the following table.[62]

$$\overline{u^2}\,\overline{u^{-1}} / \bar{u} = 1.5$$

$$\bar{u}\,\overline{(u^{-1})} = 1.27$$

$$\bar{u}/(\overline{u^2})^{\frac{1}{2}} = 0.85$$

$$\overline{u^{-1}}(\overline{u^2})^{\frac{1}{2}} = 1.38$$

$$(\bar{u})^2/\overline{u^2} = 0.847$$

$$\overline{(u^{-1})} \;/\; (\bar{u})^{\frac{1}{2}}\overline{u^{-2}} = 0.564$$

$$\overline{(u^{-1})}^2/\overline{u^{-2}} = 0.639$$

Random velocities may be replaced by the corresponding k terms.

$$\overline{u^2} = 45.5\ 10^{10} k\ T.$$

(T is the termperature of the gas). Equations 1.7.1, 1.7.2, and 1.7.3 then become:-

$$W = \frac{E}{N}\,\frac{1}{\bar{Q}_D}\,\frac{2.4\ 10^9}{(kT)^{\frac{1}{2}}} \qquad \text{1.7.4}$$

$$W/D = \frac{E\ 11.59\ 10^3}{kT} \qquad \text{1.7.5}$$

$$\lambda = 5.19\ 10^{-12}\frac{W^2}{kT} \qquad \text{1.7.6}$$

Equation 1.7.4. may be rearranged to give $\bar{Q}_D$ in terms of W and k.

$$\bar{Q}_D = \frac{E}{N}\,\frac{1}{W}\,\frac{2.4\ 10^9}{(kT)^{\frac{1}{2}}}\ \text{cm}^2 \qquad \text{1.7.7.}$$

$$= \frac{E/P}{N_o}\,\frac{1}{W(kT)^{\frac{1}{2}}}\,2.4\ 10^9\ \text{cm}^2 \qquad \text{1.7.8.}$$

N_o is the gas density at unit pressure and temperature T°A.

$$N_o = \frac{9.61\ 10^{18}}{T}$$

So, at T°A, $\bar{Q}_D$ in units of πa_o^2 is given by

$$\bar{Q}_D = \frac{E/P}{W} \frac{2.8\ 10^6}{k^{\frac{1}{2}}} (T)^{\frac{1}{2}} \quad \text{—— 1.7.9.}$$

Swarm results obtained by the Townsend School were interpreted using this simplified theory. Healey and Read[4] have tabulated most of the Townsend data. They give as functions of E/P, k, $\bar{u}$, $\bar{W}$, λ and $\bar{L}$ (electron mean free path at unit pressure), for electrons in He, Ar, Ne, H_2, N_2, O_2, air, Cl_2, Br_2, I_2, CO, NO, CO_2, N_2O, H_2O, NH_3, C_5H_{12}, C_2H_4, HCl. We have used the data to calculate $\bar{Q}_D$, the diffusion cross-section for some gases.

At 288° A, the temperature at which these early measurements were made,

$$\bar{Q}_D = \frac{E/P}{W} \frac{4.75\ 10^7}{k^{\frac{1}{2}}} \pi a_o^2 \quad \text{—— 1.7.10.}$$

Also, from equation 1.6.5. the electron energy $\frac{1}{2}m\bar{u}^2$ is related to k as follows:

$$\frac{1}{2}m\overline{u^2} = \frac{3}{2}\ 1.38\ 10^{-16}\ T\ k \text{ ergs}$$

$$= \frac{3}{2}\ 1.38\ 10^{-16}\ 6.2\ 10^{11}\ T\ k \text{ eV}$$

$$= 12.5\ 10^{-5}\ T\ k \text{ eV} \quad \text{———————} \quad 1.7.11.$$

At 288°A the electron energy in e V is given by

$$eV = 3.69\ 10^{-2}\ k$$

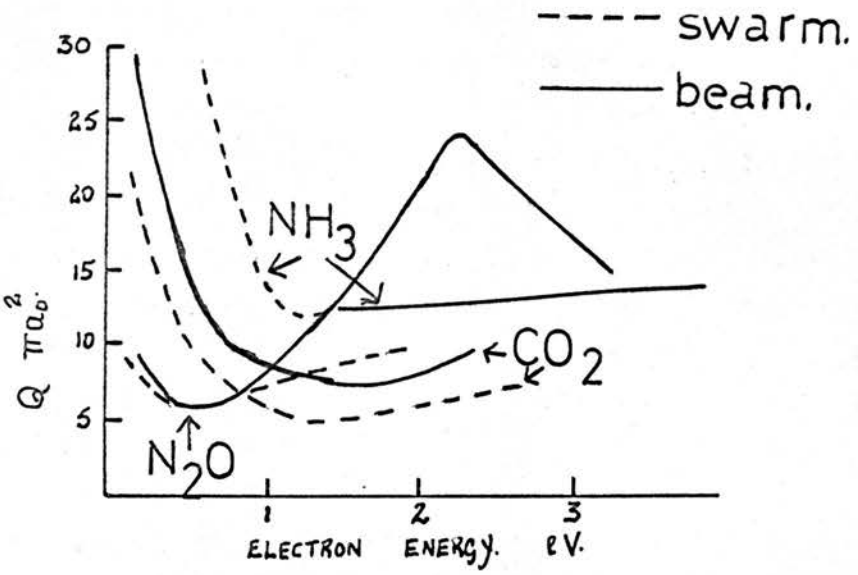

Fig.1.7.1.- Collision Cross-Sections.

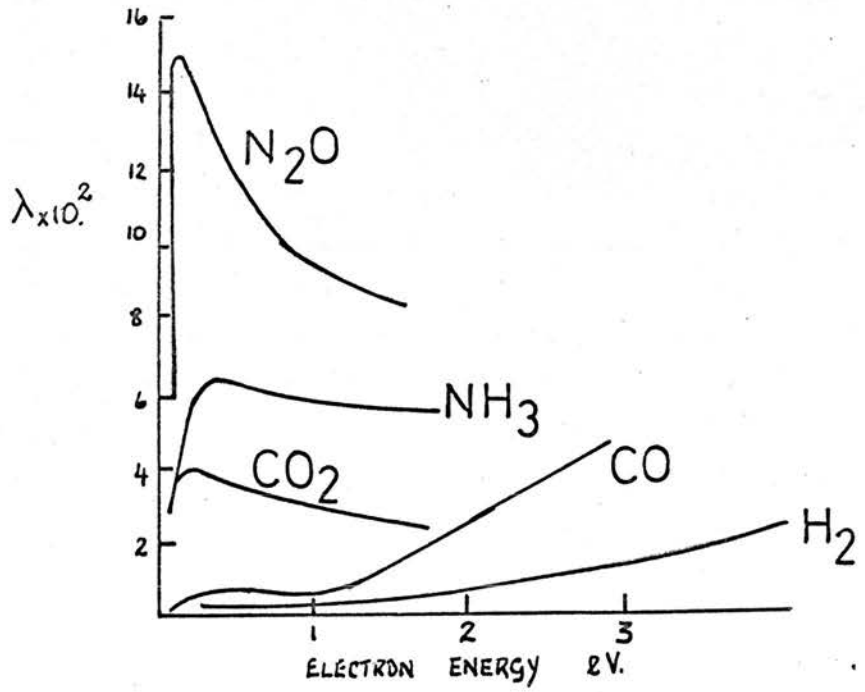

Fig.1.7.2.- Electron Energy Losses.

The calculated Q_D values are plotted as a function of electron energy in fig. 1.7.1. where they are compared with corresponding Ramsauer values, Q_R. Q_D and Q_R compare favourably in most cases, if allowance is made for the averaging involved in the evaluation of Q_D. This agreement seems to indicate that the simple theory may be successfully applied, at least to some molecules, and that λ values calculated using equation 1.7.6. may also be meaningful. Some such λ values are plotted in fig. 1.7.2. While λ approximates to the elastic value, m/M, in the inerts, in polyatomic molecules it may be quite high, indicating that a substantial proportion of the low energy impacts are inelastic. This may partly involve rotational excitation which, we have pointed out, is known to take place. However, the fact that, in some cases, λ tends to show a maximum in the vibrational energy region, is evidence favouring vibrational excitation.

1.8. Electron Velocity Distribution.

In order for accurate analysis of swarm data to be made, it is necessary that the form of the electron velocity distribution in each system studied, be known. (equations 1.6.11 etc.), and much work has been done on this problem.

At very low E/P. electrons and molecules are in thermal equilibrium and so the electron velocity is known to be Maxwellian. As E/P increases this distribution is distorted by variations in Q and by the onset of inelastic impacts. This means that the distribution function varies not only from system to system, but also within any system, as the electron energy changes. Druyvesteyn, one of the most successful early workers, studied the simplest system of:- (1) low electron densities, (2) elastic impacts only, (3) constant collision cross-section. He obtained the expression:

$$\frac{dn}{n} = A \exp.(-B\, u^4)\, u^2 du$$

now commonly known as the Druyvesteyn distribution. This compares with the Maxwellian form

$$\frac{dn}{n} = A \exp(-B u^2) u^2 du$$

Druyvesteyn's approach to the calculation was based on one used by Herz. Subsequently, Morse[84] and al reproduced the Druyvesteyn distribution using a Boltzmann approach and it is this one which has been developed to allow for inelastic impacts and varying cross-section. It involves detailed energy balancing, i.e. the number of electrons per second brought into an energy element $d\epsilon$ at ϵ and the number leaving in the same time are equated. All possible processes in which electrons gain or lose energy are considered. If the distribution function for any particular system at any energy is to be characterised, one must know the cross-sections of all the processes, elastic and inelastic, which occur. At low E/P in the inerts, inelastic impacts do not occur and so the influence of different cross-section behaviour on the distribution function may be studied. He, Ne, and Ar are particularly suitable. The cross-section of He is more or less constant at low energies; that of Ne decreases as electron energy decreases; while the Ar cross-section increases rapidly with decreasing energy. Allen[85] has calculated distribution functions in these gases, at low E/P, using Ramsauer cross-sections. More recently, Heylen and Lewis[86] have looked at velocity distribution in the inerts. They used a different approach, based on that of Smit.[87] In this one equates the number of electrons per second in a given unit volume moving upwards through the energy region and the number moving downwards, all processes being considered.

In a molecular system, the Boltzmann equation for the electron energy distribution is[88,89]

$$\frac{d}{d\epsilon}\left(\frac{e^2E^2}{3NQ_D}\frac{df}{d\epsilon}\right) + \frac{2m}{M}\frac{d}{d\epsilon}\left(\epsilon^2 N Q_D\left[f + KT\frac{df}{d\epsilon}\right]\right)$$

$$+ \sum_j \left[(\epsilon+\epsilon_j)f(\epsilon+\epsilon_j)NQ_j(\epsilon+\epsilon_j) - \epsilon f(\epsilon)NQ_j(\epsilon)\right]$$

$$+ \sum_j \left[(\epsilon-\epsilon_j)f(\epsilon-\epsilon_j)NQ_{-j}(\epsilon-\epsilon_j) - \epsilon f(\epsilon)\,NQ_{-j}(\epsilon)\right] = 0 \quad -1.8.1.$$

$\epsilon = \frac{1}{2}mu^2$

Q_j = the cross-section for excitation to the jth level.

Q_{-j} = the cross-section for de-excitation of the jth level.

This equation is very difficult to solve, even for simple molecules. Heylen and Lewis[90,91] have obtained information of the velocity distribution in molecular gases by making use of the relations between the distribution and the transport quantities given in equations 1.6.11 et seq. A cross-section of the form $Q = Q_o u^n \exp(-Ku)$ is assumed where n and K may be chosen to fit measured cross-sections, Drift velocity etc. calculated using different distribution functions. They found that, in the simple gases H_2, N_2, and O_2, calculated and experimental values agree most closely for a Maxwellian distribution. In addition, Heylen[92] has considered the influence of cross-section variation and velocity distribution on the transport quantities and has found that, provided the cross-section does not vary rapidly with electron energy or that the variation is linear, then the measured W and W/D are not particularly sensitive to these factors. But, if the cross-section is changing sharply with electron energy - as it does in the region of a Ramsauer-Townsend minimum - then W and W/D are sensitive to the form of the electron velocity distribution. An important consequence of this arises in the use of equation 1.6.17. relating W/D to k. In most cases a Maxwellian distribution may be safely assumed, as, in fact, was done by

early workers. But, if the Maxwellian distribution is assumed while W/D is distribution sensitive, the k values deduced are grossly in error.

1.9. More Advanced Swarm Analysis.

Heylen's work is of value in that it has justified the approximations made by early workers in interpreting swarm data, while at the same time emphasising the limits to which these approximations may be taken. Recently, Phelps and Co. have produced more sophisticated analyses of swarm results. At low E/P. where electrons and molecules are in thermal equilibrium, and where only rotational excitation is energetically possible, electron velocity distribution is Maxwellian.[67] Equation 1.6.11 for drift velocity may be rewritten:

$$W = \left(\frac{W}{E}\frac{N}{N}\right)\left(\frac{E}{N}\right)\frac{4}{3}\frac{e}{m}\int_0^\infty f_o \frac{d}{du}\left(\frac{u^3 N}{N Q_D u}\right) du$$

$$= \mu N\left(\frac{E}{N}\right)\frac{4}{3}\frac{e}{m}\int f_o \frac{d}{du}\left(\frac{u^3 N}{\nu}\right) du \qquad \text{1.9.1.}$$

μ is the electron mobility and ν the frequency of momentum transfer collisions. For a Maxwellian distribution:-

$$f_o = \left(\frac{m}{2\pi kT}\right)^{3/2} \exp.\left(\frac{-mu^2}{2kT}\right)$$

(here k is Boltzmann's constant)

Phelps and Co. assumed a power series representation of

$$\frac{N}{} = (Q_D u)^{-1} \qquad \text{1.9.2.}$$

$$= \sum b_j u^{-j}$$

Combining equations 1.9.2. and 1.9.1. we have:-

$$\mu N = \frac{e}{m} \sum \frac{(3/2 - j/2)!}{(3/2)!} \; b_j \left(\frac{2KT}{m}\right)^{-j/2}$$

$$= \sum B_j \left(\frac{2KT}{m}\right)^{-j/2} \qquad \text{1.9.3.}$$

From 1.9.3. and 1.9.2.

$$Q_D^{-1} = \sum b_j u^{1-j} = \frac{m}{e} \sum \frac{(3/2)!}{(3/2 - j/2)!} B_j u^{1-j} \qquad \text{1.9.4.}$$

For a cross-section which is energy invariant $j = +1$ only need be considered and in this case μN varies as $\left(\frac{2kT}{m}\right)^{-\frac{1}{2}}$. Phelps and Co. measured W at several different gas temperatures. They were thus able to choose a reasonable set of j values for each gas and to find the coefficients b_j from experimental data. These were then substituted in equation 1.9.4. to give cross-sections. Calculations were made for the following gases:[67,68].

Helium, neon, argon, krypton xenon, deuterium, carbon monoxide,

carbon dioxide, water vapour, nitrous oxide, and ammonia. In the case of Ar, drift velocities at two temperatures only were available and only a two term power series expansion in μN could be evaluated. It was found that three possible series fitted the data, giving three different cross-sections. Similarly, three different cross-sections were obtained for krypton and xenon.

This type of analysis is, of course, applicable only to very low energy regions where inelastic processes are unimportant. At higher energies, they make use of the Boltzmann equation as given in equation 1.8.1. [94,95,96,97]. They take a trial set of collision cross-sections for all the processes, elastic and inelastic, that are likely to occur in the particular energy region considered. These cross-sections are deduced from experiments or theoretical considerations etc. The equation is then solved for f(u) and measurable quantities like, W, W/D,

are calculated using equations 1.6.11 and 1.6.14 etc. Experimental and calculated data are compared and the input cross-sections tailored until theoretical and experimental agree. This method provides a set of cross-sections consistent with experimental data but not unique. H_2,[94] D_2,[94] N_2, Ar,[95] He, Ne, Kr, Xe[97] have been analysed in this way. The final momentum transfer cross-sections agree fairly well with those measured by the Ramsauer method and those deduced from simple swarm theory. In addition, in the diatomics studied, rotational and vibrational excitation must be assumed in order to reproduce experimental data. In N_2 the cross-section for vibrational excitation has a threshold in the region of one vibrational quantum and, in the energy region where they overlap, the agreement with the measured value of Schulz is reasonable.

1.10. Excitation Mechanisms.

(a) Rotational Excitation. As we have pointed out the mechanism of rotational excitation is well understood. If an electron is to rotationally excite a molecule, two conditions must be fulfilled. The electron must have sufficient energy, and it must have angular momentum about the scattering molecule that at least equals the increase in angular momentum of the molecule accompanying the excitation. Consider this latter requirement. To have even unit angular momentum about the scattering molecule, a slow electron must have a high impact parameter. [section 1.4(a)] . In many cases the impact paremeter may be too high for there to be any interaction between the electron and the molecule. However, electron/dipole and electron/quadrupole interactions are long range. Therefore, a polar molecule may be able to interact with an electron having the necessary angular momentum, sufficiently strongly for excitation to take place. In fact, calculations show that rotational excitation cross-sections for polar molecules may be quite high. Massey showed this to be so for HCl.[98] More recently,[99,100] Gerjuoy and Stein have applied the Born approximation to the problem and calculated λ values for slow electrons scattered from quadrupolar molecules, with rotational excitation of the molecule. (In this case, electrons which contribute to the cross-

section are necessarily far from the molecule and therefore only slightly distorted by it. Thus, the Born approximation which holds only if the incoming wave is slightly distorted by the scattering molecule, may be applied.) Gerjuoy and Stein did calculations on N_2 and H_2 and their results agree fairly with the experimental values. [Phelps and Co. used rotational cross-sections of Gerjuoy and Stein in their analysis of swarm data of H_2 and N_2 (section 1.9)].

Carson[101] and Morse[102] have also applied the Born approximation to the rotational excitation of H_2, but they both neglected the electron/quadrupole interactions in their calculations. They considered only the interaction due to the difference in phase of the incident wave between the two nuclei. Their cross-sections were much too low to account for the observed transport quantities.

(b) Vibrational Excitation The Laws of Conservation of Energy and Momentum show that 'direct' vibrational excitation of a molecule cannot be effected by a slow electron. Apart from the 'resonance' excitation which has been observed in electron beam experiments, both beam and swarm experiments indicate that vibrational excitation does take place in the vibrational energy region. So far, no mechanism has been offered to explain it. Massey,[104] Morse[102] and Carson[101] have all applied the Born approximation to electron scattering by hydrogen with vibrational excitation. They assumed that the only electron/molecule interaction is that due to the difference in phase of the incident electron wave between the two nuclei, and all their cross-sections are much too low to account for the observed swarm behaviour.

Wu[105] tried a different approach to the problem. He assumed that the molecule interacts with the electron through the oscillating electric moment arising from the vibration of the molecule. For the optically active vibration of H_2, he calculated the cross-section for electrons of a few electron volts to be $5.7\ 10^{-3}\ \pi a_o^2$. This is of the same order of magnitude as Carson's values.

1.11. Present Study

The first step in any chemical change is the excitation of molecular vibrations, so any process by which energy is efficiently transferred into

vibrational degrees of freedom is of particular interest to the chemist. This present study was undertaken, therefore, with a view to determining whether or not slow electrons do excite molecular vibrations 'directly'. We chose to study this by an electron swarm experiment, viz. the measurement of electron drift velocities in a number of polyatomic gases by the Electron Shutter Method (section 1.6). A swarm experiment was preferred to a beam experiment for reasons already mentioned, viz. swarm techniques are, experimentally, the simpler and they can be applied to low energy regions where the electron beam is not reliable. Although the final analysis of swarm data is complex, the Electron Shutter provides a means for measuring average drift velocities directly. Electron drift velocities through any gas depend on the number and nature of the electron/molecule impacts occurring, and we hoped, by observing drift velocity patterns in a variety of gases, to get information - albeit qualitative - on the nature of the interactions that take place when slow electrons collide with gas molecules.

II. EXPERIMENTAL.

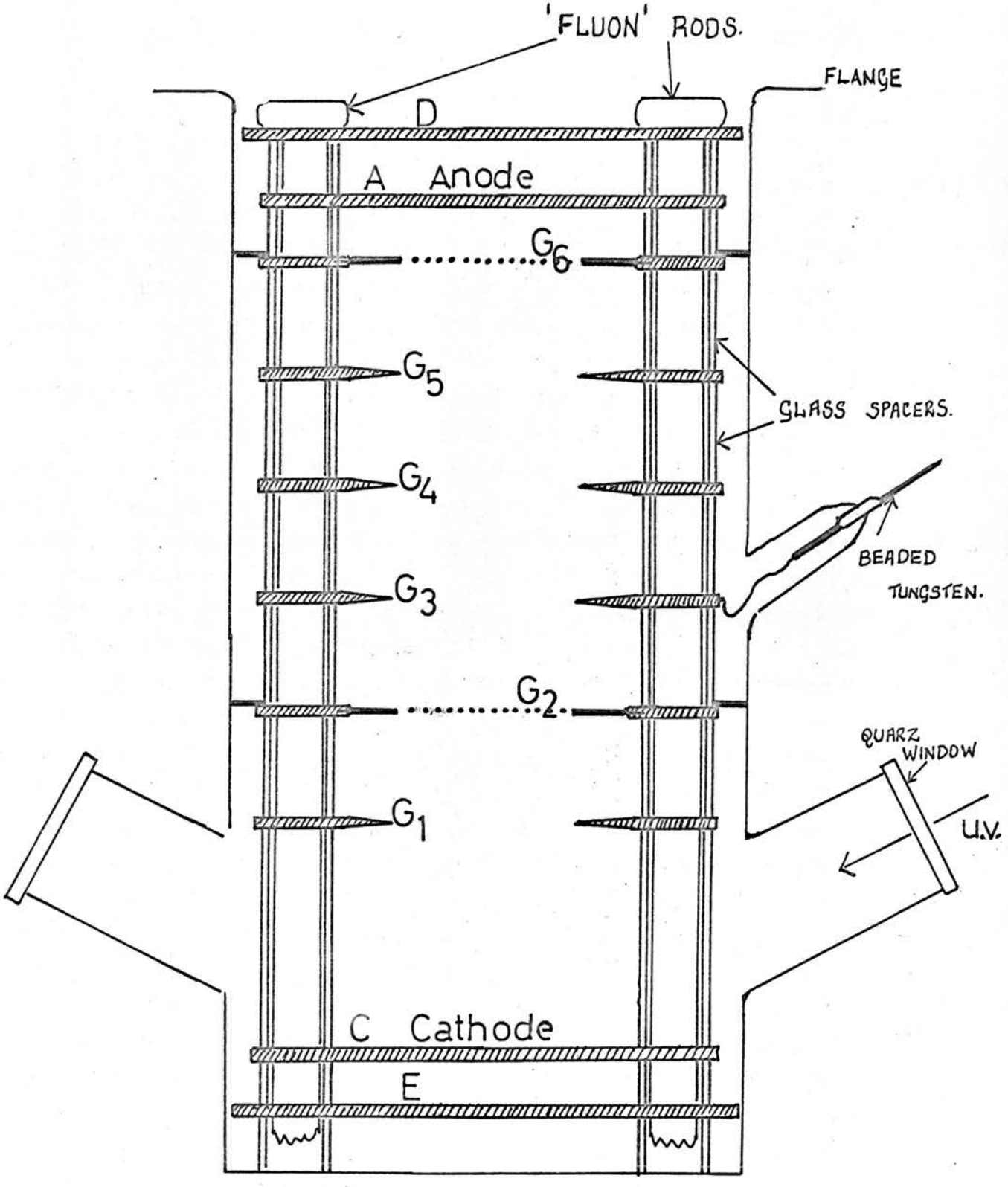

Fig II.1.1.

Drift Tube.

II. EXPERIMENTAL

II. 1. Apparatus.

The cell in which the present measurements were made is shown in fig. II.1.1.

C is a photocathode. A filament - the other possible electron source - was considered unsatisfactory, because of possible decomposition of gases on the hot filament, and because of temperature gradients which might be set up in the tube by the hot filament. The use of photoelectrons does limit the choice of gases to those that are transparent to the u.v. light, which ejects the electrons from the cathode. In this case the u.v. source was a mercury vapour lamp. The electrons were pulled upwards by a d.c. electric field maintained uniform by a series of guard rings, G_1, G_3, G_4, G_5, and collected at the anode A. All the electrodes were fashioned from brass and were nickel plated and then gold plated. The cathode was highly polished. Precision bore pyrex glass tubing was accurately ground to make spacers between the guard rings. Pyrex glass was chosen because of the necessity of a very high insulation resistance between anode and cathode $\doteqdot 10^{15}\,\Omega$. The loose fitting 'Fluon' supports inserted through the spacers down the complete length of the tube (fig.11.13.(a)) served only to aid construction as did the two gold-plated discs D and E. The electron shutters G_2 and G_6 were made by stringing fine gold wire 0.004 in. diameter, 1.5 mm apart on mica frames. In each case, the mica was held between two thin metal plates which were maintained at the appropriate potential with respect to cathode. The electrical leads attached to the guard rings, anode, and cathode are shown in fig. II.13.(b). Gold-plated platinum wire was hard-soldered to tungsten to which a glass bead had been attached. This platinum was then rivetted to the electrode with a gold-plate rivet. The electrode assembly was contained in a pyrex glass envelope which was made up in two sections. The lower section had several narrow side-arms on it, positioned so that one side-arm was level with each electrode. Construction was carried out as follows: The inner assembly - electrodes, spacers, and teflon supports - was built up in an inverted position.

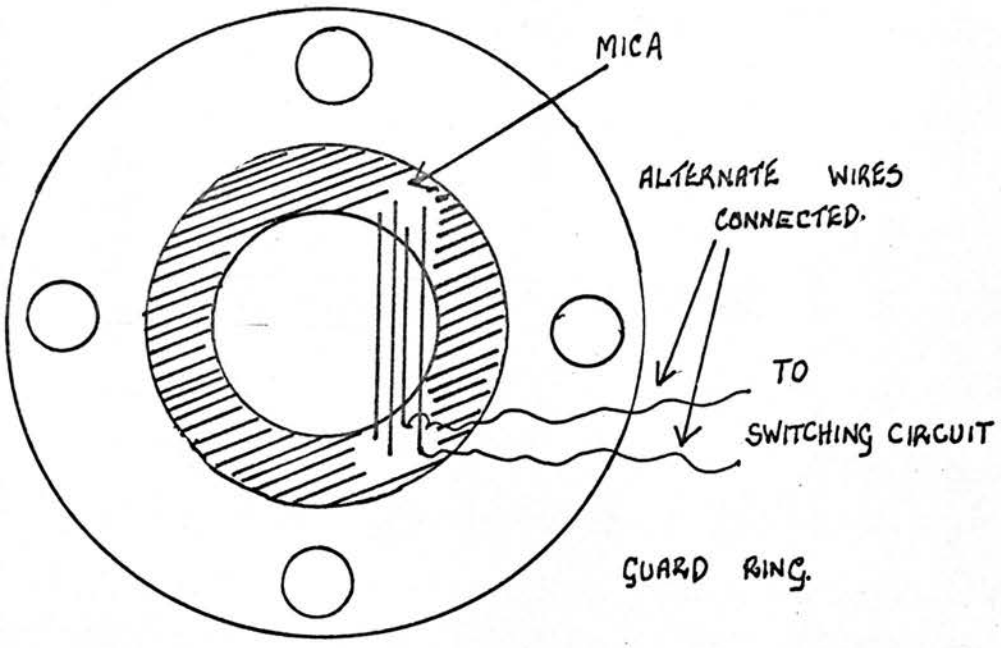

Fig. III.2.

Electron Shutters - G_2, G_6 -

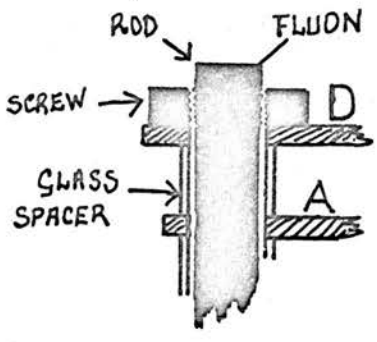

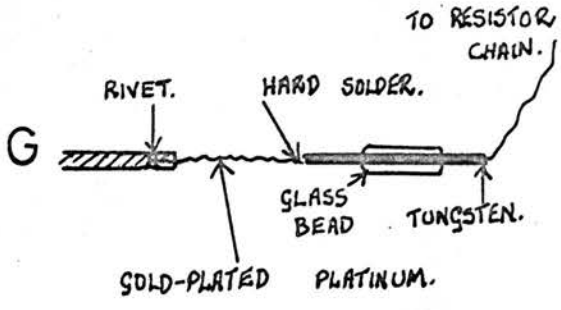

Fig III.3.

(a) Fluon Supports

(b) Electrical Leads

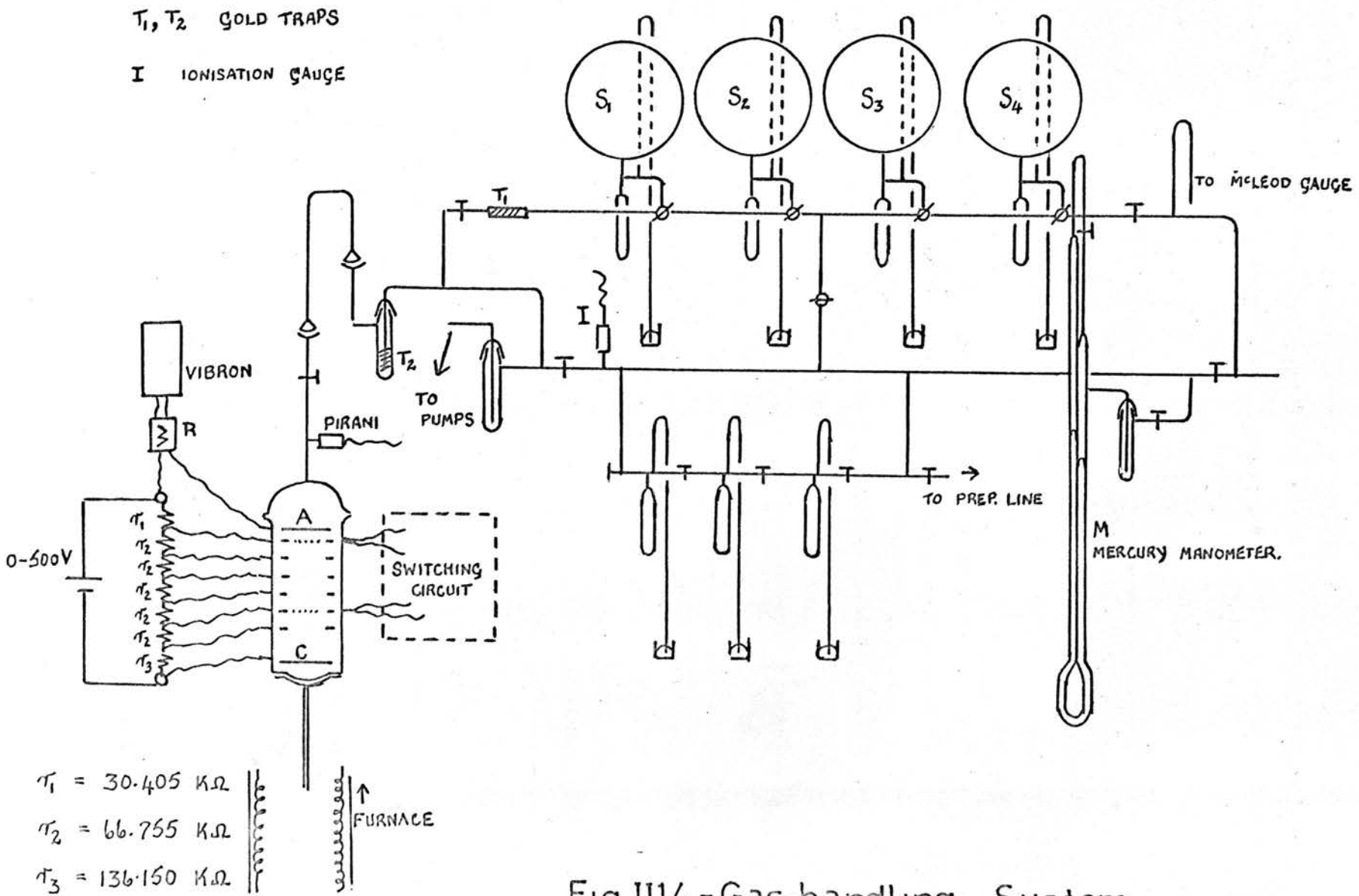

Fig. II.1.4.- Gas-handling System.

The lower portion of the envelope was slipped over it, the electrical leads being fed through their appropriate side-arms. The whole was re-inverted and the tungsten leads sealed to the sidearms. In the case of the shutters, three leads - one from each wire and one from the guard ring were taken through one side-arm. The lid of the envelope was then cemented on with a heat-resistant 'Araldite' cement. The u.v. beam was admitted through a quarz window, also cemented on with this 'Araldite'. A quarz lens focussed the beam on to the cathode. A second quarz window allowed scattered light to be reflected out of the cell.

The d.c. voltage between anode and cathode was obtained from a 0 - 500 V Solartron Power Supply. This was continuously monitored by a voltmeter. Guard ring voltages were tapped from a resistor chain of precision wire-wound resistors, correct to $\frac{1}{2}\%$. The anode current was measured on a 33B Vibron Electrometer in conjunction with a high resistance (10^8, $10^{10}\Omega$) .

Fig.II.1.4 shows the drift-tube and gas-handling system. The gas-line and cell were evacuated by a mercury diffusion pump, backed by an oil pump. When the cell was in position, a furnace could be raised up around it. The temperature of bake-out was limited to not higher than 200°C, by the 'Araldite'. After baking for ~ 10 hours, an ultimate pressure of 7.5×10^{-6} Torr as measured on the ionisation gauge I was reached. Working pressures were measured on the mercury manometer M situated at some distance from the cell and separated from it by a cold trap. This manometer was constructed of precision bore tubing, 10 mm internal diameter, and the mercury levels were measured with a travelling microscope. The gases were stored over mercury in the storage globes S_1, S_2, S_3, S_4, and before being admitted to the cell were passed slowly through the gold trap T_1. T_1 was a tightly rolled gold-plated platinum foil placed between two capillarly constrictions in the line. A second gold-plated foil T_2 was at the entrance to the drift tube.

The switching circuit, applying a square wave of variable frequency and amplitude to the wires of G_2 and G_6 is shown in fig.II.1.5.

Fig II.1.5. Grid Switching Circuit

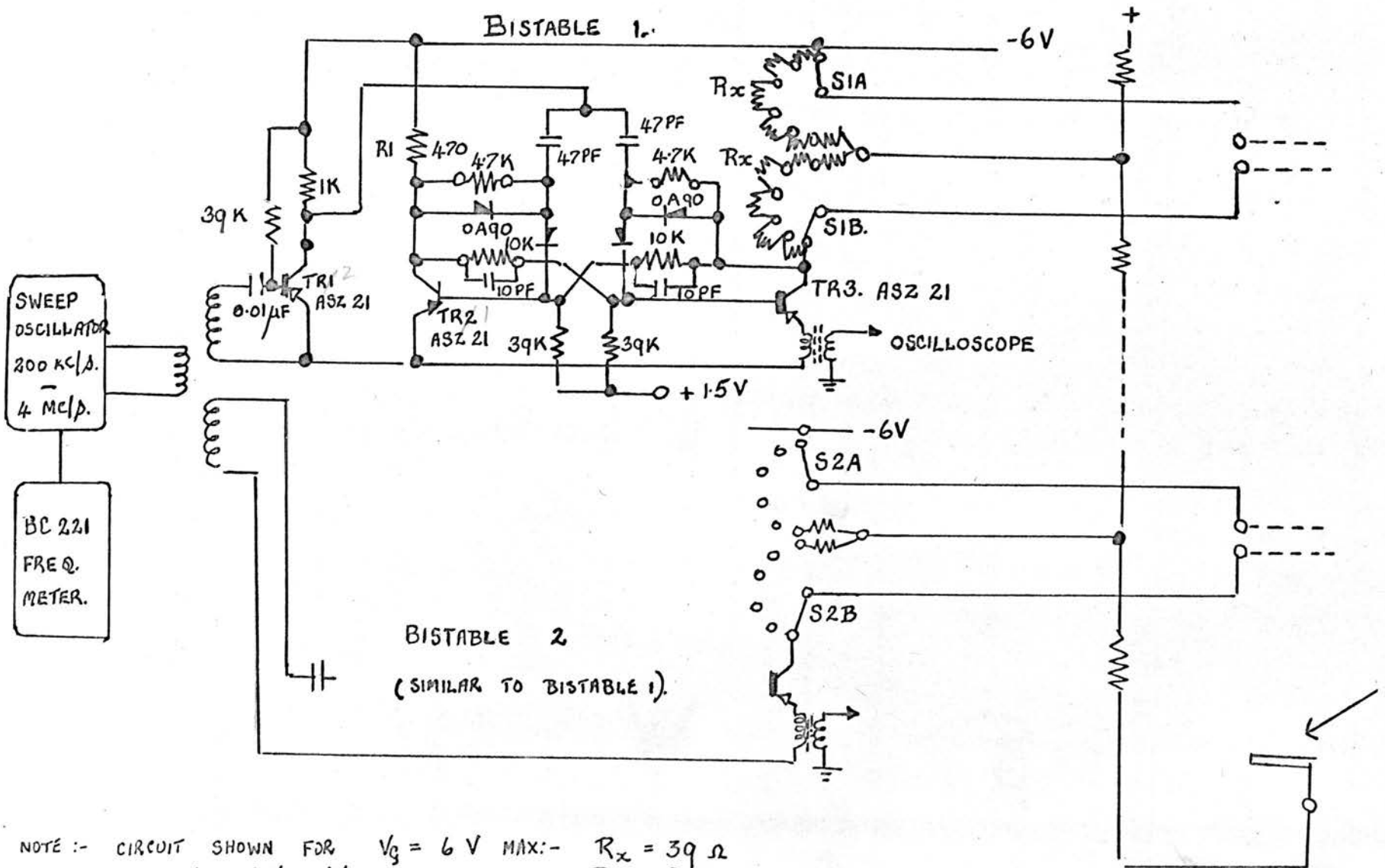

NOTE :- CIRCUIT SHOWN FOR V_G = 6 V MAX:- R_x = 39 Ω
FOR V_G = 12 V MAX :- R_x = 82 Ω
TR_1 & TR_2 = 2 EACH ASZ 21'S IN PARALLEL.
R_1 = 1 KΩ
MAIN SUPPLIES = 12 V.

An oscillator driven by a variable speed motor provided a stabilised output of 0.5 V over a frequency range of 200 kc/s to 4 mc/s. The oscillator output was fed to a wide-band transformer which drove two similar bistable circuits each supplied by its own isolated battery. Tr 1 acted as a clipping amplifier driving the bistable formed by Tr2 and Tr 3, dividing the input by two, and providing a square wave across the collector load of Tr 3 at a frequency of 100 kc/s to 2 mc/s. The maximum amplitude of this square wave was 6 V nominal, but it could be reduced in steps of 1 V to give a range of 1 - 6 V, by means of switches S 1 and S 2. The centre point of the collector loads of Tr3 was connected to the drift tube divider chain to maintain the grids at the correct potential with respect to cathode. Small pulse transformers in the emitters of Tr3 provided monitors to ensure that the two wave trains were in correct phase as observed on an oscilloscope. Phasing could be set by momentarily disconnecting and reconnecting the input. The circuit could be modified to give switching up to 12 V in 2 V steps as noted on fig.II.1.5.

Some of the cell dimensions and the nomenclature used are given below.

Anode - cathode distance	$h = 15.04 \pm 0.02$ cm.
Drift distance G_2 - G_6	$d = 8.02 \pm 0.02$ cm.
Anode volts	$V_A = 0 - 500$ V.
Amplitude of switching voltage	$V_G = 0 - 12$ V.
Frequency of switching	$f = 100\ kcs^{-1} - 2\ mcs^{-1}$.
Electrometer signal	$S =$
Electrometer signal when G_2 and G_6 are at field potential	$S_o = 10^{-10} - 10^{-12}$ A.
Electrometer signal with G_2 and G_6 'closed	S_C
Grid efficiency	$\phi = (S_o - S_C)/S_o$

Experimental measurements were made as follows. With the gas in the cell at the appropriate E/P, S_o was noted. The effiency of each shutter was then obtained for a number of sideways voltages V_G, and the minimum

voltage to give 95 - 100% grid efficiency at that E/P was chosen as the working V_G. With this V_G (in any run, V_G was the same for G_2 and G_6), a quick scan of the frequency range gave the approximate positions of the anode maxima. Each peak was then slowly scanned. The motor drive was reversible allowing a peak to be approached from the high frequency or low frequency end. The oscillator was stopped 'on' a current maximum. A frequency meter, connected to the oscillator was then tuned to this frequency of maximum current f_o and the peak again slowly scanned to check that the frequency meter 'blip' and the current maximum coincided. If not, the frequency meter was adjusted until 'blip' and maximum did coincide and f_o read correct to $\frac{1}{2}\%$ from the frequency meter. The value of f_o located in this way depended on whether the peak was approached from the high frequency or low frequency side. However, by plotting graphically anode signal v oscillator frequency it was verified that

$$f_o = \frac{f_o(\text{from below}) + f_o(\text{from above})}{2}$$

This method of locating current maxima (by stopping the oscillator on the peak) eliminated errors due to random fluctuations of the electrometer and f_o could be located to $\pm$ 0.01 mc/s.

When drift velocities were very low, the position of the first current maximum [corresponding to n = 1 in the equation $W = \frac{d f_o}{n}$] lay below the lower limit of the oscillator, i.e. at less than 0.2 mc/s. In such cases, several subsidiary maxima were located (corresponding to n = 2,3,4,.....) and the position of the fundamental estimated from them. As several peaks could be positioned, there was never any doubt about the frequency of the first maximum. For example:-

GAS	E/P		Frequencies of Current Maxima.					
CH_3Cl	2.5		0.363,	0.423,	0.483,	0.543,	0.610	mc/s.
		n =	6	7	8	9	10	
fundamental			0.0605,	0.0604,	0.0604,	0.0603,	0.0610	mc/s

II.2. Materials

Drift velocities were measured as a function of E/P in CH_4, CD_4, SiH_4, SiD_4, C_2H_6, C_3H_8, C_2H_4, C_2H_2, C_2D_2, CH_3Cl, AsH_3, AsD_3 CH_3COCH_3, CH_3OCH_3, C_2H_5OH.

Methane. Although all reported electron drift velocities in CH_4 were high at low E/P, no two concordant sets of results appeared in the literature. As the differences could have been due to impurity effects, several samples of CH_4 were used.

Sample 1(a). A stream of commercial CH_4 was passed through P_2O_5 and part of the stream condensed in a liquid N_2 trap. The supernatant vapour was pumped away; the condensed gas was vapourised, recondensed, and pumped several times.

Sample 1(b). Gas 1(a) was distilled several times through P_2O_5.

Sample 1(c). Gas 1(b) was fractionally distilled in a Clusius-Riccobini[106] low temperature distillation column. The column used has been previously described.[110] This distillation is believed to be one of the most efficient means of purifying CH_4. The final sample had a v.p. of 10.0 Torr in liquid N_2 (lit. 10.00 Torr), and 83.1 Torr in liquid O_2 (lit. 83.0 Torr).

Sample 2. High purity CH_4 was supplied by 20th Century Electronics Ltd., who quoted a minimum purity of 99%.

Tetradeuteromethane. High purity CD_4 was supplied by 20th Century Electronics Ltd. - minimum purity quoted 99 atoms % D

Silane. The sample used has been previously described.[107] It was prepared by the reduction of $SiCl_4$ with $LiALH_4$. The molecular weight, as determined by the method of limiting densities was 32.05 $\pm$ 0.04 (theoretical 32.12). Infra-red analysis showed no detectable impurities.

Tetradeuterosilane. The sample used has been previously described.[107] It was prepared by the reduction of $SiCl_4$ with $LiAlD_4$. The molecular weight was 36.07 $\pm$ 0.04 (theoretical 36.15) Infra-red analysis showed less than 0.5% SiH_4 to be present.

Ethane. Cylinder ethane was bubbled slowly through a purification train of fuming H_2SO_4, KOH, and P_2O_5. The acid removed C_2H_4, the major

impurity. The stream of gas was condensed in a liquid N_2 trap, and then fractionated. The lowest boiling fraction was retained and the fractionation repeated, until only trace quantities of C_2H_4 showed up as a barely detectable peak at 950 cm^{-1} in the infra-red spectrum. Further purification failed to remove this.

Propane. A sample was supplied by the Matheson Co. Inc. Gas chromatographic analysis showed less than 0.3% impurities.

Ethylene.

Sample 1. Cylinder ethylene was distilled from liquid N_2 and passed through P_2O_5. Only the middle portion was retained, and the process repeated several times. Infra-red analysis showed no detectable impurities.

Sample 2. Sample 1 was distilled over sputtered sodium, to remove traces of O_2 or H_2O.[108]

Acetylene. Cylinder acetylene was passed slowly through a purification train of strong $NaHSO_3$ solution, aqueous NaOH, aqueous chromic acid, alkaline hydrosulphite, $CaCl_2$, and P_2O_5. The gas was condensed in liquid N_2 and distilled several times over P_2O_5, the middle portion being retained in each case. Infra-red analysis showed no detectable impurities.

Dideuteroacetylene. This sample was prepared by the reaction of D_2O and CaC_2. The evolved gas was distilled over P_2O_5. Infra-red analysis showed no detectable impurities.

Methyl Chloride. Cylinder methyl chloride was passed slowly through a purification train of conc. H_2SO_4, NaOH, and P_2O_5. The acid removed all traces of dimethylether, the major impurity. Infra-red analysis showed no detectable impurities.

Arsine. The sample used has been previously described.[109] It was prepared by dropping H_2O on to freshly prepared calcium arsenide. Infra-red analysis showed no detectable impurities.

Trideuteroarsine. The sample has been previously described.[109] It was prepared from D_2O and calcium arsenide. Infra-red analysis showed an absorption band at 2136 cm^{-1} which has been ascribed to traces of AsH_3.

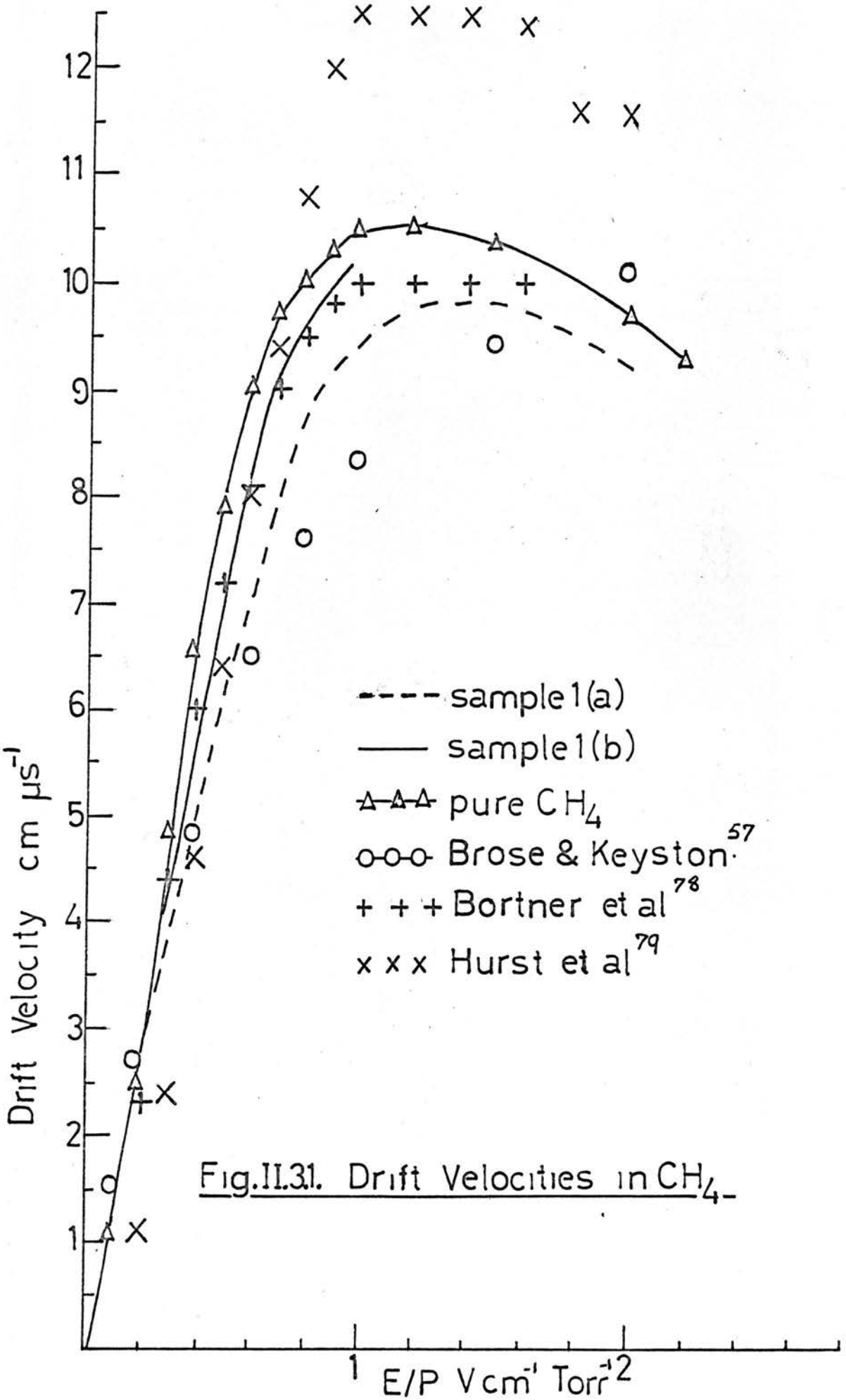

Fig.II.31. Drift Velocities in CH_4.

Acetone. 'Analar' acetone was used.

Dimethylether. High purity ether was supplied by the Matheson Co. Inc.

Ethanol 'Analar' ethanol was used.

II.3. Results.

The apparatus was calibrated with N_2. Drift velocities in N_2 agreed with those of Bradbury and Nielson within the limits of experimental error. The results are compared below.

Drift Velocities in N_2.

E/P	W		cm us^{-1}
	present	Bradbury and Nielson	
0.49	0.52	0.52	
0.58	0.57	0.57	
0.67	0.62	0.62	
0.81	0.70	0.70	
1.16	0.90	0.88	
1.34	0.95	0.95	
2.0	1.21	1.29	
V cm^{-1} $Torr^{-1}$			

Methane. Drift velocities in the high purity CH_4 samples 1(c) and 2 are tabulated in table II.3.1. The estimated experimental error is $\pm$0.2cm us^{-1} (section II.5.) and drift velocities in the two samples agree to within these limits. The resultant 'best' values are plotted against E/P in fig. II.3.1. and fig. II.3.2. In fig. II.3.1. they are compared with results for samples 1(a) and 1(b) and with those obtained by other workers.[57,78,79] In fig. II.3.3 is given a typical graph of anode current

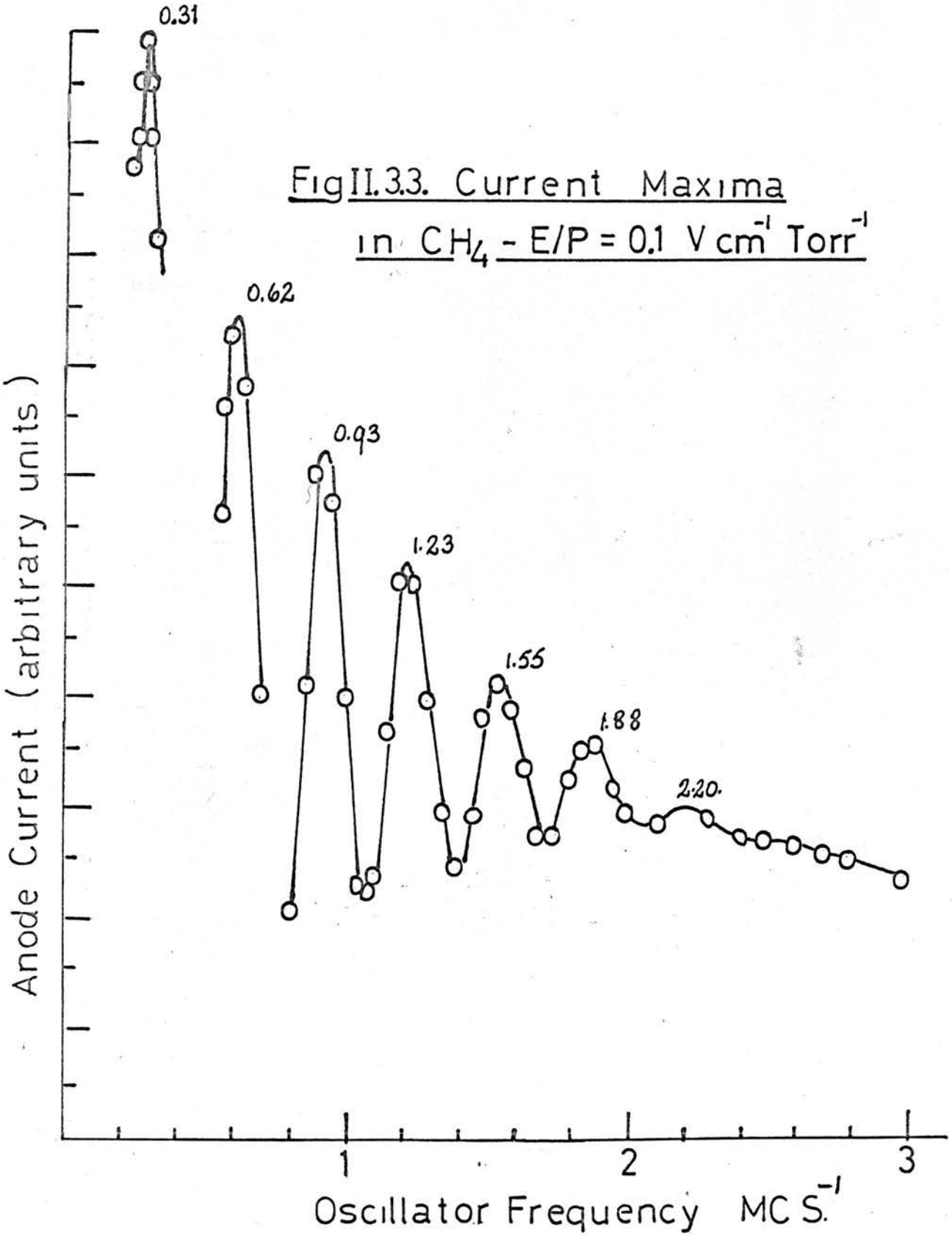

Fig II.3.3. Current Maxima in CH_4 - E/P = 0.1 V cm^{-1} $Torr^{-1}$

versus switching frequency, obtained for electrons in CH_4 at $E/P = 0.1$ V cm^{-1} $Torr^{-1}$. Seven maxima are defined, corresponding to $n = 1 - 7$ in the equation $W = df_o/n$.

Tetradeuteromethane. Results are tabulated in table II.3.2. and experimental points are given in fig. II.3.2. Estimated experimental error = $\pm$ 0.2 cm μs^{-1}

Silane. Results are tabulate in table II.4.3. and experimental points are given in fig. II.3.2. Estimated error = $\pm$ 0.2 cm μs^{-1}

Tetradeuterosilane. Results are tabulated in table II.3.4 and experimental points given in fig. II.3.2. Estimated error = $\pm$ 0.2 cm μs^{-1}

Ethane. Results are tabulated in table II.3.5 and experimental points given in fig. II.3.4. Estimated error = $\pm$ 0.2 cm μs^{-1}

Propane. Results are tabulated in table II.3.6 and experimental points given in fig. II.3.4. Estimated error = $\pm$ 0.2 cm μs^{-1}

Ethylene. Results for samples 1 and 2 are tabulated in table II.3.7. and experimental points given in fig. II.3.5. Although the drift velocities in the two samples agree to within the limits of experimental error, it was found necessary to subject sample (1) to further purification because of anomolous grid behaviour observed in it. Let S^6 square denote the electrometer signal when a square wave is applied to G_6 alone, G_2 being at field potential, S^2 square is similarly defined. Normally S square will be $\geqslant \frac{1}{2}S_o$ depending on grid efficiency. However, at low E/P and pressures greater than a few Torr, S squ. $< \frac{1}{2}S_o$ in sample (1), approaching zero in some cases; i.e. current carriers were not being transmitted through the 'open' grids. The effect was always more marked at G_6

Table II.3.16

GAS	P	E/P	V_G	S_o	S^6 square	S^2 square
C_2H_4 (1)	5.26	1.0	6	540	30	90
			5		80	120
			4		200	200
			3		340	

In this case, current maxima were detected when the shutters were operated together, but the peak heights were very low. Below, in table II.3.17. are given the heights of the peaks above background current for different V_G

Table II.3.17.

E/P	V_G	Peak height mV	Background Current mV
1.0	6	14	4
	5	12	15
	4	11	60

Peak height remained almost constant on a varying background. In each case f_o corresponded to the expected drift velocity.

This anomolous behaviour was observed only to a slight extent in sample (2) at E/P = 0.1 and P > 20 Torr.

Acetylene. Results are tabulated in table II.3.7. and experimental points given in fig. II.3.5. Estimated error = $\pm$ 0.2 cm μs^{-1}.

Dideuteroacetylene. Results are tabulated in table II.3.8. and experimental points given in fig. II.3.5. Estimated error = $\pm$ 0.2 μs^{-1}.

Methyl Chloride. Results are tabulated in table II.3.10 and experimental points given in fig. II.3.2. and II.3.6. Estimated error = $\pm$ 0.05 cm μs^{-1}.

Arsine. Results are tabulated in table II.3.11 and experimental points given in fig. II.3.6. Estimated error = $\pm$ 0.05 cm μs^{-1}.

Trideuteroarsine. Results are given in table II.3.12 and experimental points given in fig. II.3.6. Estimated error = $\pm$ 0.05 cm μs^{-1}.

Acetone. Results are tabulated in table II.3.13 and experimental points given in fig. 11.3.7. The point marked * were obtained 2 hours after the gas had been put into the cell. The increase in W with time is due to decomposition of the gas by the u.v. beam. The curve drawn for the drift velocity thus represents an upper limit.

Dimethylether. Results are tabulated in table II.3.14 and experimental points given in fig. II.3.7. Estimated error = $\pm$ 0.05 cm μs^{-1}.

Ethanol. Results are tabulated in table II.3.15 and experimental points given in fig. II.3.7. Estimated error = $\pm$ 0.05 cm μs^{-1}.

Table II. 3.1 Drift Velocities in CH_4 cm μs^{-1}

P / E/P	4.76	8.00	8.25*	9.49	10.00*	21.6*	24.46	51.06	best	Torr
0.1						1.1	1.1	1.2	1.1	
0.2						2.9			2.9	
0.25		3.4				3.9		3.9	3.9	
0.3			4.5			4.7			4.6	
0.35			5.5			5.7			5.6	
0.40			6.7	6.6					6.6	
0.45						7.3		7.5	7.4	
0.50			8.0	7.8		8.0			8.0	
0.55			8.6			8.6			8.6	
0.60			8.9	8.9		9.1			8.9	
0.65						9.4				
0.70			9.8	9.6					9.7	
0.75						10.0				
0.80			10.2	9.9					10.0	
0.85						10.2				
0.90		10.2	10.5	10.2	10.6	10.6	10.2	10.5	10.4	
1.0	10.3	10.3	10.6	10.2	10.6		10.3		10.4	
1.1			10.6						10.6	
1.2	10.5		10.4				10.5		10.5	
1.3							10.6			
1.4		10.4			10.0					
1.5	10.3	10.4			10.4				10.4	
1.6					9.8				9.8	
1.8					9.8				9.8	
2.0					9.6				9.6	
3.0					8.0				8.0	
V cm^{-1} $Torr^{-1}$										

* sample 1 (c).

Table II 3.2 **Drift Velocity in $C D_4$ cm μs^{-1}**

E/P \ P	5.53	6.57	8.88	10.45	21.21	best	Torr
0.2			2.8	2.8		2.8	
0.3			4.5			4.5	
0.4	6.1		6.2			6.2	
0.5	7.5	7.4		7.5	7.6	7.5	
0.6	8.4	8.3	8.2		8.4	8.3	
0.7	8.5	8.6	8.7		8.7	8.6	
0.8		8.7	8.9		8.7	8.7	
0.9		8.7	8.8			8.7	
1.0		8.6	8.6		8.6	8.6	
1.1		8.4	8.3			8.4	
1.2		8.1	7.6			8.1	
1.3							
1.4		7.7	7.6			7.7	
1.6		7.2				7.2	
1.8		6.7				6.7	
2.0		6.3				6.3	
V cm^{-1} $Torr^{-1}$							

Table II 3.3 Drift Velocity in SiH_4 cm μs^{-1}

P / E/P	3.76	5.17	13.05	best	Torr
0.2			0.45	0.45	
0.4			1.0	1.0	
0.6			1.55	1.55	
0.8					
1.0			2.7	2.7	
1.2			3.35	3.35	
1.4			3.95	3.95	
1.6			4.5	4.5	
2.0			5.9	5.9	
2.5			7.45	7.5	
3.0		8.6	8.6	8.6	
3.4		9.6		9.6	
3.6		10.05		10.1	
3.8		10.32		10.3	
4.0		10.6		10.6	
4.2		10.85		10.9	
4.4		11.05		11.1	
4.6		11.13		11.13	
4.8		11.25		11.3	
5.0		11.4		11.4	
5.5		11.4		11.4	
6.0	11.4	11.4		11.4	
7.0	11.13			11.13	
7.5	11.07			11.1	
8.0	10.75			10.75	
V cm^{-1} $Torr^{-1}$					

Table II. 3.4 Drift Velocity in SiD_4 cm μs^{-1}

P / E/P	2.23	3.87	6.11	14.13	best	Torr
0.5				1.3	1.3	
0.75				2.1	2.1	
1.0				2.9	2.9	
1.25				3.7	3.7	
1.5				4.5	4.5	
1.75				5.4	5.4	
2.0			6.2	6.4	6.3	
2.25			7.1	7.3	7.2	
2.5			8.0		8.0	
2.75			8.6		8.6	
3.0			9.2		9.2	
3.25			9.6		9.6	
3.5			10.0		10.0	
3.75			10.2		10.2	
4.0		10.2	10.2		10.2	
4.25			10.25		10.25	
4.5			10.3		10.3	
4.75			10.2		10.2	
5.0		10.1	10.1		10.1	
5.25		10.0	10.0		10.0	
5.5		9.9			9.9	
6.0		9.6			9.6	
6.5		9.3			9.3	
7.0		9.0			9.0	
7.5		8.6			8.6	
8.0	8.32	8.4			8.4	
8.5		8.2			8.2	
9.0	7.9				7.9	
10.0	7.4				7.4	
V cm^{-1} $Torr^{-1}$						

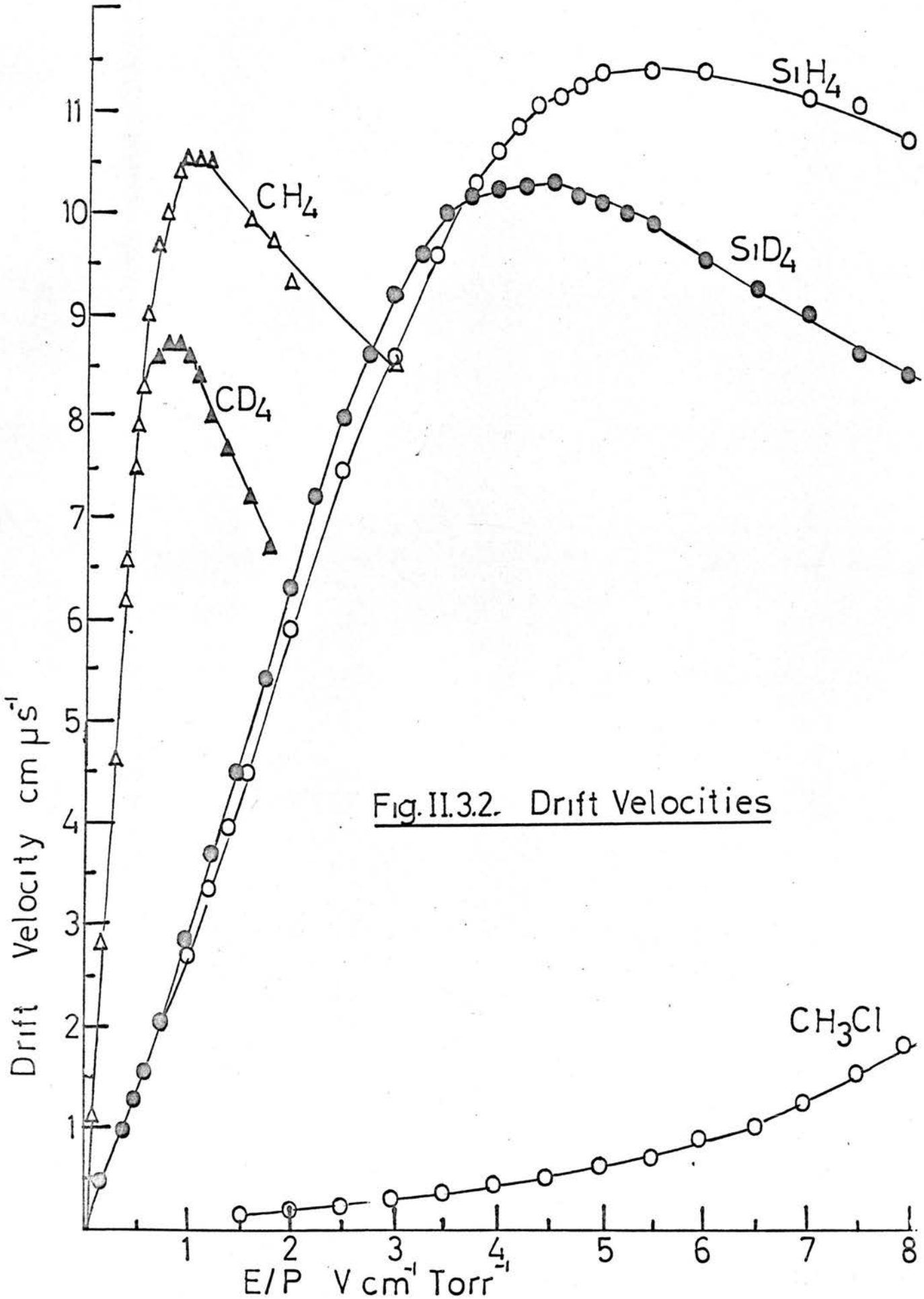

Fig. II.3.2. Drift Velocities

Table II. 3.5 Drift Velocity in C_2H_6 cm us^{-1}

E/P \ P	9.53	19.79	best	Torr
0.1		1.3	1.3	
0.15		1.8	1.8	
0.2	2.1	2.3	2.2	
0.25	2.8	2.7	2.8	
0.3	3.2	3.2	3.2	
0.4	3.8		3.8	
0.5	4.2		4.2	
0.6	4.5		4.5	
0.7	4.7		4.7	
0.8	5.0		5.0	
1.0	5.1	5.1	5.1	
1.2	5.2		5.2	
1.3	5.25		5.25	
1.4	5.3		5.3	
1.5	5.35	5.35	5.35	
1.6	5.4		5.4	
1.7	5.4		5.4	
1.8	5.4		5.4	
2.0	5.43		5.4	
2.25	5.45		5.45	
2.5	5.45		5.45	
3.0	5.4		5.4	
V cm^{-1} $Torr^{-1}$				

Table II. 3.6 Drift Velocity in C_3H_8 cm μs^{-1}

P / E/P	4.3	7.45	7.94	10.33	18.45	19.04	23.	Best	Torr
0.3					1.5		1.6	1.6	
0.4		2.0			2.0		2.1	2.0	
0.5		2.4			2.4		2.5	2.4	
0.6		2.7					2.9	2.8	
0.7		3.0			3.1		3.1	3.1	
0.8		3.3				3.4	3.4	3.4	
0.9		3.4			3.5	3.9	3.6	3.6	
1.0	3.6	3.6	3.6	3.7	3.7	3.7	3.7	3.7	
1.2		3.9	3.8		4.0		4.0	3.9	
1.4		4.0	4.0					4.0	
1.6		4.2	4.1					4.2	
1.8		4.3	4.2					4.3	
2.0	4.4	4.4	4.4	[illegible]5				4.4	
2.2		4.6	4.5					4.5	
2.4			4.6					4.6	
2.6		4.7	4.6					4.7	
2.8			4.7					4.7	
3.0		4.8	4.7	4.8				4.8	
3.2		4.8	4.8					4.8	
3.4			4.8					4.8	
3.6		4.8	4.8					4.9	
4.0	4.9	4.9	4.9					5.0	
4.2	5.0							5.0	
4.4	5.0							5.0	
4.6	5.0							5.0	
5.0	5.0							5.0	
V cm^{-1} / Torr $^{-1}$									

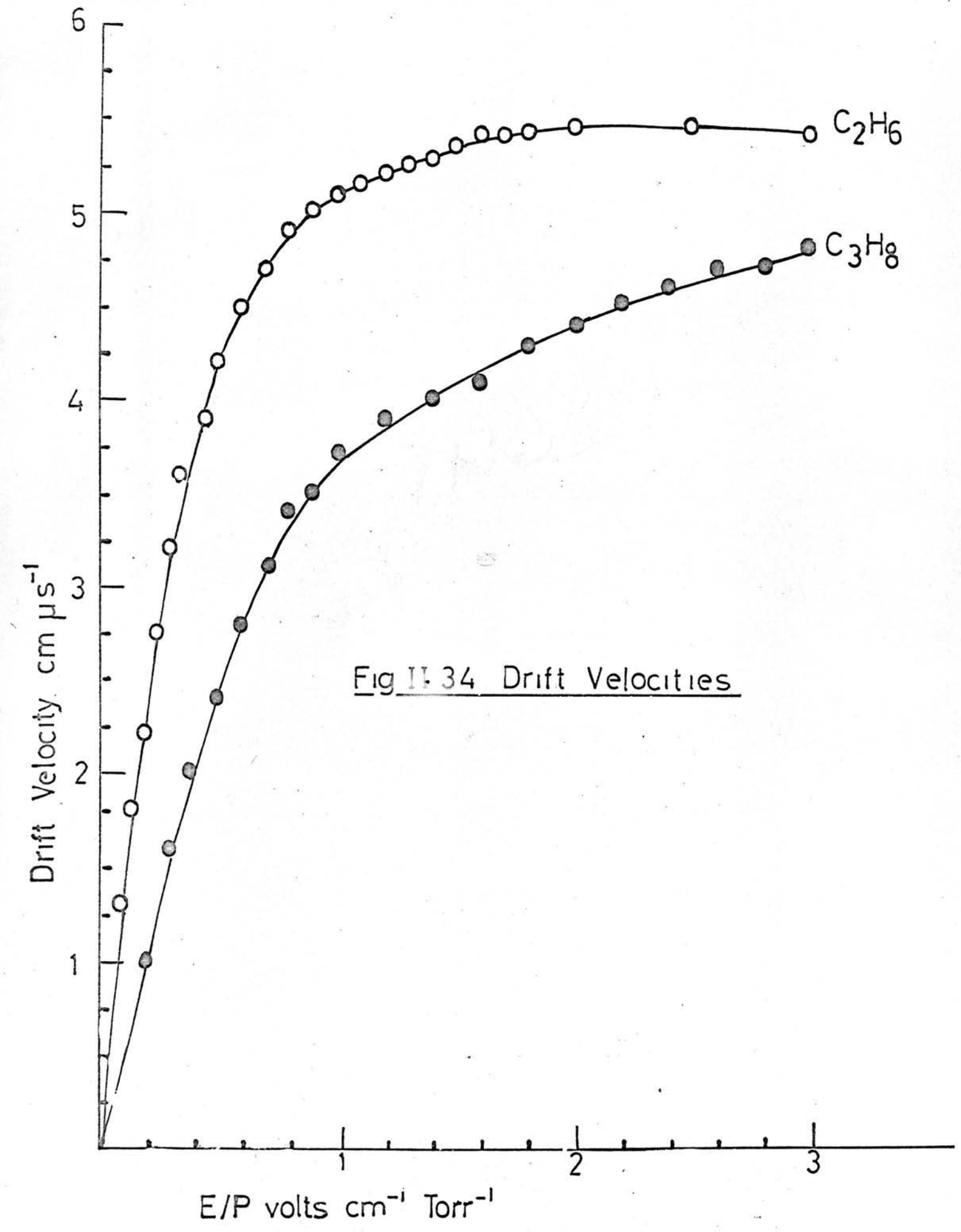

Fig II 34 Drift Velocities

Table II. 3.7 Drift Velocities in C_2H_4 cm μs^{-1}

P / E/P	1.43*	3.68*	5.26*	10.05*	10.76	15.9*	29.13	43.93	best	Torr
0.1							0.9		0.9	
0.2					1.7			1.8	1.8	
0.3					2.4			2.4	2.4	
0.4				2.8	2.9				2.9	
0.5		3.2		3.3	3.4			3.4	3.3	
0.6				3.7	3.7				3.7	
0.7					4.0				4.0	
0.8					4.2				4.2	
0.9					4.4				4.4	
1.0	4.4	4.5	4.5	4.5	4.6				4.5	
1.1					4.8				4.8	
1.2					4.9				4.9	
1.3					4.9				4.9	
1.4					5.0				5.0	
1.5			5.1		5.1				5.1	
1.6					5.0				5.0	
1.8					5.1				5.1	
2.0					5.1				5.1	
2.5			5.2	5.1					5.1	
3.0		5.0							5.0	
3.5		4.9							4.9	
4.0		4.8							4.8	
4.5	4.7	4.7							4.7	
5.0	4.8									
5.5	4.6								4.6	
6.0	4.6									
V cm^{-1} $Torr^{-1}$										

* sample (1)

Table II. 3.8 Drift Velocities in C_2H_2 cm μs^{-1}

P / E/P	3.48	4.77	9.53	best	Torr
0.2			0.5	0.5	
0.4			1.25	1.25	
0.5			1.5	1.5	
0.6			1.8	1.8	
0.8			2.3	2.3	
1.0			2.7	2.7	
1.2			3.1	3.1	
1.4			3.4	3.4	
1.6			3.7	3.7	
1.8			3.9	3.9	
2.0			4.1	4.1	
2.2			4.3	4.3	
2.4			4.5	4.5	
2.6			4.6	4.6	
2.8			4.75	4.75	
3.0	4.8	4.8	4.8	4.8	
3.5		5.0		5.0	
4.0		5.2		5.2	
4.5		5.3		5.3	
5.0		5.35		5.35	
5.5		5.4		5.4	
6.0	5.4	5.4		5.4	
7.0	5.4			5.4	
8.0	5.4			5.4	
9.0	5.5			5.5	
V cm^{-1} $Torr^{-1}$					

Table II. 3.9 Drift Velocities in C_2D_2 cm μs^{-1}

P / E/P	3.43	7.61	17.48	best	Torr
0.2					
0.4	1.2		1.2	1.2	
0.6			2.2	2.2	
0.8					
1.0			2.6	2.6	
1.2			3.0	3.0	
1.4		3.4	3.3	3.4	
1.6		3.7		3.7	
1.8		3.8		3.8	
2.0		4.0		4.0	
2.5					
3.0		4.4		4.4	
3.5		3.5		3.5	
4.0	4.5	4.5		4.5	
4.5					
5.0	4.5			4.5	
6.0	4.5			4.5	
7.0	4.5			4.5	
V cm^{-1} Torr^{-1}					

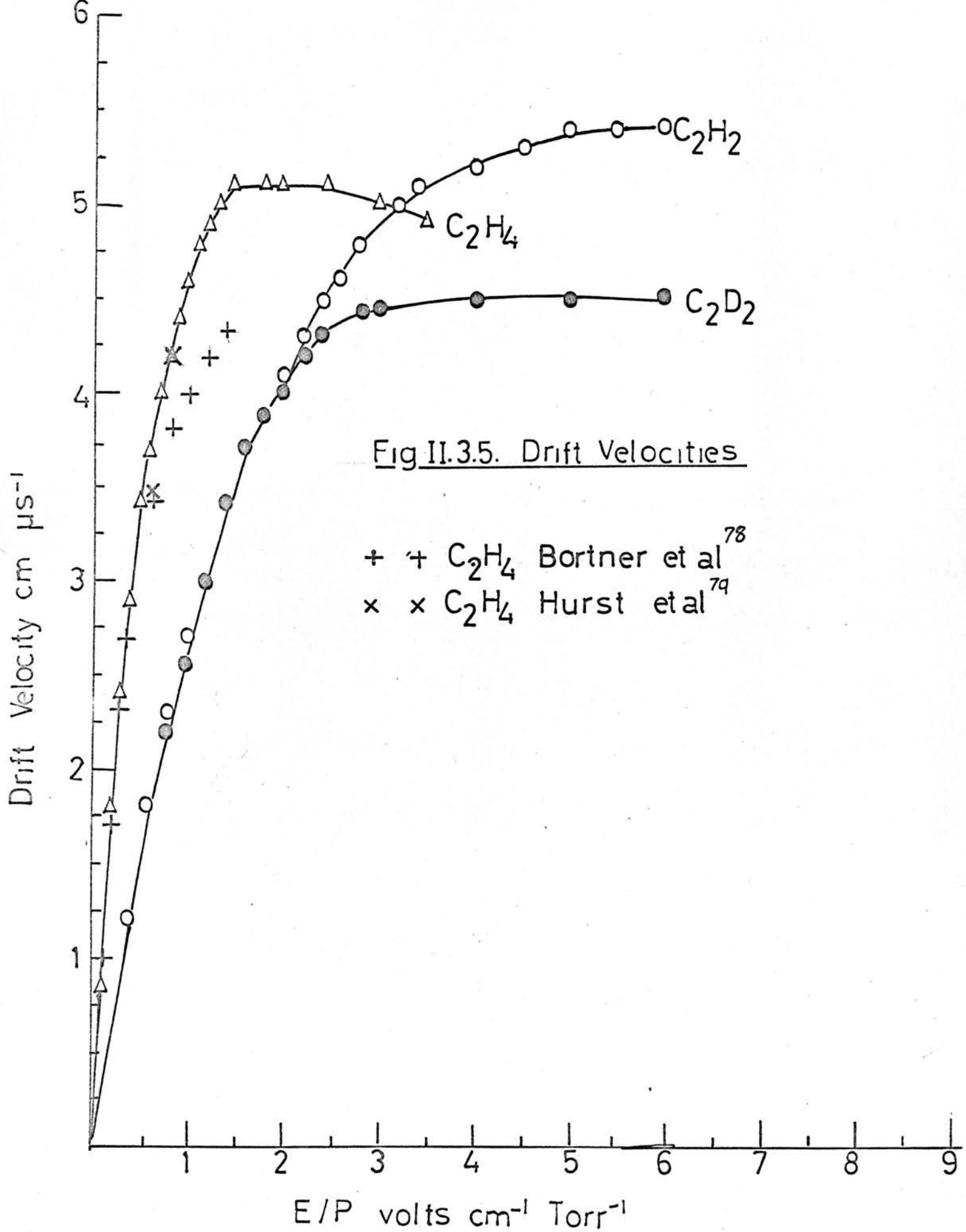

Fig II.3.5. Drift Velocities

Table II. 3.10 Drift Velocities in CH_3Cl

P / E/P	3.47	12.01	best	Torr
1.0	0.15		0.15	
2.0	0.18		0.18	
2.5	0.24	0.24	0.24	
3.0	0.30		0.30	
3.5	0.36		0.36	
4.0	0.43		0.43	
4.5	0.51		0.51	
5.0	0.61	0.60	0.61	
5.5	0.72		0.72	
6.0	0.88		0.88	
6.5	1.1		1.1	
7.0	1.24		1.24	
7.5	1.5		1.5	
8.0	1.8		1.8	
8.5	2.1		2.1	
9.0	2.3		2.3	
9.5	2.6		2.6	
$V\ cm^{-1}$ $Torr^{-1}$				

Table II. 3.11 Drift Velocities in AsH_3 μs^{-1}

P / E/P	3.31	8.39	best	Torr
1.0		0.2	0.2	
1.5		0.3	0.3	
2.0		0.4	0.4	
2.5		0.6	0.6	
3.0	0.7	0.75	0.7	
3.5	0.9	0.96	0.9	
4.0	1.2		1.2	
4.5	1.4		1.4	
5.0	1.7		1.7	
	2.0		2.0	
6.0	2.4		2.4	
6.5	2.8		2.8	
7.0	3.3		3.3	
7.5	3.7		3.7	
8.0	4.0		4.0	
8.5	4.5		4.5	
9.0	4.8		4.8	
9.5	5.3		5.3	
10.0	5.6		5.6	
V cm^{-1} Torr $^{-1}$				

Table II. 3.12 Drift Velocities in AsD$_3$, cm μs^{-1}

P / E/P	3.23	6.57	best	Torr
1.0		0.20	0.20	
1.5		0.32	0.32	
2.0		0.46	0.46	
2.5		0.60	0.60	
3.0		0.78	0.78	
3.5		1.0	1.0	
4.0		1.3	1.3	
4.5		1.7	1.7	
5.0	2.1	2.1	2.1	
5.5	2.5		2.5	
6.0	3.0		3.0	
6.5	3.4		3.4	
7.0	3.9		3.9	
7.5	4.3		4.3	
8.0	4.7		4.7	
8.5	5.1		5.1	
V cm^{-1} Torr^{-1}				

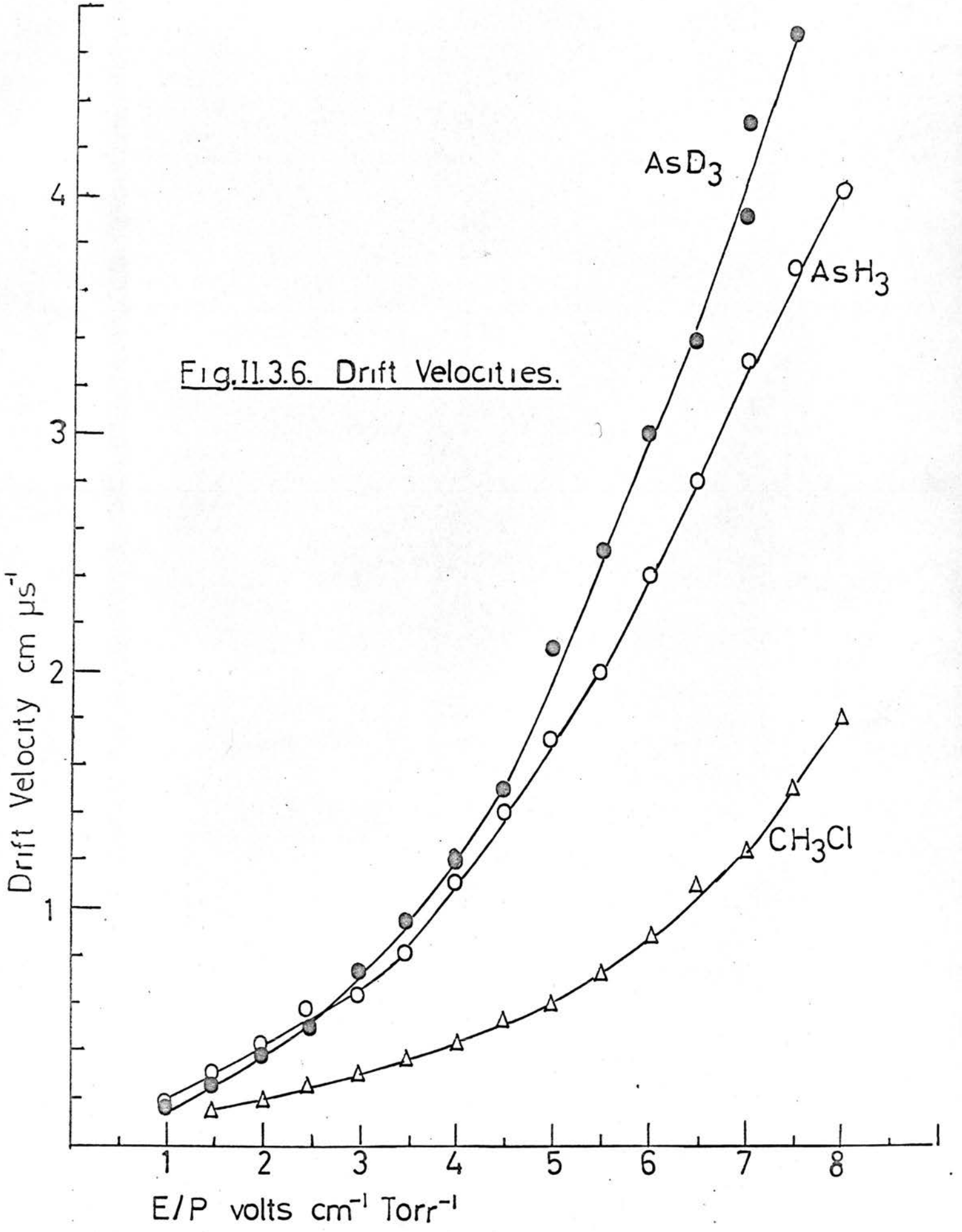

Fig.II.3.6. Drift Velocities.

Table II. 3.13 Drift Velocities in CH_3COCH_3 cm μs^{-1}

P / E/P	3.25	7.35	best	Torr
3.0		0.16	0.16	
4.0	0.25	0.24	0.24	
4.5		0.28	0.28	
5.0	0.34		0.34	
5.5				
6.0	0.43		0.43	
6.5	0.48		0.48	
7.0	0.54		0.54	
7.5	0.63*			
8.0	0.67		0.67	
8.5	0.80*			
9.0	0.85			
10.0	1.08			
V cm^{-1} Torr^{-1}				

* after 2 hours

Table II. 3.14 Drift Velocities in $(CH_3)_2O$ cm μs^{-1}

P / E/P	4.21	10.02	best	Torr
1.0	0.25	0.23	0.24	
1.5	0.38	0.35	0.37	
2.0	0.55		0.55	
2.5	0.70	0.66	0.68	
3.0	0.90	0.85	0.88	
3.5	1.2		1.2	
4.0	1.4		1.4	
4.5				
5.0	2.1		2.1	
5.5	2.4		2.4	
6.0	2.8		2.8	
7.0	3.7		3.7	
7.5	4.0		4.0	
V cm^{-1} Torr^{-1}				

Table II. 3.15 Drift Velocities in CH_3CH_2OH cm μs^{-1}

P / E/P	4.97	5.61	9.8	best	Torr
1.1		0.16		0.16	
2.0		0.25	0.26	0.26	
2.5			0.32	0.32	
3.0	0.38	0.38	0.38	0.38	
3.5		0.45		0.45	
4.0		0.54		0.54	
4.5		0.60		0.60	
5.0	0.68	0.69			
5.5		0.77		0.77	
6.0	0.84			0.84	
V cm^{-1} Torr^{-1}					

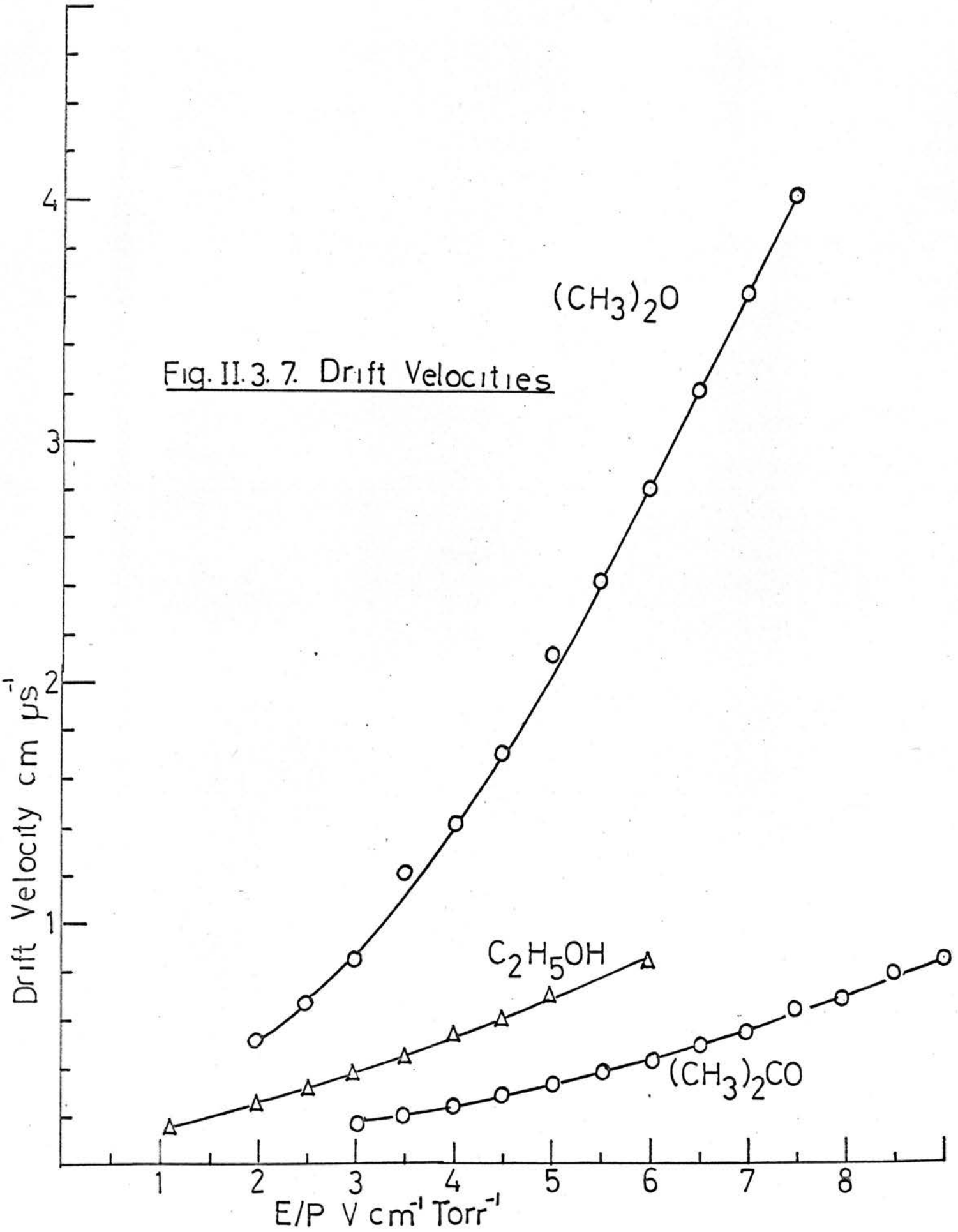

Fig. II. 3. 7. Drift Velocities

II.4. Preliminary Work.

The final drift tube was perfected after preliminary experiments on test cells. The test cells were non-bakable, and many difficulties were met in them - difficulties which were removed only when attention was paid to purifying the system. The preliminary work is described, briefly, below.

Cell I. The cathode was of polished zinc. The drift distance d was 5 cm and only two guard rings were used - one below the first shutter and one mid-way between the shutters. The spacers were 'Fluon' rods. The grid wires - 0.010 in nickel - were strung 1 mm apart on 'Fluon' frames. The electrical leads were taken horizontally through 'Picien' wax in the side-arms of a pyrex envelope. A brass lid was cemented on to the envelope with 'Picien'.

A different switching system was employed. A pulse generator supplied two pulse transformers - one fed from a prepulse and one, after a suitable delay, from a main pulse. Each pulse transformer had two secondary windings connected to corresponding base inputs of the switching bistable pairs. (fig. II.1.5.). When operating the prepulse switched the bistables to the 'closed' position and after the desired delay, the main pulse opened the shutters; so pulses of variable length and repetition time could be applied to the wires. The pulse length could be varied from 1 μs - 1,000 μs and repetition time from 2 μs to 2,000.μs. Experimentally, current maxima were located by plotting anode current against pulse repetition time. Usually square pulses were applied.

This cell was unsatisfactory because of low, fluctuating, currents and inefficient grids. Currents rarely exceeded 10^{-12}A, in the region of the lower limit of the electrometer. However, some reasonable values for drift velocities in air, N_2O, and C_2H_4 were obtained, over a limited E/P range.

Cell 2. The inner assembly of Cell 2 resembled that of the final drift tube. All electrodes were of gold-plated brass, separated by glass spacers. However, G_1 and G_2 were interchanged, i.e. the drift distance d was 10 cm. and there was no 'smoothing' guard ring before the first

shutter. The shutters were constructed of gold-plated nickel wire, strung 1 mm apart on mica frames. All electrical leads were taken up the side of the glass envelope and through glass-metal seals in a brass 'lid' which was 'Piciened' to the envelope.

The currents were good, the grids were efficient, but anode current did not depend on the switching frequency of the grids. This was assumed to be most probably due to there being a wide spread of drift velocities either because of distortion of E by the vertical electrical leads, or because of the disturbing effect of the first shutter on the oncoming electrons.

Cell 3. Cell 3 was a non-bakable version of the final cell. The smoothing guard ring G_1 was placed before the first shutter making the drift distance 8 cm. Once more the leads were taken horizontally through the side of the containing envelope through 'Picien' seals.

Currents and grid efficiency were further improved and some reliable drift velocities were obtained in air, N_2O and C_2H_4 the results agreeing well with literature values. However, the range over which drift velocities could be obtained was limited, in N_2O and C_2H_4 to moderate E/P and low P. The anomolous grid behaviour already described for C_2H_4 was more marked in Cell 3. i.e. at low E/P and P $>$ a few Torr, all the current carriers were stopped by a square wave of a few μ s long. However, when pulse repetition time was increased 10^2 - 10^3 times, half the current carriers did reach the anode.

Table II.4.1.

Gas	Grid	SmV	Square Wave Repetition Time μs	Square Wave frequency	s^2 square
C_2H_4	G_2	42	2	0.5 mc/s	0
			20	5×10^4 c/s	0
			200	5×10^3 c/s	21
			2000	5×10^2 c/s	21

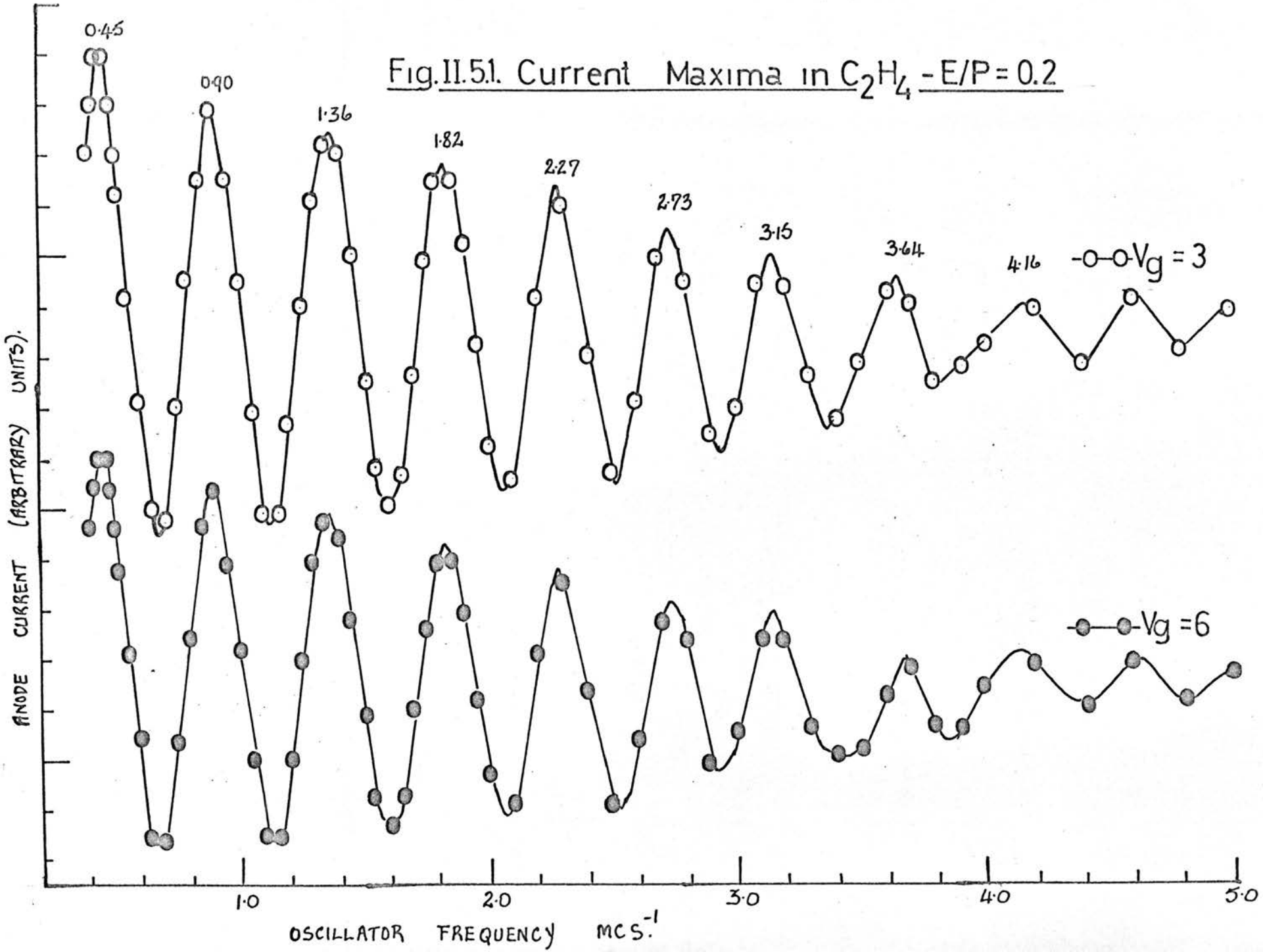
Fig. II.5.1. Current Maxima in C_2H_4 - E/P = 0.2
0·45
0·90
1·36
1·82
2·27
2·73
3·15
3·64
4·16
-o-o-Vg = 3
-o-o-Vg = 6
ANODE CURRENT (ARBITRARY UNITS).
1·0
2·0
3·0
4·0
5·0
OSCILLATOR FREQUENCY MCS.$^{-1}$

The interpretation of these results is discussed later.

Cell 4. This is the final bakable cell which has been fully described. The drift velocities obtained in it are believed to be reliable within the limits quoted.

II.5. Discussion of Experimental Error.

(a) Distortion of Field E. The precautions taken in the construction of the cell to ensure field uniformity have been described in section II.1.; the guard rings were made fairly large, tapering to a knife edge; all electrical connections were taken horizontally through the side of the envelope. The gold-plating of all surfaces and junctions within the cell reduced contact potentials to a minimum. It also minimised gas absorption and any resulting surfaces charges, which might distort the drift field. It is unlikely that these effects (contact potentials and surface charges) were completely eliminated, so measurements were never made at E less than 3 Vcm^{-1}. where the error might be significant. Distortion of the field in the region of the shutters is, of course, inevitable and so measurements were made at the least possible V_G giving efficient grids. However, the influence of this distortion on W must be small, as W did not depend on the magnitude of V_G. This is seen in fig. II.5.1 where electrometer signal is plotted as a function of oscillator frequency for E/P = 0.2 in C_2H_4. at two different V_G.

(b) Temperature and Pressure. Electron drift velocity is, strictly speaking a function of E/N where N is the gas density. We discuss it as a function of E/P. At 20° C, E/P = (E/N) 3.29×10^{16} A temperature change of 3°C for a gas at constant pressure is required to change E/N by 1% at 20°C. Even in CH_4 where W is a sharply varying function of E/N, the corresponding change in W is too low to be significant. Although the present system was not thermostatted, all measurements were made at 20 ± 2°C. W is also a function of gas temperature. However, variation of W due to temperature fluctuations may also be neglected compared with other errors. As has been described, the pressure measurements were made on a mercury manometer. The mercury levels were read, correct to

$\pm$ 0.025 mm with a travelling microscope. Positions of both top and bottom of the menisci were noted and a correction applied to compensate for the difference in meniscus height.[111] The maxumum possible error in the pressure reading was $\pm$ 0.1 Torr. This was considered to be the main source of experimental error.

(c) Space Charge Effects. The current received at the anode under comparable conditions varied from gas to gas. However, if it exceeded about 10^{-9}A considerable electrometer fluctuations resulted. These fluctuations were removed by reducing the current, which was not allowed to exceed about 10^{-10}A. In no case did the drift velocity show a dependance on current over the range 10^{-10} - 10^{-12}A.

(d) Switching Frequency and Phase. As has been described, the waves applied to the shutters were phase-locked. The method of locating current maxima was most reliable, allowing them to be placed to $\pm$ 0.01 mcs^{-1}. The fact that f_o/n is constant where several maxima were located shows that errors due to phase differences or incorrect frequency measurements are negligible.

(e) Impurities. The presence of impurities in the drift tube can alter drift velocities or interfere with the measurements. This has been shown in:-

(1) CH_4 where drift velocities were low in the less pure gas samples.
(2) Acetone, where decomposition of the gas by the u.v. radiation caused W to rise with time.
(3) C_2H_4 where anomolous grid behaviour was observed in the impure gas sample.

Details of the precautions taken to ensure absolute purity of the system have been described - gold-plating of all surfaces, baking out etc. etc. Only in the case of acetone did W change with time; so contamination due to desorption from the metal surfaces may be neglected.

(f) Diffusion Effects. The estimated relative error in W due to diffusion of the electrons is[71] $\frac{3}{d(W/D)}$ which is small for long drift

distance d and high gas pressures. Any diffusion effects should show up in a pressure dependence of W. No such dependence was observed outwith the limits of experimental error.

Independent measurements of W/D have been made in this laboratory (Appendix 1) for a number of gases and may be used to estimate the magnitude of the diffusion error:

GAS	P	E/P	(r_x 100)
CH_4	9.3	1.1	0.8
	23.5	1.1	0.25
	33.4	1.05	0.20
	Torr.	Vcm^{-1} $Torr.^{-1}$	

so diffusion effects would not be expected to be detected in the present system. Further evidence that they are negligible is obtained from the curves in figs. II.3.3 and II.5.1. The above estimated error applies to the limiting case of a shutter being open for a very short time. As the pulse width increases the error decreases. As switching frequency increases, the electron pulses get narrower; so, if diffusion effects were marked, f_σ/n would increase with increasing n. No such frequency dependency was observed where more than one peak was located.

The drift velocities given are believed to be correct to $\pm$ 2%.

III. DISCUSSION.

III. Discussion

III.1. Anomolous Behaviour with Ethylene.

The anomolous behaviour described for C_2H_4 was obviously due to the presence of traces of O_2 or H_2O which were removed by passage over sputtered Na. In general, as P was increased and E/P decreased, the fraction of the current carried by electrons appeared to decrease - the rest being carried by a species that did not get through the open grid when it was operating at high frequency. (Table II.3.16). The following explanation is offered. The current-carrying species was a negative ion, formed by electron attachment to C_2H_4. The attachment was stabilised by traces of impurity and also by high P. The geometry of the tube and grids, and the mobility of the ion were such, that, an ion pulse transmitted during the 'open' period did not have time to move out of the sphere of influence of a grid before it shut. This pulse was, therefore, removed, along with ions in the immediate vicinity of the wires, during the next 'closed' period. Any free electrons present behaved normally and their drift velocities could be measured. (Table II.3.17). When the pulse width was increased, the slow moving ion pulse had sufficient time to move away from the grid before it shut, and ideal behaviour was again observed. (Table II.4.1.). (The system could not be easily adapted to scan this low frequency region, so that ionic mobilities could not be measured). The effect was more marked at the second shutter because of the greater concentration of ions at this shutter.

Bannon and Brose,[56] who have also measured transport quantities in C_2H_4, did not make measurements for $E/P < 1.26$ because, they report, as E/P was reduced an increasing fraction of the current was carried by negative ions. They detected the ions in a Diffusion Tube in which they were obtaining k values for the electrons (section I.6.(a)). At low E/P, k was found to be energy dependent, increasing with increasing P. In this apparatus (fig. I.6.1.) heavy ions tend to concentrate on to the central disc of the anode. If allowance is not made for these ions, calculated k values for the electrons are high.

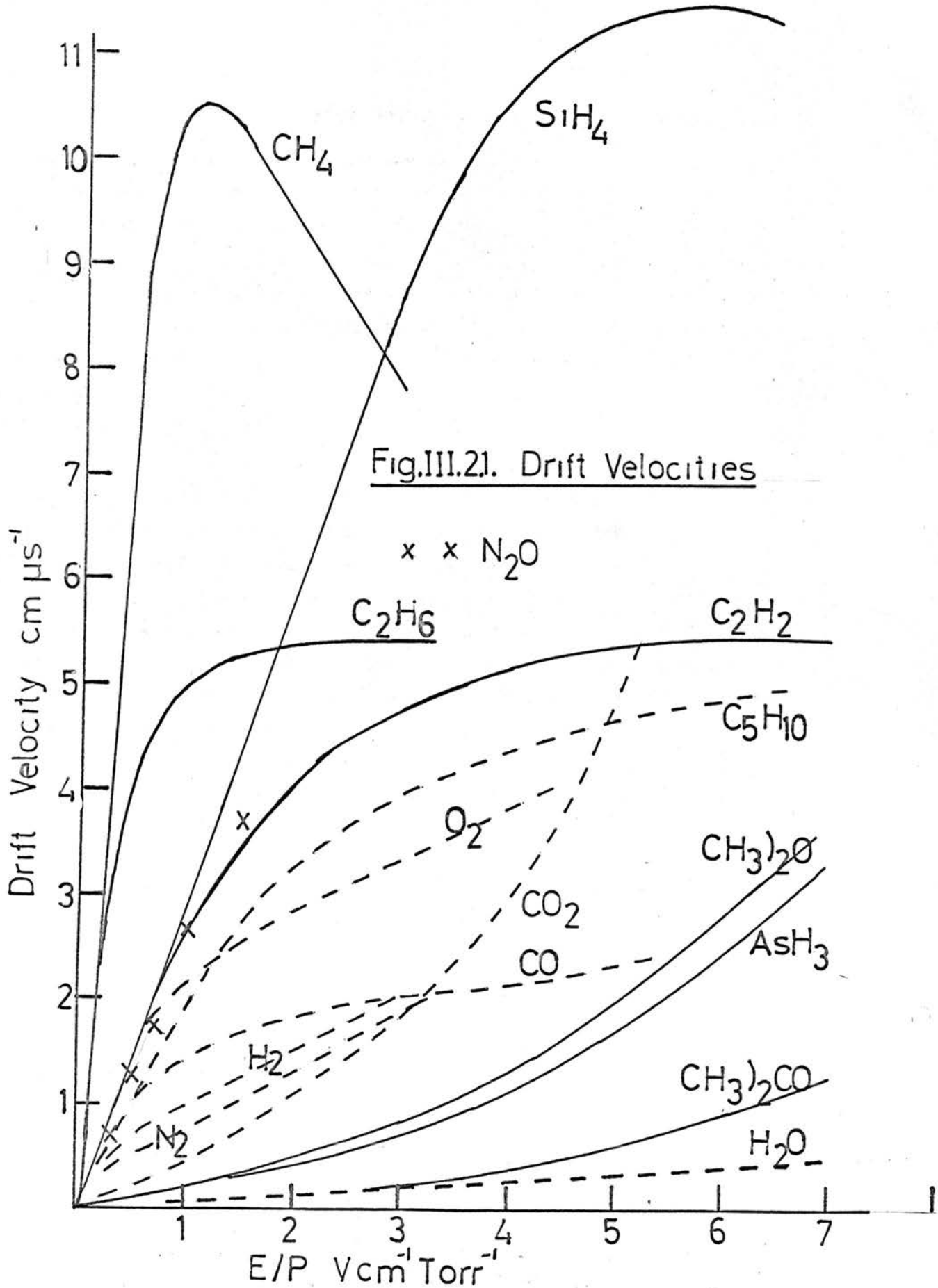

Fig.III.21. Drift Velocities

III.2. Qualitative Discussion of Drift Velocities.

In fig. III.2.1. are drawn drift velocity curves for several polyatomic gases. Full lines represent present results; broken lines are taken from the literature[68,63,55](only reliable results have been used). Drift velocities in the inerts[68]are given in fig. III.2.2. In this section we shall discuss these drift velocities qualitatively.

The outstanding features of these figures are:-

(1) the tendency for drift velocity curves, in fig. 1, to divide themselves into groups according to whether the molecules are symmetrical, quadrupolar or dipolar; symmetrical molecules - high W showing a maximum; quadrupolar molecules - intermediate W, tending in some cases to reach a plateau; dipolar molecules - low W, rising steadily;

(2) the difference in the drift velocities in Ar and CH_4. Despite the similarity in the Ramsauer Cross-sections of Ar and CH_4 (section I.4(a)) a slow electron can obviously tell the difference between them.

At any E/P, electron drift velocity depends on the number and nature of the electron/molecule impacts that occur. Collisions by randomising direction of motion, impede progress in any one direction; so the lower the total collision cross-section, the higher will be the drift velocity, at any E/P.

$$\text{low } Q \quad - \quad \text{high } W.$$

In addition, an electron emerging from an inelastic impact finds itself with a reduced random velocity u. As $u > W$, it is u that determines collision frequency. At any E/P., the lower u, the lower will be the collision frequency and the higher W.

$$\text{high } Q_{\text{inelastic}} \quad - \quad \text{high } W.$$

i.e. at any E/P, a high W is favoured by a low total collision cross-section, a large proportion of which is inelastic. This can be shown by combining equations 1.7.6. and 1.7.8. to give

$$W = \frac{a}{\bar{Q}_D} \left(\frac{\lambda}{}\right)^{\frac{1}{2}} \frac{E}{P} \qquad \text{III.2.1.}$$

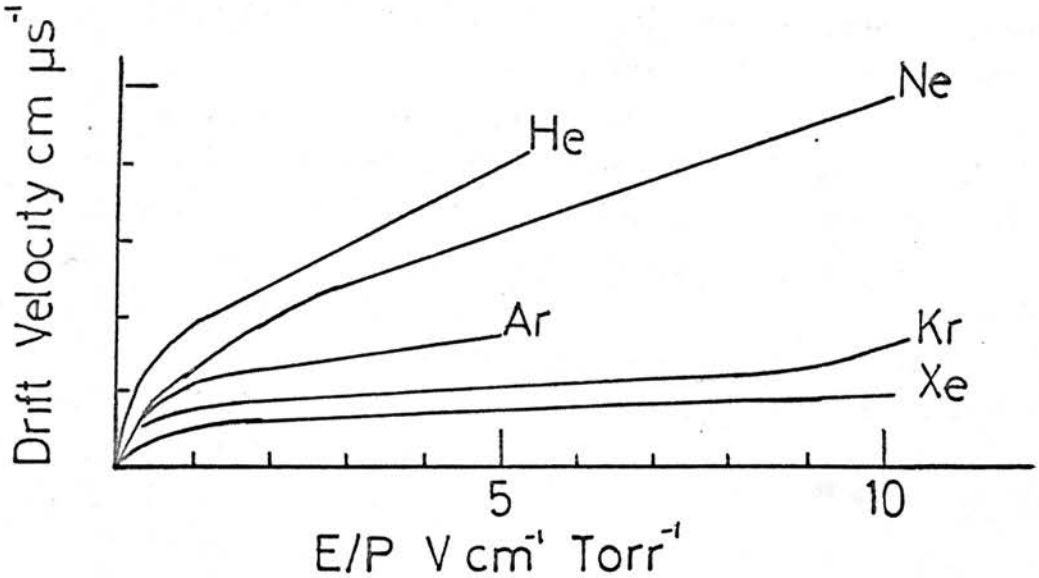

Fig III.2.2. Drift Velocities

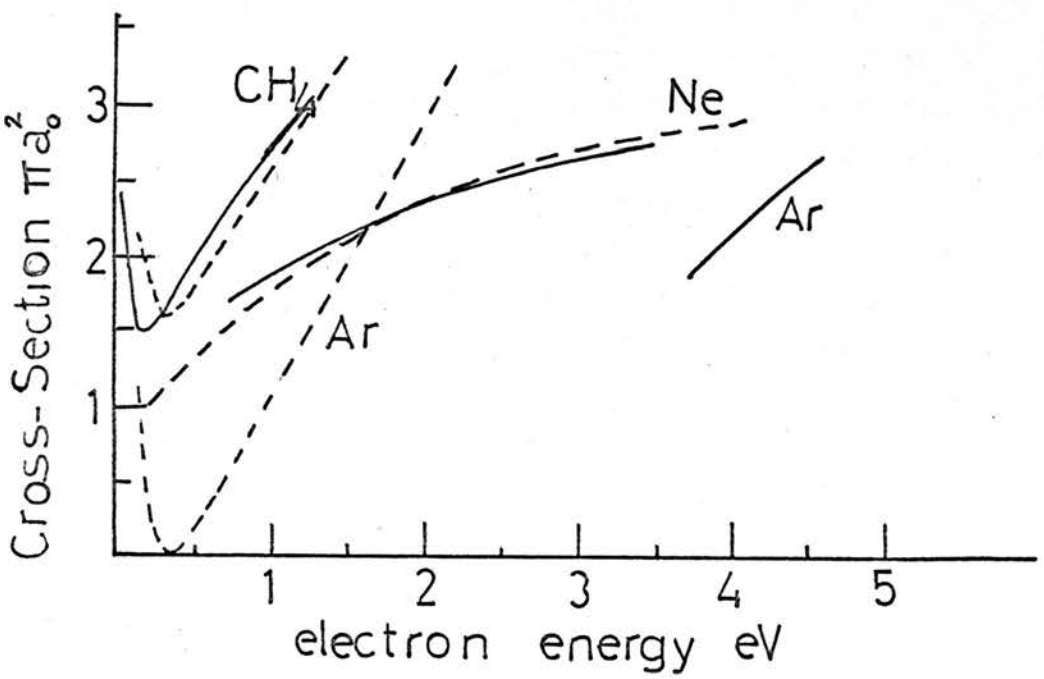

Fig. III.3.1. Collision Cross-Sections

——— Q_D(swarm

------ Q_R(beam)

a is an energy dependent factor and the relation holds only if $\overline{Q}_D$ is not a rapidly varying function of electron energy.

The reason for the very low drift velocities in dipolar gases is at once obvious. The electron/dipole interaction is a long range one; so the cross-sections of dipolar molecules are large at low energies. (fig. 1.7.1.) Furthermore, because of the large Q, the electrons have little opportunity to gain energy from the field in between collisions so that u is low and inelastic losses unimportant.

III.3. Methane and the Inerts - Comparison. At low E/P, only elastic impacts are energetically possible in the inerts; so differences in drift velocities in these gases can be attributed to differences in the cross-section behaviour. This is illustrated in fig. III.2.2. In He and Ne, gases whose cross-sections do not show a Ramsauer-Townsend minimum, (fig. 1.4.2.) the drift velocities rise fairly steeply with increasing E/P. In Ar, Kr, and Xe - molecules which do have Ramsauer-Townsend minima in their cross-sections - drift velocity rises slowly to an almost constant value and W increases in order of decreasing cross-section. The upward curve seen at the high end of the Kr curve is probably due to electronic excitation, (first electronic excitation potential = 9.98 eV). The CH_4 cross-section resembles that of Ar and Kr in both form and order of magnitude, and yet drift velocities in CH_4 are markedly higher than in the inerts. The shape of the CH_4 drift curve may, in part, be attributed to the Ramsauer-Townsend minimum, but it seems, at first sight, that another factor must be introduced to account for the very high drift velocities in CH_4 - viz. inelastic losses in CH_4. We shall consider this, and other possible causes for the drift velocity differences, further.

We have constructed a Townsend Diffusion Apparatus in which to measure W/D for electrons in gases (section 1.6.(a)). Making the usual simplifying assumptions about electron velocity distribution and molecular collision cross-sections, k values for electrons in CH_4 have been deduced. k as a function of E/P is given in Appendix 1, and the results used to evaluate $\overline{Q}_D$ for CH_4. From equation 1.7.9, at 293°A (the temperature at which present measurements were made)

$$\bar{Q}_D = 4.8\ 10^7 \frac{E/P}{W(k)^{\frac{1}{2}}} \quad \pi a_o^2$$

and from equation 1.7.10, the electron energy in eV is

$$eV = 3.7\ 10^{-2} k$$

$\bar{Q}_D$ as a function of electron energy are tabulated in table III.3.1. and plotted in fig.III.3.1, where they are compared with measured cross-sections Q_R.

Table III.3.1 Cross-sections - CH_4

E/P V cm^{-1}	W cm μs^{-1}	k	energy eV	Q_D πa_o^2
0.2	2.9	1.9	0.07	2.36
0.4	6.6	3.3	0.12	1.56
0.6	8.9	4.6	0.17	1.51
0.8	10.0	6.2	0.23	1.53
1.0	10.4	8.0	0.30	1.63
1.2	10.5	10.0	0.38	1.73
1.4	10.2	12.1	0.45	1.88
1.6	9.8	14.4	0.54	2.05
1.8	9.7	16.8	0.63	2.16
2.0	9.6	19.2	0.72	2.28
2.5	9.4	28	1.05	2.39
3.0	8.0	33.6	1.26	3.09

Similar calculations have been made on the literature swarm data for Ar and Ne, and the results plotted in fig.III.3.1.

The agreement between Q_D and Q_R is good for CH_4 and Ne but not for Ar. This indicates that:-

(a) simple swarm theory can be successfully applied to electrons in CH_4. As k(E/P) is involved both in calculating the magnitude of Q_D and in positioning it along the x-axis, it is unlikely that the agreement between Q_D and Q_R is fortuitous.

(2) Slow electrons are scattered isotropically from CH_4. This is predicted by scattering theory. A Ramsauer-Townsend effect is shown only by an attractive scattering potential for which only $l = 0$ is involved in the expression for Q

$$Q = \frac{4\pi}{k^2} \sum_{l=0}^{l=\infty} (2l+1) \sin^2 n_l$$

When only $l = 0$ is important, scattering tends to become isotropic as the electron energy tends to zero.[15], This means that the high drift velocity in CH_4 is not due to preferential forward scattering of electrons from CH_4.

(3) The approximate swarm theory cannot be applied to Ar, or the swarm data for Ar is incorrect.

Drift velocities in Ar have been well established. The k values are less certain, although they are known to be high. The Q_D curve for Ar could be shifted along the x-axis to coincide with the Q_R curve by adjusting k (E/P). At electron energy greater than 0.7 eV, Q_R for Ar may be represented by the linear equation:-

$$Q_R = (2.2\epsilon - 1.3)\ \pi a_o^2$$

while

$$Q_D = 4.8 \frac{E/P}{W(k)^{\frac{1}{2}}}\ 10^7\ \pi a_o^2$$

$$= Y/\epsilon^{\frac{1}{2}} \qquad Y = 0.92\ 10^7 \frac{E/P}{W}$$

Equating Q_D and Q_R

$$2.2\epsilon^{\frac{3}{2}} - 1.3\epsilon^{\frac{1}{2}} - Y = 0 \quad \text{——} \quad \text{III.3.1.}$$

Y may be evaluated at each E/P and equation III.3.1. solved to give that k(E/P) required to bring Q_D into coincidence with Q_R

Table III.3.2.

GAS	E/P	W cm us^{-1}	Y	$\epsilon^{\frac{1}{2}}$ eV$^{\frac{1}{2}}$	ϵ eV	k	k_m	k/k_m
Ar	0.125	0.31	3.7	1.35	1.8	47.5	100	0.5
	0.195	0.32	5.5	1.5	2.25	59	120	0.5
	0.355	0.36	9.12	1.7	2.89	76	160	0.5

k_m is k deduced from measured W/D using equation 1.7.5. This shows that either the W/D measurements for electrons in Ar are grossly in error or that the W/D measurements are reliable and simple theory cannot be used to relate them to k. Heylen[92] has suggested that the latter is true and ascribes it to the presence of the Ramsauer-Townsend minimum. That this does not appear to upset the swarm theory in CH_4 may be due to the fact that the cross-section minimum in Ar is unique in that it is very nearly zero. This may cause rapid variations in electron velocity distribution in the region of the minimum. As k values are not available for Kr, a comparison cannot be made with this molecule. However, it seems that, if minor differences in cross-section behaviour have major effects on transport quantities, then, of the species, CH_4, Ar, Kr, and Xe, - Ar will be the odd molecule. In fact, CH_4 is the anomolous one, indicating that another factor must be considered in this case. The obvious factor is inelastic losses to CH_4.

III.4. Drift Velocities in Quadrupolar Molecules.

Quadrupolar molecules, in general, have intermediate cross-sections and, as expected, intermediate drift velocities. In addition, drift velocity curves for the hydrocarbons tend to lie above those for the diatomic quadrupolars, i.e. there is a further sub-division into polyatomic and diatomic molecules. Some molecules, viz. CO_2, O_2, and N_2O do not follow the general pattern. CO_2, a non-polar linear polyatomic, has a drift velocity curve more like those of the dipolars. However, at low energies, the CO_2 cross-section is high, resembling that of NH_3 and other dipolar molecules. (Fig. 1.7.1.) N_2O, a polar polyatomic, has a very high drift velocity curve. However, Ramsauer type measurements indicate that the N_2O cross-section is low at low energies (fig. 1.7.1.) (the reason is not obvious), and, in addition, Schulz has shown that vibrational excitation of N_2O[21] by resonance scattering, takes place at low energies. The drift velocity curve for O_2 lies above those of the other diatomics, but, like N_2O, the O_2 cross-section is low at low energies, and O_2[23] is vibrationally excited by slow electrons. The excitation mechanism has not yet been established.

It is difficult to assess the influence of the cross-section behaviour on the shape of the drift velocity curves for these molecules. The cross-sections of the hydrocarbons resemble each other and this may, in part, account for the plateau-like regions in the drift curves. However, the O_2 drift curve is also high, while its cross-section does not resemble the hydrocarbon cross-sections. It seems likely that the common factor is large χ in both O_2 and the polyatomics. That is, the higher drift velocities in the polyatomic species is due, to larger inelastic losses to these molecules.

III.5. Isotope Behaviour.

The collision cross-sections of hydrides and the corresponding deuterides are likely to be closely similar, so that differences in their transport quantities will be due to differences in electron energy losses.

From equation III.2.1., at any E/P

$$\left(\frac{W_h}{W_d}\right)^2 \doteq \frac{Q_d}{Q_h}\left(\frac{\lambda_h}{\lambda_d}\right)^{\frac{1}{2}} \qquad \text{III.5.1.}$$

$$\doteq \left(\frac{\lambda_h}{\lambda_d}\right)^{\frac{1}{2}} \qquad \text{III.5.2.}$$

if energy losses are small and Q not sharply energy dependent.
(The subscripts h and d indicate drift velocities etc. in hydrides and corresponding deuterides.)

For elastic losses:-

$$\frac{\lambda_h}{\lambda_d} \doteq \frac{2m}{M_h}\frac{M_d}{2_m} \qquad \text{III.5.3.}$$

$$\doteq \frac{M_d}{M_h} \qquad \text{III.5.4.}$$

For rotational losses:-

$$\frac{\lambda_h}{\lambda_d} \doteq \frac{(\text{moment of inertia})_d}{(\text{moment of inertia})_h} \qquad \text{III.5.5.}$$

$$\doteq \frac{M_d}{M_h} \qquad \text{III.5.6.}$$

For vibrational losses:-

$$\frac{\lambda_h}{\lambda_d} = \frac{(h\nu)_h}{(h\nu)_d} \qquad \text{III.5.7.}$$

$$= \left(\frac{\mu_d}{\mu_h}\right)^{1/2} \qquad \text{III.5.8.}$$

where μ is the reduced mass of the vibrating atoms.

Thus, if the collision cross-section is not sharply energy dependent, it might be possible, from the ratio of the drift velocities at any E/P, to tell whether there is (a) elastic or rotational excitation, or (b) vibrational excitation. It will not be possible to distinguish between energy losses in elastic impacts and impacts exciting rotations.

Table III.5.1.

Drift Velocity Ratios for Some Hydrides and Deuterides.

W_h / W_d

E/P	CH_4/CD_4	C_2H_2/C_2D_2	SiH_4/SiD_4	H_2/D_2 [61]	AsH_3/AsH_3
0.2	1.04				
0.4	1.06	1.04			
0.8	1.15	1.04			
1.0	1.33	1.03	0.94	1.1	1.0
2.0	1.52	1.02	0.95	1.15	0.87
3.0		1.1	0.95	1.18	0.9
4.0		1.15	1.04	1.15	0.93
5.0		1.19	1.13	1.17	0.81
6.0		1.2		1.15	0.8
7.0		1.2	1.19	1.17	0.85
8.0			1.28	1.26	0.85
Calculated					
Elastic Rotational	1.06	1.02	1.03	1.19	1.01
Vibrational	1.08	1.08	1.09	1.09	1.09

Calculated values are obtained from equations: III.5.4, III.5.6 and III.5.8.

From this table, it appears that losses to H_2 and D_2 are elastic or rotational over the whole E/P range considered. Losses to the methanes, acetylenes and silanes are elastic or rotational at low E/P. At higher E/P in these molecules, the drift velocity ratio increases over the calculated value. This calculated ratio

$$\frac{W_d}{W_h} = \left(\frac{\lambda_h}{\lambda_d}\right)^{\frac{1}{4}}$$

assumes that $Q_h = Q_d$ at each E/P. This is true only if the absolute energy losses are small and if Q is not a sharply energy dependent function. The greater the inelastic losses, the greater will be the difference between Q_h and Q_d at any E/P; so, although no conclusive results can be drawn from this comparison, the results are not inconsistent with low energy losses at low E/P and greater inelastic losses at high E/P. In all cases the drift velocity ratio is such as to make Q_d great than Q_h at high E/P. As $k_d > k_h$ for all the energy loss processes considered, this means that Q increases with increasing energy in CH_4, C_2H_4, and SiH_4. This is known to be true for CH_4 and C_2H_4.

Because of the large mass of the As atom, the W ratio for elastic and rotational losses is very nearly unity. AsH_3 is dipolar, so electron energies are likely to be low and cross-sections high in this gas. Furthermore, at low energies, the collision cross-section of NH_3 and other polar species increases sharply with decreasing electron energy. This may also be true for AsH_3, in which case, even small energy losses, making k_h slightly less than k_d, may mean that $Q_h > Q_d$ i.e. $Q_d/Q_h < 1$. If $(\lambda_h/\lambda_d)^{\frac{1}{4}}$ is very nearly 1, this will mean that W_h / W_d will be less than 1. That is, the AsH_3 results could be explained by elastic or rotational losses in a region where the cross-section increases sharply with decreasing electron energy.

III.6. Evaluation of λ in Methane and Ethylene.

Using the k values reported in Appendix and the present W values, λ values for electrons in methane have been evaluated from the equation 1.7.6.

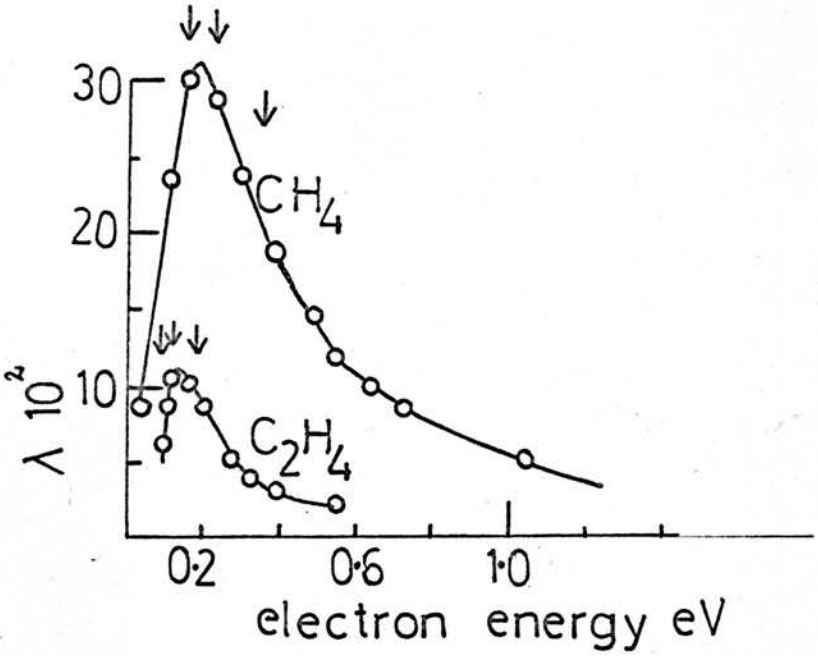

Fig III.6.1. λ values

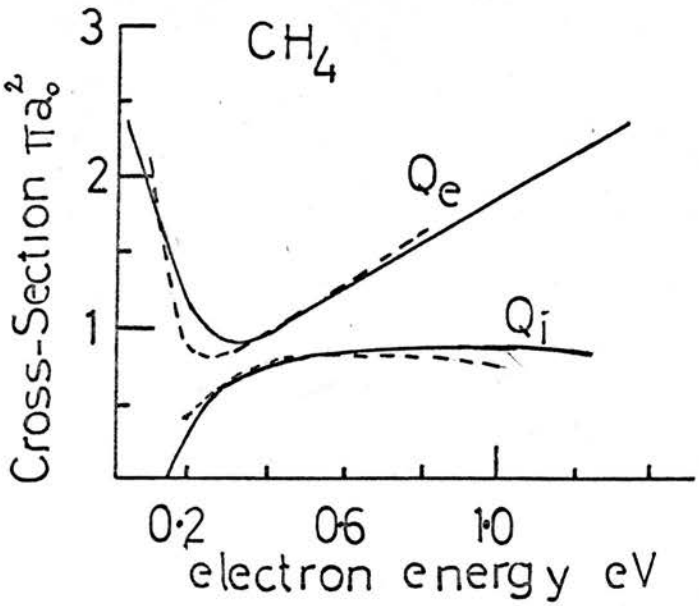

Fig.III.9.1. Collision Cross-Sections -CH_4-

e elastic

i inelastic

——— swarm

- - - - - mathematical curves

at 293°C

$$\lambda = 1.77\ 10^{-14}\ \frac{W^2}{k} \quad \text{—} \quad \text{III.6.1.}$$

(λ is the fractional energy loss per electron per collision). Results are tabulated in table III.6.1.

Table III.6.1.

λ Values for Electrons in Methane.

E/P	k	W cm us^{-1}	energy (eV)	λ x 10^2
0.2	1.9	2.9	0.07	8.5
0.4	3.3	6.6	0.12	23.6
0.6	4.6	8.9	0.17	30.6
0.8	6.2	10.0	0.23	28.9
1.0	8.0	10.4	0.30	24.2
1.2	10.0	10.5	0.38	19.7
1.4	12.1	10.2	0.45	15.1
1.6	14.4	9.8	0.54	11.8
1.8	16.8	9.7	0.63	10.0
2.0	19.2	9.6	0.72	8.7
2.5	28	9.4	1.05	5.5
3.0	33.6	8.0	1.26	3.4

For elastic losses only, $\lambda \doteq 2m/M \doteq 7 \times 10^{-5}$.
Despite the question of the validity of equation III.6.1. these very high λ values are strong evidence in favour of inelastic impacts between slow electrons and methane. The results are plotted in fig.III.6.1. The arrows on the graph denote the positions of the methane vibrations.

The maximum value of λ lies in the vibrational energy region. This could be interpreted as 'direct' vibrational excitation of methane by slow electrons. A similar calculation has been carried out for C_2H_4 using present drift velocities and the k values reported by Cochrane and Forrester[60]. The results are tabulated in table III.6.2. and shown graphically in fig. III.6.1. Again arrows represent vibrational modes of the molecule.

Table III.6.2.

λ Values for Electrons in Ethylene.

E/P	k	W cm μs^{-1}	energy eV	$\lambda \times 10^2$
0.4	2.7	0.85	0.1	5.7
0.6	2.9	1.7	0.11	8.8
0.8	3.0	4.2	0.114	10.5
1.0	3.5	4.6	0.13	10.8
1.2	4.0	4.9	0.15	10.7
1.4	4.4	5.0	0.16	10.2
1.6	4.6	5.0	0.17	9.7
1.8	5.4	5.1	0.20	8.6
2.0	5.8	5.1	0.22	8.0
3.0	9.1	5.0	0.27	4.9
3.5	10.8	4.9	0.34	4.0
4.0	12.9	4.8	0.4	3.2
4.5	15.0	4.7	0.56	2.6

Like methane, this shows a well defined maximum in the vibrational energy region.

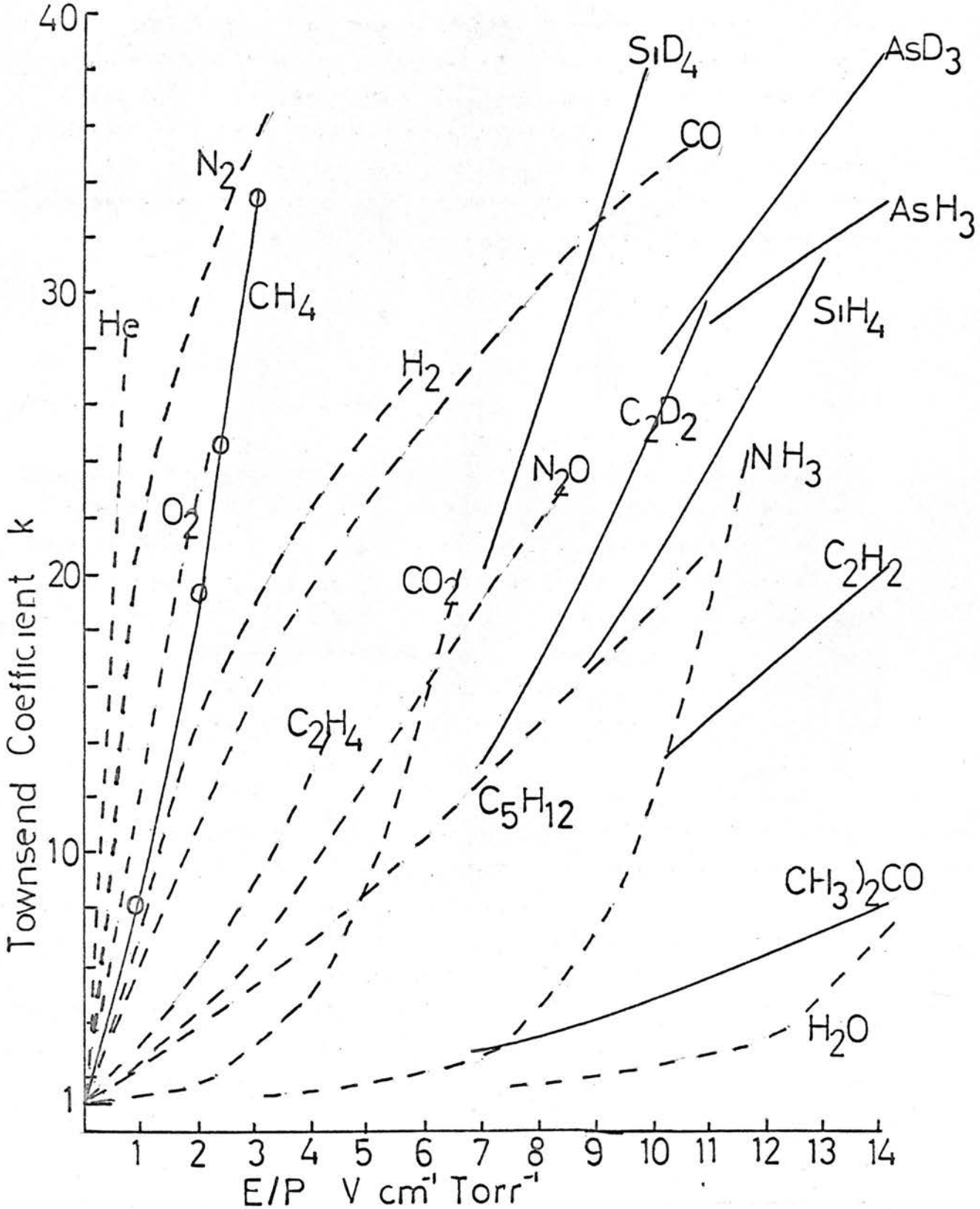

Fig. III.7.1. k values

III. 7. Further Evidence of Inelastic Impacts. In addition to the work described in Appendix 1, in this laboratory, some preliminary experiments have been done on the measurement of W/D for electrons in some gases.[112] As yet, only results at high E/P are available. k values derived from these measurements by the simplified theory are shown in fig. III.7.1. Also shown (broken lines) are other k values taken from the literature.[36-60] Re-arrangement of equations 1.7.6. and 1.7.8. gives

$$k = b \frac{1}{\overline{Q}_D \lambda^{\frac{1}{2}}} \frac{E}{P} \qquad \text{III.7.1.}$$

where b is an energy dependent factor. This illustrates that, at any E/P, high k is favoured by low Q and low λ .

There is little doubt that electron energies in the inerts are much higher than in other molecules - including CH_4 with its inert-like cross-section. The low k values in the polar gases can be explained by their high cross-sections. The k curves for polyatomics lie below those of the diatomics indicating, possibly, greater λ values in the polyatomic gases. Finally, k values for deuterides invariably lie above those of the corresponding hydrides. These k values are not sufficiently reliable to be used to try to differentiate between the different possible energy loss processes.

Using the k values in fig. III.7.1. and drift velocities either from the literature or present work, some λ values have been evaluated for a number of systems. They are given in fig. III.7.2. The λ pattern is interesting. Only in the inerts does λ approach the low, elastic value. In all the polyatomic molecules, λ is high and tends to show a maximum in the vibrational energy region. The maxima are particularly well defined in the less polar molecules. (A similar calculation on SiH_4 and SiD_4 using k values obtained by extrapolating the curves in fig. III.7.1. gives a λ maximum in the vibrational energy region.) Values in the diatomics are too high to be accounted for by elastic losses, but lie well below those in the polyatomics.

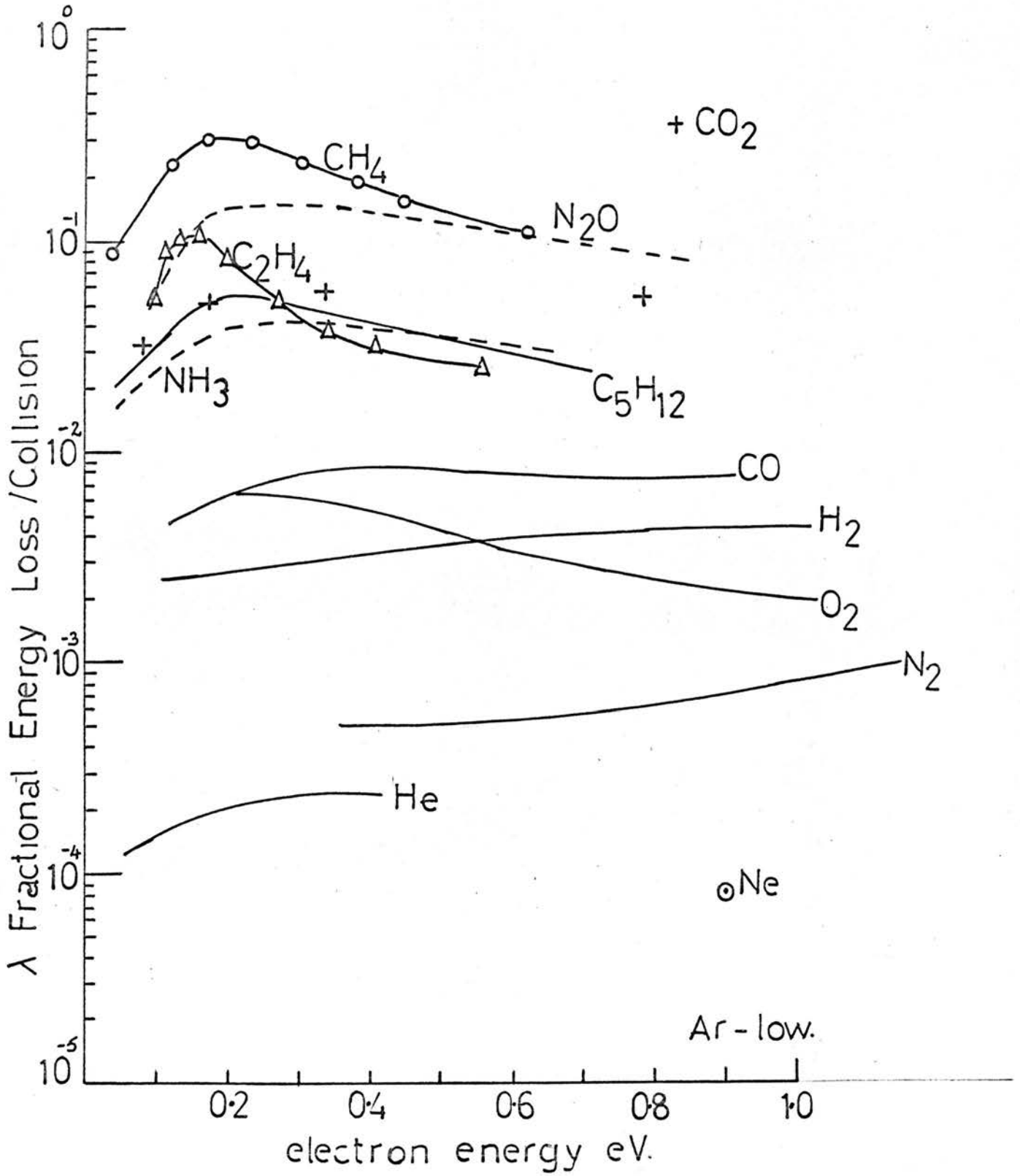

Fig. III. 7.2. λ Values

Rotational excitation may, to some extent, account for the high λ values. However, rotational excitation of CH_4 by the accepted mechanism is unlikely. In addition, as has been pointed out, the fact that CH_4 shows a Ramsauer-Townsend effect means that only 'head-on' electrons are deflected by the scattering potential. Such electrons, having zero angular momentum, cannot excite rotational motion. Electronic excitation of CH_4 by electrons in the high energy tail of the distribution may be discounted, as, at the low energies at which the λ maxima appear, the energy distribution curve is quite sharp.

It thus seems that, to account for the observed electron behaviour in gases, low energy inelastic processes - other than rotational excitation - must be introduced. The only possible process is vibrational excitation, in the vibrational energy region. Furthermore, according to present evidence, the excitation is more efficient for polyatomic molecules than for diatomic molecules. The observed patterns in W and k, the relation between transport quantities in hydrogen and deuterium isotopes, the form of the λ curves may be explained by the efficient vibrational excitation of polyatomic molecules by slow electrons. In the polar species, this excitation will be accompanied by rotational excitation, which may account for the flatter λ maxima in these molecules.

The fact that the vibrational excitation is less efficient for the diatomic molecules may be due to either of two factors:-

(a) The vibrational mode excited is a bending one. The position of the λ maximum in CH_4 favours this.

(b) The excitation mechanism is not available to the diatomic molecule.

Until the mechanism is established, the tenability of (b) is uncertain. However, at the present time, the drift velocity patterns we have observed may be explained by excitation of bending modes in molecules, by slow electrons.

III.8. Excitation Mechanism

So far, the only known mechanism by which slow electrons excite vibrations is that involving the resonance or compound electron/molecule intermediate, described in section I.5. It may be that these intermediates play a dominant role in collisions between electron and molecules, other than N_2, CO, and N_2O.

Resonances in the low-energy scattering of electrons is shown by a potential well which has a 'virtual' energy level just above the top of the well.[113] Such a potential well exhibits a resonance in the scattering of a slow electron having the same l valve as the virtual level. If the well is sufficiently deep and broad for the level to fall in the well, resonance will not occur. Physically, the incident electron has nearly the right energy to be bound by the potential well and so tends to concentrate there. The incident wave function is thus highly distorted. These resonance states can occur in elastic scattering, and have recently been seen in the scattering of electrons from the inerts, just below the first electronically excited states.[114]

If, as seems likely, the vibrational excitation of molecules by slow electrons proceeds via such intermediates, this means that there exists a set of molecular energy levels, hitherto undetected. The present indications are that beam techniques are not sufficiently sensitive to reliably detect inelastic processes in these low energy regions; so that it will remain for electron swarm experiments to investigate further the possible existence of such states. This will demand increasingly more sophisticated analysis of swarm data. At present, the approach of Phelps and Co. involving the solution of the Boltzmann equation for each system is the most satisfactory method.[94] However, this is extremely complex. An alternative method has been suggested by Fluendy,[115] in which a Monte-Carlo technique is used. In this, the experiment is, effectively, reproduced in an electronic computer. The physical situation is this: an electron of fixed velocity starts a random walk, down-hill through gas molecules. Its velocity increases until it collides. After a collision its velocity has changed and it moves away from the molecule

with randomised direction of motion. The walk is continued until the electron reaches the foot of the hill or 'home', and its time of travel is recorded. Because of the large number of choices which face the electron at various points in its travel, and because of the very large number of electrons which must be considered, to reproduce this situation by a physical model is almost impossible. However, it can be done mathematically and, by random sampling techniques, the result produced by a fast computer in a fairly short time.

In this treatment, energy dependent collision cross-sections must be assumed. These can then be tailored until calculated and experimental drift times agree. To a first approximation they may be obtained from swarm experiments.

III.9. Inelastic Cross-Sections

The following expression may be written for λ

$$\lambda = \lambda_{el} \frac{Q_{el}}{Q_{total}} + \lambda_{inel} \frac{Q_{inel}}{Q_{total}}$$

If vibrational excitation takes place, then the first term in the above equation may be neglected.

$$\lambda = \lambda_{inel} \frac{Q_{inel}}{Q_{total}}$$

Consider CH_4 in which rotational excitation is forbidden and assume that, in an inelastic impact, one vibrational quantum $h\nu$ is lost by the electron.

$$\lambda = \frac{h\nu}{\epsilon} \frac{Q_{inel}}{Q_{total}}$$

$$Q_{inel} = \frac{\epsilon}{h\nu} \lambda \, Q_{total}$$

ϵ is the electron energy.

The following table has been compiled using the ϵ and λ values of table III.6.1 and the Q_{total} of table III.3.1. $h\nu$ is taken as 0.16 eV, the lowest vibrational quantum of CH_4.

Table III.9.1.

Cross-Sections for Methane.

GAS	$h\nu$ eV	ϵ eV	λ	Q_{tot} Πa_o^2	Q_{in} Πa_o^2	Q_{el} Πa_o^2
CH_4	0.16	0.07	-	2.4	-	2.4
		0.12	-	1.6	-	1.6
		0.23	30.6	1.51	0.44	1.09
		0.27	28.9	1.53	0.64	0.87
		0.30	24.2	1.63	0.74	0.89
		0.38	19.7	1.73	0.81	0.92
		0.45	15.1	1.88	0.80	1.08
		0.54	11.8	2.05	0.82	1.23
		0.63	10.0	2.16	0.85	1.31
		0.72	8.7	2.28	0.89	1.39
		1.05	5.5	2.39	0.86	1.53
		1.26	3.4	3.09	0.83	2.26

Q_{inel} and Q_{el} are plotted as functions of electron energy in fig. III.9.1.

(page 80)

Over the energy region in which we are interested, these cross-sections may be represented by the equations:-

$$Q_{el} = (3.3 - 12.5\epsilon)\text{II } a_o^2 \qquad \epsilon < 2h\nu$$

$$Q_{el} = (1.42\epsilon + 0.4)\text{ II } a_o^2 \qquad \epsilon \geq 2h\nu$$

$$Q_{inel} = 0.82 \left[1 - 9.8(\epsilon - 3h\nu)^2\right]^{\frac{1}{2}} \qquad \text{when positive and real}$$

These curves are shown as dotted lines in fig. III.9.1.

Cross-sections of the above form have been used as in-put cross-sections in a Monte-Carlo analysis of electron transport through CH_4. A programme for the Atlas computer has been written[115] and the calculation is being done at the present time. It is hoped that the results will show whether or not the electron behaviour in CH_4 can be accounted for by vibrational excitation of the molecules. If the answer is 'yes' refined cross-sections will be produced and facilitate further investigations on the excitation mechanism. If the answer is 'no', an alternative explanation for the observed transport quantities must be sought. Either way, there is still valuable information, on the nature of electron/molecule interactions, to be gained from electron swarm studies.

APPENDIX.

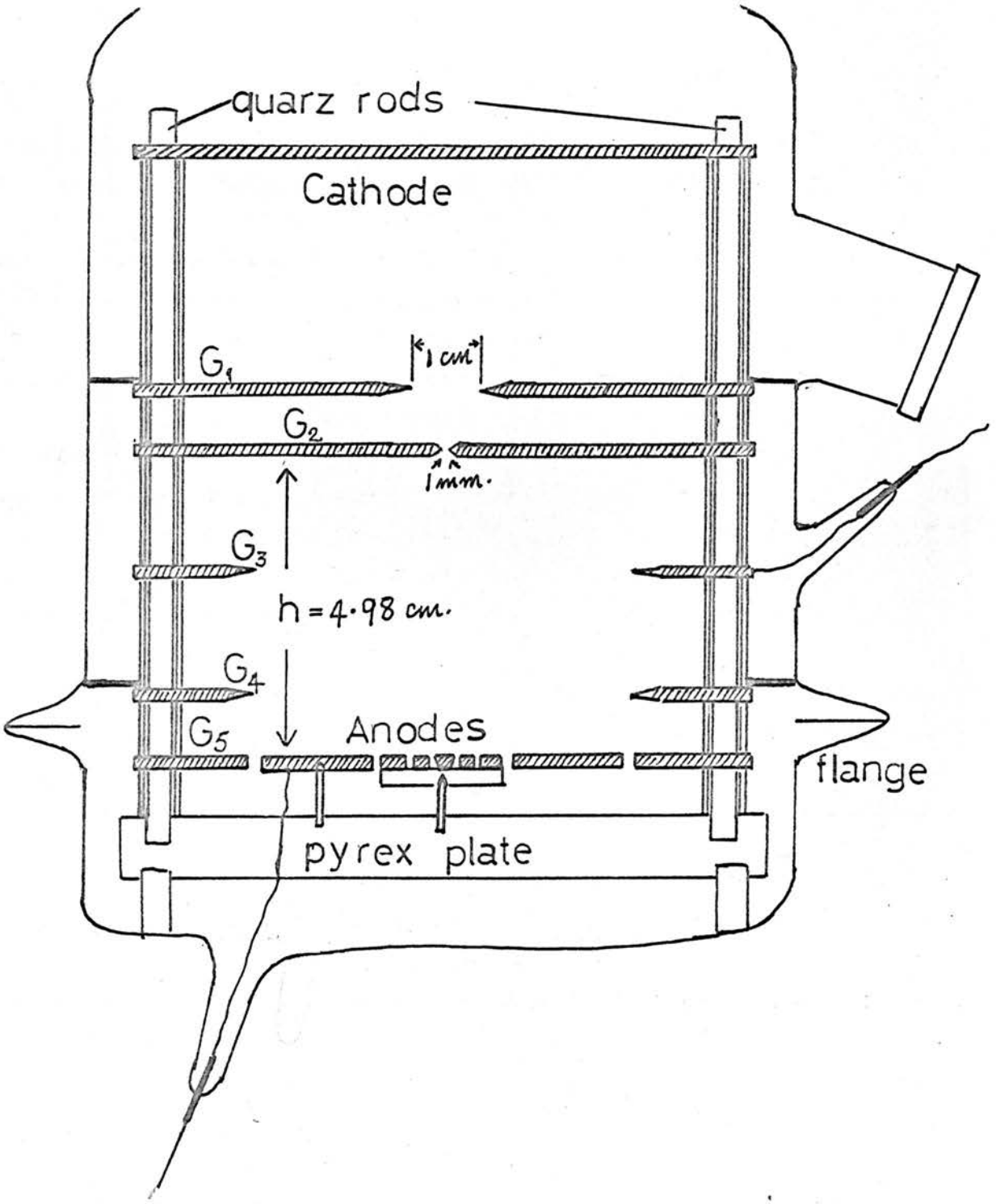

Fig.A.1. Diffusion Cell

APPENDIX I

Measurement of k values in CH_4

k values for electrons in CH_4 were deduced from measurements of W/D made in a Townsend diffusion apparatus. The principles of this have been described (section I.6(a)).

The present cell is shown in fig. A.1. and in general design resembles the drift cell (fig. II.1.1.) Photoelectrons, ejected from the cathode by u.v. light, moved downwards under the influence of an electric field E to be collected on the anode. This anode consisted of a central disc surrounded by 3 annuli - all the components being insulated from each other.

As previously, the electrodes were of gold-plated brass, separated from each other by accurately ground glass spacers. Unlike the drift tube, the internal assembly was built up from the bottom. Four quarz rods, fixed into a pyrex glass base plate, ran through the glass spacers and guard rings, up the length of the tube. This gave stability to the structure. The anode components were also supported on this base plate. Anodes A_1,A_2 and A_3, were screwed on to a pyrex disc which was then mounted on to the base plate, supported by three pyrex rods, as shown (fig. A.1, and A.2). Anode A_4 was similarly supported on glass rods. This assembly was quite rigid and gave the necessary insulation resistance between the anodes of $\sim 10^{14}$ ohms.

The guard ring leads, constructed as before, were taken horizontally through the sides of the containing pyrex vessel. The anode leads and the lead from G_5 were taken through tungsen/glass seals in the bottom of the envelope. When operating the anode was maintained at earth potential and the cathode negative with respect to earth. The cathode/anode voltage was provided by a 0-500 V Solartron Power Supply and the guard ring voltages tapped from a resistor chain of precision wire-wound resistors. Currents were measured on a 33C Vibron electrometer in conjunction with a high resistance (10^{11},10^{12} ohms). Each anode lead was tied to the centre point of a miniature knife switch which could be connected either to the

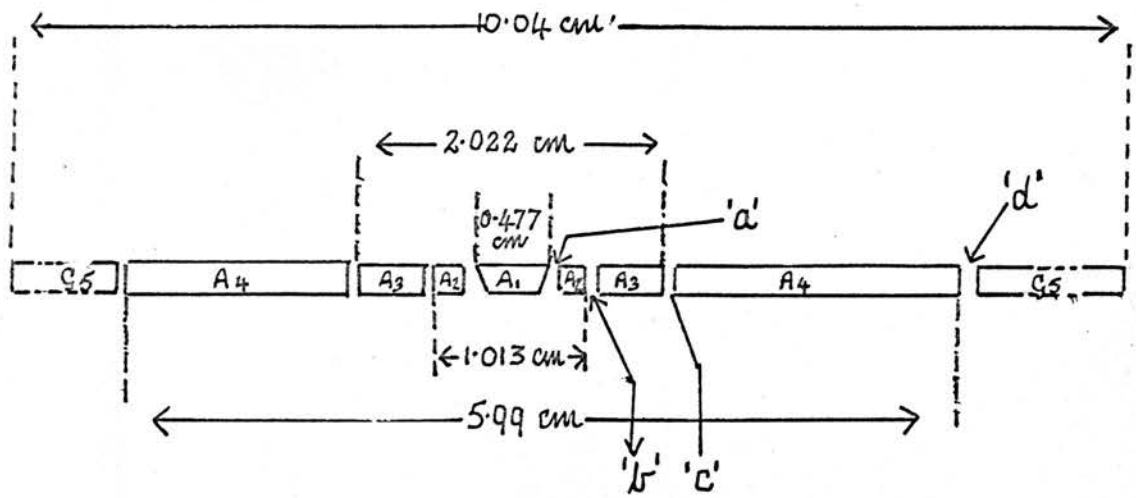

'a' = 0·02 cm
'b' = 0·025 cm
'c' = 0·030 cm
'd' = 0·05 cm.

(a)

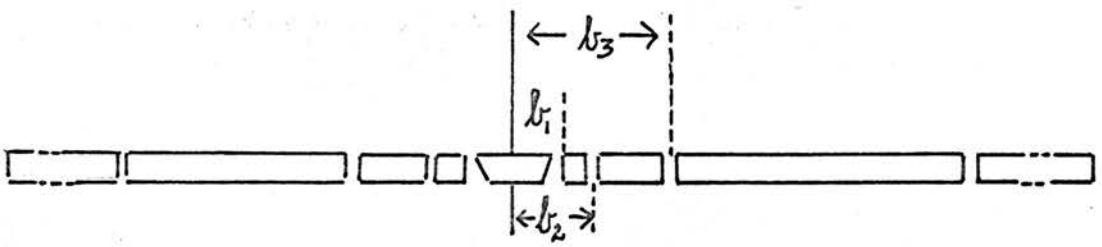

b_1 = 0·259 cm
b_2 = 0·591 cm
b_3 = 1·026 cm.

(b)

Fig.A.2. Anode Dimensions

electrometer or to earth. Currents arriving at the different anode components could thus be measured separately. The anode electronics were housed in a shielded box directly below the cell, and all leads were made as short as possible.

The gas-handling system was similar to that described previously. However, in this case, the furnace, allowing bake-out of the cell at temperatures up to 200°C, was always in position around the cell, acting as a shield. Normally a 'dark' current (i.e. current registered on the electrometer when the cathode was not illuminated) of 10^{-14} A was recorded, and, as this could be a significant proportion of the total current arriving at any one anode, care had to be taken (by shielding electronics and leads etc.) to keep this dark current to a minimum. This dark current was subtracted from the 'light' current at any anode in all measurements. In addition, the usual precautions to keep experimental error to a minimum were taken.

The dimensions of the individual anodes are given in fig. A.2.

Recall, that, if i_a is the current falling on an anode disc of radius b and i_t the total current arriving at the anode, then

$$\frac{i_a}{i_t} = R = 1 - \frac{h}{d} \exp -g(d-h) \quad \text{——} \quad \text{A.1.}$$

where h is the distance between entrance hole and anode and $d^2 = b^2 + h^2$. g is the factor W/2D which is related to k, the electron Townsend factor, by equation 1.7.5. (if the simple theory is assumed to hold).

$$W/D = \frac{E}{kT} \quad 11.59\ 10^3 \quad \text{———} \quad \text{A.2.}$$

Rearranging equation A.1. we get

$$g = \frac{1}{(d-h)} \ln \frac{h}{d} - \frac{1}{d-h} \ln(1-R) \quad \text{——} \quad \text{A.3.}$$

If i_a is very low, a small error in current reading due to random electrometer fluctuations introduces a large error into R and hence k. Optimum results are therefore obtained if $R \doteq 0.5$. In the present apparatus, at each E/P, we were able to test various anode combinations to find that b giving R nearest to 0.5. Three ratios were possible.

$$R_1 = i_1/i_t \quad R_2 = (i_1 + i_2)/i_t \quad R_3 = (i_1 + i_2 + i_3)/i_t$$

Initially, the radii (b) of the anodes were measured to the centre of the anode air gaps. However, it was found that, to give consistent results, the whole of the air gap 'a' (fig. A.2.) had to be included in the central disc radius, giving 'b' values as shown in fig. A.2(b). Under such conditions, and provided $0.1 > R > 0.9$, the k values deduced at any E/P from R_1 R_2 and R_3 agreed to within 5%. The differences appeared to be purely random, and due to electrometer fluctuations.

Pressures ranged from 8 - 30 Torr and no pressure dependence was observed.

The measurements were made at 293°C where equation A.2. becomes

$$W/D = \frac{E}{k} 39.5$$

In the table below are listed the 'best' k values.

Table A.1

k values - CH_4

E/P V $cm^{-1}Torr^{-1}$	k
0.2	1.9
0.4	3.3
0.6	4.6
0.8	6.2
1.0	8.0
1.2	10.0
1.4	12.1
1.6	14.4
1.8	16.8
2.0	19.2
2.5	28
3.0	33.6
3.5	40.0

These measurements were made by Mr. I.A. Stenhouse.

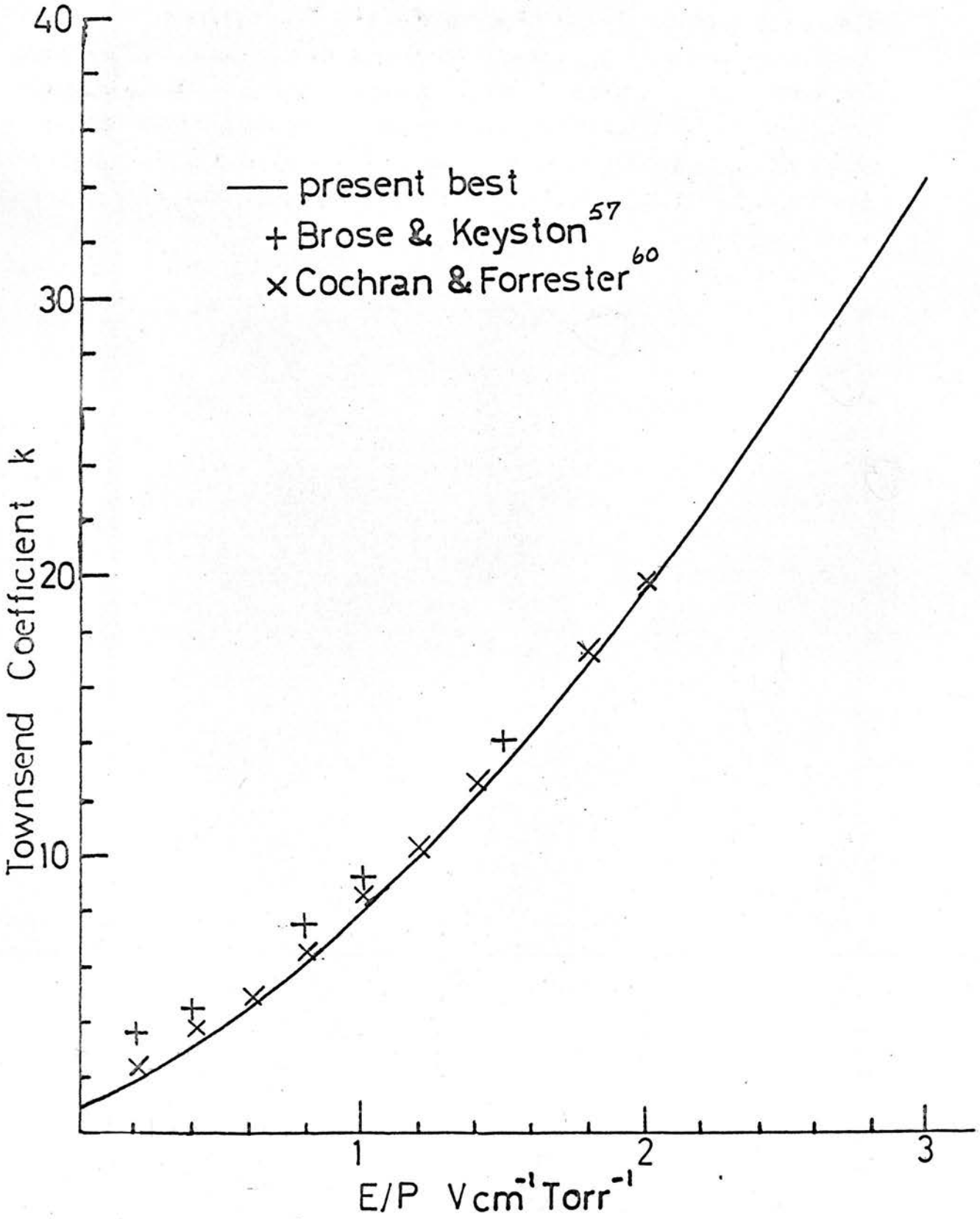

Fig.A.3. k values - CH_4

In fig. A.3 they are plotted as a function of E/P and compared with those of Brose and Keyston[57] and Cochran and Forrester.[60] (Cochran and Forrester give their results in terms of W/D at various E/P. In order to evaluate k from W/D, it is necessary to know E and P We assumed that their values were 'normalised' to unit pressure and evaluated E/P from their data accordingly. The comparison with our results suggests that this treatment is correct.)

These k values were used along with our drift velocities to evaluate molecular collision cross-sections and electron λ values for electrons in CH_4.

References

1. H.S.W. Massey and E.H.S. Burhop.
   'Electronic and Ionic Impact Phenomena' (1952) Oxford University Press.
2. D.R. Bates (Ed) 'Atomic and Molecular Processes' (1962) Academic Press.
3. L.B. Loeb 'Basic Processes in Gaseous Electronics' (1955) University of California Press.
4. R.H. Healey and J.W. Reed 'The Behaviour of Slow Electrons in Gases' (1941) Amalgamated Wireless (Australasia) Ltd.
5. J.S. Townsend 'Motion of Electrons in Gases' (1925) Oxford University Press.
6. J.B. Hasted 'Physics of Atomic Collisions' (1964) London, Butterworths.
7. A. Kuppermann, L.M. Raff. J. Chem.Phys. 1962, 37, 2497.
8. Landau and Lifshitz. 'Quantum Mechanics' 1958, Pergamon Press, page 400.
9. C. Ramsauer, Ann.der Physik 1921, 64, 513.
   C. Ramsauer, Ann.der Physik, 1921, 66, 546.
10. R.B. Brode, Phys.Rev. 1925, 25, 636.
11. C.E. Normand, Phys. Rev. 1930, 35, 1217.
12. C. Ramsauer, and R. Kollath, Ann.der Physik. 1929, 3, 536; 1930, 4, 91.
13. E. Bruche:- see ref. 1 page 209.
14. J.S. Townsend, V.A. Bailey, Phil. Mag. 1922, 43, 539.
15. Ref. 8, chapter XIV et seq.
16. J.B. Fisk, Phys. Rev. 1936, 49, 167 and Phys. Rev. 1937, 51, 25.
17. R.A. Buckingham, H.S.W. Massey, S.R. Tibbs, Proc.Roy.Soc. 1941, A178,119.
18. G.J.Schulz, Phys. Rev. 1958, 112, 150.
19. G.J. Schulz, Phys. Rev. 1959, 116, 1141.
20. G.J. Schulz, " 1962, 125, 229.
21. G.J. Schulz, J. Chem.Phys. 1961, 34, 1778.
22. G.J. Schulz, " 1960, 33, 1661.
23. G.J. Schulz and J.T. Dowell, Phys. Rev. 1962, 128, 174.
24. G.J. Schulz, Phys. Rev. 1964, 135, A988.
25. R. Haas, Z.Physik. 1957, 148, 177.
26. A. Herzenberg and F. Mandl, Proc.Roy.Soc. 1963, A274, 253.
27. J.G.C. Chen, J.Chem.Phys. 1964, 40, 3513.
28. J.S. Townsend, 'Electricity in Gases' 1914. Oxford University Press.
29. J.S. Townsend, Proc.Roy.Soc. 1908, A80, 207 and A81, 464.

30. L.G.H. Huxley, Aust.J.Phys. 1957,10.118.
31. " " " 1960,13,718 and 578.
32. Ref. 4, chapter 1.
33. R.W. Crompton and R.L.Jory, Aust.J.Phys. 1962, 15, 451.
34. L.G.H. Huxley, Phil.Mag. 1940, 30, 396.
35. L.G.H. Huxley and R.W. Crompton, Proc.Phys.Soc. 1955, B68, 381.
36. J.S. Townsend and V.A.Bailey, Phil.Mag. 1923, 46, 657.
37. V.A. Bailey, Phil.Mag. 1924, 47, 379.
38. J.S. Townsend and V.A. Bailey, Phil.Mag. 1922, 44, 1033.
39. J.S. Townsend and V.A. Bailey, Phil.Mag. 1921, 42, 873.
40. H.L. Brose, Phil.Mag. 1925, 50, 536.
41. R.H. Healey and Kirkpatrick, from ref. 4 page 94.
42. J.S. Townsend and H.T. Tizard, Proc. Roy.Soc. 1913, A88, 336.
43. V.A. Bailey, Phil.Mag. 1925, 50, 825.
44. V.A. Bailey and R.H. Healey, Phil.Mag. 1925, 19, 725.
45. J.E. Bailey, R.E.B.Makinson and J.M. Somerville, Phil.Mag. 1937, 24, 177.
46. R.H. Healey, Phil.Mag. 1938, 26, 940.
47. M.F. Skinker and J.V. White, Phil.Mag. 1923, 46, 630.
48. V.A. Bailey and J.M. Somerville, Phil.Mag. 1934, 17, 1169.
49. J.B. Rudd, from ref. 4 page 98.
50. M.F. Skinker, Phil.Mag. 1922, 44, 994.
51 V.A. Bailey and J.B. Rudd, Phil.Mag. 1932, 14, 1033.
52. V.A. Bailey and W.E. Duncanson, Phil.Mag. 1930, 10, 145.
53. V.A. Bailey and A.J. Higgs, Phil,Mag. 1929, 7, 277.
54. V.A. Bailey and J.D. McGee, Phil.Mag. 1928, 6, 1073.
55. J.D. McGee and J.C. Jaeger, Phil.Mag. 1928, 6, 1107.
56. Bannon and Brose, Phil.Mag. 1928, 6, 817.
57. Brose and Keyston, Phil.Mag. 1935, 20, 902.
58. R.W. Warren and J.H. Parker, Phys.Rev. 1962, 128, 2661.
59. R.W. Crompton and D.J. Sutton, Proc.Roy.Soc. 1952, A215, 467.
60. L.W. Cochran and D.W. Forrester, Phys.Rev. 1962, 126, 1785.
61. B.I.H. Hall, Aust.J.Phys. 1955, 8, 468.
62. L.G.H. Huxley and A.A. Zaazou, Proc.Roy.Soc. 1948, A196, 402.
63. R.W. Crompton, L.G.H. Huxley and D.J. Sutton, Proc.Roy.Soc. 1953, A218, 507.
64. L.G.H. Huxley, Phil.Mag. 1937, 23, 219.
65. N.E. Bradbury and R.A. Nielson, Phys.Rev. 1936, 49, 388.

66. R.A. Nielson, Phys. Rev. 1936, 50, 950.
67. J.L. Pack and A.V. Phelps, Phys.Rev. 1960, 121, 798.
68. J.L. Pack, R.E. Voshall, and A.V. Phelps, Phys.Rev. 1962, 127, 2084.
69. R.A. Duncan, Aust.J.Phys. 1957, 10, 118.
70. R.W. Crompton, B.J. Hall, and W.C. Macklin, Aust.J.Phys. 1957, 10, 366.
71. J.J. Lowke, Aust.J.Phys. 1962, 15, 39.
72. P. Herreng, Compt.Rendu, 1943, 217, 75.
73. J.A. Hornbeck, Phys.Rev. 1951, 83, 374.
74. L. Colli and U. Facchini, Rev. SC.Instr. 1952, 23, 39.
75. J.M. Kirshner and D.S. Toffolo, J.Appl.Phys. 1952, 23, 594.
76. E.D. Klema and J.S. Allen, Phys.Rev. 1950, 77, 661.
77. W.N. English and G.C. Hanna, Can.J.Phys. 1953, 31, 768.
78. T.E. Bortner, G.S. Hurst, and W.G. Stone, Rev. Sc.Instr. 1957, 28, 103.
79. G.S. Hurst, J.A. Stockdale, and L.B. O'Kelly, J.Chem.Phys. 1963, 38, 2572.
80. J.C. Bowe, Phys.Rev. 1960, 117, 1411.
81. G.S. Hurst, L.B.O'Kelly, E.B. Wagner, and J.A. Stockdale, J.Chem.Phys. 1963, 39, 1314.
82. M.J. Druyvesteyn, Physica, 1934, 1, 1003.
83. M.J. Druyvesteyn, Physica, 1936, 10, 61.
84. P.M. Morse, W.P. Allis, and E.S. Lamar, Phys.Rev. 1935, 48, 412.
85. H.W. Allen, Phys. Rev. 1937, 52, 707.
86. A.E.D. Heylen and T.J. Lewis, Proc.Roy.Soc. 1963, A271, 531.
87. J.A. Smit, Physica, 1936, 3, 543.
88. H. Margenau, Phys.Rev. 1946, 69, 508.
89. T. Holstein, Phys.Rev. 1946, 70, 367.
90. A.E.D. Heylen, Proc.Phys.Soc. 195, 76, 779.
91. T.J. Lewis, Proc.Roy.Soc. 1958, A244, 166.
92. A.E.D. Heylen, Proc.Phys.Soc. 1962, 79, 284.
93. A.E.D. Heylen, Proc.Phys.Soc. 1962, 80, 422.
94. A.G. Engelhardt and A.V. Phelps, Phys.Rev. 1963, 131, 2115.
95. A.G. Engelhardt and A.V. Phelps, Phys.Rev. 1964, 133, A375.
96. A.G. Engelhardt, A.V. Phelps and C.G. Risk, 1964, 135, A1566
97. L.S. Frost and A.V. Phelps, Phys.Rev. 1964, 136, 1538.
98. H.S.W. Massey, Trans.Fer.Soc. 1935, 31, 556.

99. E. Gerjuoy and S. Stein, Phys.Rev. 1955, 97, 1671.
100. E. Gerjuoy and S. Stein, Phys.Rev. 1955, 98, 1848.
101. T.R. Carson, Proc.Phys.Soc. 1954, A67, 908.
102. P.M. Morse, Phys.Rev. 1953, 90, 51.
103. S. Altshuler, Phys.Rev. 1957, 107, 114.
104. H.S.W. Massey, Trans.Far.Soc. 1935, 31, 556.
105. T-Y.Wu, Phys.Rev. 1947, 71, 111.
106. Clusius and Riccobini, Z.Phys.Chem. 1938, B.38, 81.
107. T.L. Cottrell and A.J. ,atheson, Trans.Far.Soc. 1962, 58, 2336.
108. Storch, J.Amer.Chem.Soc. 1934, 56, 374.
109. T.L. Cottrell et al, Trans.Far.Soc. 1964, 60, 241.
110. A.J. Matheson, Thesis, Edinburgh University, 1962.
111. Cawood and Patterson, Trans.Far.Soc. 1933, 29, 514.
112. T.L. Cottrell and D. Maydan, unpublished results, Edinburgh University, 1965.
113. Mott and Massey 'The Theory of Atomic Collisions' 1949, Oxford.
114. G.J. Schulz, Phys.Rev. 1964, 136, A650.
115. M.A.D. Fluendy, Edinburgh University, 1965.

ACKNOWLEDGEMENTS

I wish to record my sincere thanks to Professor T.L. Cottrell who supervised this research. I am grateful, also, to Dr. A.W. Read who gave much help and advice, particularly during the early stages of the work; to Mr. A.H. Young, who designed and built the electronic circuits; to Mr. T.D. Sheddan and his team of technicians whose skill was invaluable in the design and construction of the apparatus; to D.S.I.R. who provided a maintenance grant for two years; and to the University of Edinburgh for the provision of laboratory facilities.

I.C. Walker.